SEDIMENT IMPACT ON THE FORMATION OF HYPOXIC WATERS IN THE NORTHERN GULF OF MEXICO: A SYNTHESIS OF SEDIMENT TEXTURE, COMPOSITION, ERODIBILITY AND TRANSPORT

by

Rangley Claude Mickey

Submitted in Partial Fulfillment of the

Requirements for the Degree of Master of Science in

Coastal Marine and Wetland Studies in the

College of Science

Coastal Carolina University

2013

_____	_____
Dr. Kehui Xu	Dr. Susan Libes
Major Professor	Committee Member

_____

Dr. Jenna Hill

Committee Member

Acknowledgements

The author would like to acknowledge all those participants who supported in field work, laboratory work, funding, and design of this Master's of Science Thesis study at Coastal Carolina University. I would first like to thank my advisor, Dr. Kehui Xu, for all the opportunities offered to me during my graduate career, as well as my thesis committee members for their support during this project. I would like to acknowledge with much appreciation all the principle investigators and students who are part of the Mechanisms Controlling Hypoxia Research Group for their research efforts, support with modeling, and for allowing my participation in the ongoing research. I would like to express my appreciation to Dr. James Geaghan and Xi Chen of the Louisiana State University Experimental Statistics Department for the help with my project. I also thank the National Oceanic and Atmospheric Association and the National Science Foundation for their funding of this research project.

Abstract

Annual hypoxic events have been found to occur over the past several decades in the northern Gulf of Mexico (nGOM) and have prompted researchers to begin studying the mechanisms that control hypoxia formation so they may advise policy makers on the appropriate mitigating responses. This has led to the development of 3-dimensional modeling systems that incorporate marine physical, biological, geological, and chemical processes that may impact the formation and duration of hypoxic regimes in the nGOM. This study used field, laboratory, and modeling techniques to examine how sediment may be eroded from the seabed and where/how it is transported across the nGOM. Analysis of sediment texture, composition, and erodibility through field studies and Regional Ocean Model System (ROMS) simulations have shown that spatial variability in sediment grain size and erodibility relates mostly to the proximity to the major river deltas (Mississippi and Atchafalaya) and to the remnants of historic shifts in the Mississippi deltaic lobe system. Temporal variability stems mostly from changes in seasonal weather patterns, with more energetic weather in winter and spring setting up an active bottom boundary layer (BBL) which agitates seabed sediment and therefore increases its erodibility, compared to summer quiescent periods that can allow for seabed consolidation due to a low-energy BBL. This study has also found evidence that there is an organically enriched flocculent layer of material at the water-sediment surface that is highly erodible. Based on comparisons of model simulations and experiments, the shear stress levels during the quiescent periods may be strong enough to resuspend this material and reintroduce it into the lower water column where it may be decomposed by bacteria. Modeling studies have illustrated that understanding the interactions among physical, chemical, biological, and geological dynamics is a challenging but necessary in order to determine what mitigating practices will be most beneficial. This study only examines a part of the complex hypoxic water system, but it provides a stepping stone for future studies that examine the complex interaction of the different regimes that influence hypoxia formation.

Table of Contents **Page**

Tables

Figures

Abbreviations

τ_b: The stress applied to the bed

τ_c: The depth-varying critical stress for erosion

τ_{cr}: critical shear stress for erosion

BBL: Bottom boundary layer

CCU: Coastal Carolina University

CSTMS: Community Sediment Transport Modeling System

CTD: Conductivity, Temperature, Depth

E: Erosion rate

E_{rate}: Erosional rate

Floc: flocculent

FMI: Fluid Meter Inc.

FVCOM: Finite Volume Coastal Ocean Model

HYCOM: Hybrid Coordinate Ocean Model

LATEX: Louisiana-Texas

M: the depth-varying erosion rate ‘‘constant’’

MCH: Mechanisms Controlling Hypoxia

MMT: million metric tons

NARR: North American Regional Reanalysis

NCEP: National Center for Environmental Prediction

nGOM: Northern Gulf of Mexico

NOAA: National Oceanic and Atmospheric Association

NSF: National Science Foundation

OM: organic matter/organic material

Pa: Pascal

RDAS: Regional Data Assimilation System

ROMS: Regional Ocean Modeling System

SOC: Sediment oxygen consumption

SOD: Sediment oxygen demand

SSC: Suspended sediment concentration

SWAN: Simulating Waves Nearshore

Tau_C: current generated shear stress

Tau_{CW}: total applied shear stress (wave plus current)

Tau_W: wave generated shear stress

TSS: Total Suspended Solids

VSS: Volatile Suspended Solids

W_s: settling velocity

WWIII: Wave Watch III

Sediment Impact on the Formation of Hypoxic Waters in the Northern Gulf of Mexico: A Synthesis of Sediment Texture, Composition, Erodibility and Transport

1 Introduction

1.1 Northern Gulf of Mexico Hypoxic Zone

One of the largest hypoxic events occurs annually in the northern Gulf of Mexico (nGOM) during the warmer months of the year. This area of the nGOM has become so heavily impacted by annual hypoxic (dissolved oxygen < 2 mg/L) events that it is now being referred to as a "Dead Zone" (Rabalais et al., 2007). The development of hypoxia in the nGOM is described to be the result from a combination of eutrophication from excessive nutrient loading from the Mississippi River watershed and water column stratification during warm times of the year (Rabalais et al., 2007). The Mississippi River is the largest river in the United States and drains nearly 41% of the continental US into the nGOM (Xu et al., 2011). The Mississippi River system has two main distributaries entering the gulf: the Mississippi and Atchafalaya Rivers. The main stem of the Mississippi River has 30% of its discharge being diverted, by control structures, into the Atchafalaya River (Meade and Moody, 2010). The input of nutrients from these two watersheds causes high productivity in the spring months, which increases the amount of detritus being introduced into the lower water column and seabed surface, leading to increased aerobic respiration by heterotrophic bacteria (Rabalais et al., 2007). Bottom water hypoxia becomes most prevalent during the late spring and summer months due to strong stratification of the water column, which decreases the amount of mixing and re-oxygenation occurring in the lower water column below the pycnocline. The spatial extent of this hypoxic event increases dramatically within weeks to cover an area ranging from 8,000-20,000km^2, with an average around 13,000km^2 annually from 1985 to 2007 (Rabalais et al., 2007).The large nutrient loads that are transported into the nGOM from the Mississippi and Atchafalaya Rivers become utilized by phytoplankton and result in massive algal blooms. These large amounts of nutrients, specifically nitrogen, come from the watershed of the Mississippi River which drains from vast areas of agricultural lands. The runoff from these areas tends to have large amounts of agricultural fertilizers containing high concentrations of nitrogen and phosphorus. Studies indicate that

there is a linear correlation between the increased size of the hypoxic zone and the increased amounts of nitrogen input over the past few decades (Turner et al., 2006; 2008). The increase in these nutrients allows phytoplankton growth to increase above the normal abundances seen under normal ambient nutrient concentrations, which tend to be a limiting factor for growth if occurring naturally (Rabalais et al., 2007). When these large algal blooms begin to die off or are consumed by zooplankton and turned into fecal matter, the detrital material begins to sink through the water column onto the seabed and is respired by heterotrophic bacteria (Dagg et al., 2008). Other processes of aggregation—disaggregation, sorption—desorption, photo-oxidation, and mineralization that occur in the upper water column also affect the amounts and composition of materials entering the lower water column and settling on the sediment surface (McKee et al., 2004). Studies that analyze the amount of biologically bound silica from decomposing diatoms have served as a proxy for the increased amount of primary productivity and indicate that eutrophication and this increase in silica are fairly recent events, starting around 30 years ago (Turner et al., 2008). Large accumulations of the bound silica correlate linearly with increases in the amounts of nutrient loading coming from the Mississippi watershed (Turner et al., 2008).

As productivity increases due to these large nutrient loads across the shelf, there is more organic matter (OM) being deposited on the sediment surface in a flocculent (floc) layer of fine loose material. This floc layer lies on top of the sediment and contains mostly materials that are easily resuspended due to their small particle size and low density, such as fine particulate organic matter (Wainright and Hopkinson, 1997); this floc layer at the sediment-water interface has been observed to be a major site for aerobic respiration by bacteria (Rowe et al., 2002). In fluvial and marine systems the frictional force at the seabed which influences the amount of particles that are resuspended is referred to as shear stress; wave and current combined shear stress acts on the seabed setting up a bottom boundary layer (BBL) present just above the sediment surface. The degree of shear stress greatly influences the amount of seabed material that becomes eroded and introduced into the lower water column, which may influence hypoxic regimes in this area of the nGOM.

Hypoxic events like the one observed in the nGOM have many negative effects on the food web dynamics of this ecosystem. The most important effect on the biota during these events is a shift in the

transfer of carbon; instead of transferring to higher trophic levels carbon is transferred straight to the microbial community; the losses of benthic biomass are estimated to be as much as 1.4 MT C/km^2 (Diaz and Rosenberg, 2008). There have also been studies that have shown some species such as Atlantic croaker and brown shrimp experience habitat loss during hypoxic events in bottom waters in the nGOM (Craig and Crowder, 2005). Craig and Crowder (2005) observed that both species tend to migrate to areas along the edge of the hypoxic zone; and even these areas were observed to have moderately low oxygen levels, which along with increased water temperatures can have detrimental effects on the development of these species.

1.2 Policy Action for Hypoxia Mitigation

There has been some policy action in the US regarding hypoxia in the nGOM that aims at reducing the hypoxic zone size to an average of 5000 km^2 by the year 2015 (Mississippi River/Gulf of Mexico Watershed Nutrient Task Force, 2001). Scientists and policy makers are working together using newly developed techniques and adaptive ecosystems based management practices to better monitor and assess the development of hypoxia. The Mississippi River/Gulf of Mexico Watershed Nutrient Task Force was setup in 1997 to begin research and monitoring of hypoxic events in the Gulf of Mexico to understand the mechanisms that control hypoxia formation. The main focus for this task force was to review and unify all the available data from scientific research and public forums on hypoxic events in the Gulf of Mexico into an adaptive management plan for mitigating these hypoxic events. The task force has identified large nutrient loading as the main concern for scientists, farmers, stakeholders, and policy makers. More specifically reduction of nitrogen loading from non-point sources in the Mississippi watershed could have the most direct effect on hypoxia formation (Mississippi River/Gulf of Mexico Watershed Nutrient Task Force, 2001). The management plan issued by the task force calls for monitoring of nutrient loading not only at the Mississippi Delta but all along the watershed basin. This will increase the data available for adequate management practices by capturing effects of non point sources.

These management practices have been implemented for over 5 years and in 2008 the task force released another Action Plan that reflects adaptations made to the previous plan from 2001. This new plan has identified areas where more action is needed and demonstrates the effectiveness of adaptive

management practices. The main realization of this new plan is that there is a need for task force action on all fronts of the action plan if the goals are to be reached by the estimated dates (Mississippi River/Gulf of Mexico Watershed Nutrient Task Force, 2008). This reassessment has shown that the goal of <5000km^2 hypoxic zone is still a reasonable outcome but the time in which to achieve this goal may be longer than previously predicted. The research performed after the 2001 Action Plan has shown that there are other mechanisms that may contribute to hypoxia formation besides eutrophication and water column stratification such as coastal upwelling (Mississippi River/Gulf of Mexico Watershed Nutrient Task Force, 2008).

The negative effects on coastal ecology that have been studied have shown that the long term occurrence of these events may have irreversible changes to the species diversity and food web dynamics of this coastal ecosystem, a phenomenon often referred to as “a change to an alternate state”. A change to an alternate state is defined as “the gradual change in environmental conditions, such as human-induced eutrophication and global warming, may have little apparent effect on the state of these systems, but still alter the “stability domain” or resilience of the current state and hence the likelihood that a shift to an alternate state will occur” (Turner et al., 2008). Studies have also found that excessive loading of phosphorous can contribute to hypoxia formation and that the reduction of both phosphorous and nitrogen are key for mitigating the extent and duration of these events (Mississippi River/Gulf of Mexico Watershed Nutrient Task Force, 2008). The reassessed action plan also acknowledges that increased awareness of the need for reductions of nutrient loading will be required to stimulate accelerated management responses by stakeholders, policy makers, and the public.

The purpose for this project is to analyze the physical and geological conditions occurring at the sediment-water interface and within the BBL by examining the erodibility and composition of the floc layer and surficial sediment on seabed, with special regards to the amounts of sediment and OM that may become resuspended under varying levels of shear stress in multiple areas across the Louisiana-Texas (LATEX) continental shelf. This study will also perform grain size analysis of surficial sediment at stations across the LATEX shelf to determine spatial variability and will also perform grain size analysis on the top 10-12cm of sediment at several specific stations to study any temporal variability. Model efforts will be

made to simulate sediment erosion, transport, and deposition across the LATEX continental shelf during the year 2005, with a special focus on Hurricanes Katrina and Rita. All of the results from the experiments and analyses conducted during this study will provide more insight into the physical conditions occurring at the sediment water interface; these insights may aid future studies that analyze the influence of these physical conditions on the biogeochemical dynamics that contribute to hypoxia formation and duration. With better knowledge of these physical and biogeochemical interactions, more advanced 3-D modeling systems can be developed that would be able to more accurately hindcast hypoxic events by coupling the physical model conditions with those of the biogeochemical models.

There are five chapters in this study, including the introductory chapter, which analyze different aspects of sediment transport dynamics in the nGOM where hypoxia is prevalent during summer months. Chapter 2 will focus on analyzing and discussing differences in the surficial sediment texture in multiple areas sampled across the nGOM hypoxic zone. Chapter 3 discusses how surficial sediment and associated organic material is eroded from the seabed in response to increasing shear stress levels applied to the sediment surface. Chapter 4 will discuss the use and application of a 3-dimensional coupled hydrodynamic sediment transport modeling system to better understand the mechanisms necessary for sediment resuspension and transport across the LATEX continental shelf system, with special focus on the effects of major hurricanes. Chapter 5 will discuss how the results from the previous chapters impact the dynamics of sediment transport and how those dynamics may affect mechanisms controlling hypoxia formation across the nGOM.

2 Sediment Grain Size across the Northern Gulf of Mexico

2.1 Introduction

Sediment grain size is an essential factor controlling sediment resuspension and transport across continental shelves. The physical oceanic forces of wind driven waves and currents affect sediment particles differently based on their size, which will determine the amount of sediment transported across a continental shelf system. All of these physical oceanic conditions must be quantified and analyzed for realistic physical modeling of sediment transport. The objective of this part of the study was to measure and analyze sediment grain sizes spatially and temporally in this region for integration into a hind-cast physical sediment transport modeling system. Initial observations suggest that sediment grain sizes are finer in areas in closer proximity to major river mouths compared to areas on the inner shelf more distal from river mouths, such as those within the central hypoxic region (Buczkowski et al., 2006).

The sizes of sediment particles are influenced by the chemical and physical weathering processes as they are transported from land to sea. Physical, or mechanical, weathering of parent rock material results from the many processes such as: frost wedging, plant root wedging, and abrasion during transport (Friedman and Sanders, 1978). Sediment grain sizes are also affected by erosion and transport processes such as sliding, rolling, and saltation from wind, water, or glacier movement which can cause particles to collide and break apart (Jones, 1999; Wright, 1999). Chemical weathering processes of parent rock material are products of water and aqueous solutions or oxidative reactions acting on the rock material by carrying away ions which can convert some materials like feldspar into clay minerals. Chemical weathering processes result in the transformation of parent material into altered minerals which cannot be physically reconstructed where as physical weathering is just the breakdown of parent material into smaller particles. An example of chemical weathering is hydrolysis, which is the breakdown of feldspar crystals in water to form hydroxyl ions and the release of potassium; the chemical reactions break the crystal lattices of the feldspar to form smaller clay particles and metallic ions (Friedman and Sanders, 1978). These chemical weathering processes that create clay material are what lead to the formation of fine-grained particles because of clay's weak molecular structure (Stanley, 1999). Depending on the type of weathering process that affects the source material, whether it's chemical or physical,

different sedimentary products will be produced; physical weathering usually produces sediment particles that are much larger compared to chemical weathering processes that produce finer particles of sediment material (Jones, 1994).

Shear stress, as stated earlier, is a frictional force acting on the seabed to cause sediment resuspension. The top of each water layer is acted upon by a shear stress due to the layer above, which is moving faster and tending to drag it along, as well as by a shear stress due to the layer below, which is moving more slowly and tending to drag it back (Wright, 1999). These frictional forces at each level influence the amount of shear stress acting upon the sediment-water interface. At this interface water is flowing over a solid surface and is slowed down by friction along the boundary creating a current stress; the region of flow influenced by proximity to the sediment surface is referred to as the BBL (Wright, 1999).There are two distinct BBL regions that develop from combined wave and current flows: the immediate vicinity of the bottom, 3-5 cm above sediment during mild conditions and 10-30 cm layer during more energetic conditions (Grant and Madsen, 1986). The maximum force needed to overcome frictional and gravitational forces to cause resuspension of sediment particles is defined as the critical shear stress, which varies with differing sediment sizes (Kirchner et. al., 1990). Other factors, besides grain size, that influence sediment resuspension at the BBL are sediment density, sediment cohesion, seabed consolidation, seabed smoothness, wave velocity, and current velocity (Grant and Madsen, 1986). Simple models for sediment transport have been created using spatial changes in sediment grain size descriptors such as mean, sorting, and skewness as indicators for the direction of sediment transport. These models are based on transfer functions that take into account sediment size and transport process energy such as those proposed by McLaren and Bowels (1985). Based on their model the distributions of sediment in transport are related to their source by a sediment transfer function; their sediment transfer functions define the probability that a grain within each particular sediment size class will be eroded and transported. These functions indicate that as grain size decreases, the probability of transport for that grain increases (McLaren and Bowels, 1985).Their transfer functions were derived empirically from flume experiments that illustrated with decreasing energy from high energy regimes deposited sediments from transport may become coarser, better sorted, and positively skewed; however, if starting with a low energy regime that then decreases the deposits may become finer, better sorted, and negatively skewed

(McLaren and Bowels, 1985). Complications can arise with the models as some sediment types, particularly fine-grained sediments, tend to be cohesive due to electrostatic attractions between grains. These fine sized particles tend to aggregate into larger particles that will require higher shear stress levels to cause resuspension (Mehta et al., 1989). This point is supported and illustrated by Hjulstrom's diagram, which graphs the average current velocities needed to resuspend these types of consolidated particles, as well as larger ones (Hjulstrom, 1935). Hjulstrom's diagram illustrates how finer sediments comprised of clayey and silty material will require higher current velocities in order to be resuspended due to cohesion; though as grain size increases lower current velocities are able to resuspend sediments until the grain sizes become too large thus requiring higher velocities for resuspension. The resulting curve of erosion velocity follows a 'U' shaped pattern going from fine grain sizes to larger ones. The grain size, shape, and cohesiveness of the sediments also influence the permeability and porosity of the seabed. Finer grained sediments tend to have lower permeability than larger grained sediments due to increased grain packing and consolidation (Shepard, 1989). The settling of the sediment particles of differing sizes will influence the shape of seabed smoothness which plays an important role in setting up adequate bottom boundary fluid dynamics that allow for sediment resuspension and transport. The differences in seabed smoothness may influence the current flow at the sediment-water interface which can cause it to become turbulent or laminar (Wright, 1999); based on the dominant flow type at the sediment-water interface, there will be varying amounts of sediment resuspension.

Understanding the physical and chemical dynamics occurring at the sediment-water interface has become a prominent area of study due to the annual hypoxic regimes of bottom waters in the nGOM. Modeling systems that can accurately hind-cast these physical and biogeochemical conditions will be an essential tool for better management and mitigating practices for these impacted areas of the gulf. Therefore, coupling a physical sediment transport model with a biogeochemical model will allow for better understanding of sediment-water interactions with hypoxic regimes that may arise from sediment and associated organic matter reintroduction into the lower water column.

2.2 Sediment Grain Size Analysis Methods

Sediment grain sizes in this study are categorized based on the Wentworth grain size scale into four size classes from largest to smallest, respectively: gravel, sand, silt, and clay; these four classes are then subcategorized allowing for more detailed distinctions (Fig. 2-1) (Wentworth, 1922). To determine spatial and temporal variability of sediment grain size across the nGOM hypoxic zone, measurements were taken over a 2 year period consisting of 5 research cruises (Table 2-1). Spatial variability analysis of seabed surficial sediments was made from the National Science Foundation (NSF) RAPID cruise during early August 2011 at the 27 stations (Fig.2-2); temporal variability analysis was conducted for all cruises but for only 4 of the 27 stations (AB5, 10B, 08C, Atch in Fig. 2-2). Sediments were collected using two different coring methods: multi-core and *Hypox* core retrieval. The diameters of all cores were 10 cm and the lengths were between 50 and 60 cm. Coring methods varied for each cruise due to mechanical and technical availability, i.e. the multi-corer available only for the NSF RAPID cruise. The *Hypox* corer (Fig. 2-3) is a newly designed coring device manufactured by the Geochemical and Environmental Research Group at Texas A&M University and was used for sediment core retrieval on all other cruises during this project. The device was designed by Dr. Wayne Gardner of the University of Texas Marine Science Institute. This coring device is essential for the purposes of this study which is to analyze the sediment material at the sediment-water interface; and this device allows for the collection of intact sediment cores that preserves the floc layer as well as capturing overlying water at or just above the sediment-water interface (Gardner et al., 2009). This coring method is similar to the methods used for a multicore device in that weights allow for penetration but for only one core, the only difference is there is no firing mechanism to close the top of the core once sediment penetration occurs; a spring inside the core head allows for the top flap to remain closed throughout the deployment. This actually can cause surface water to become trapped in the core as it is lowered through the water column though some bottom water is incorporated into the core near the sediment water interface; temperature, salinity, and dissolved oxygen data collected in August 2012 supports this claim (Table 2-3). Once the sediment cores were retrieved from the seabed, subsamples of the top 6-12cm were immediately taken using a modified syringe with a 2.5 cm diameter (Fig. 2-4) and divided into 1cm sections for grain size analysis; the subsamples were bagged, labeled, and frozen for transport back to Coastal Carolina University (CCU). Grain size analyses were performed using CCU's Beckman-Coulter LS 13 320 Laser Diffraction Particle Size Analyzer for

each 1cm sample. From each sample approximately 0.5g of sediment was placed into a vial with deionized water, shaken by hand and with mechanical shaker, as well as stirred for at least 10 minutes to break all aggregates, then poured into the analyzer. This analyzer has a size detection range from 0.02µm to 2000µm diameter. The analyzer software generates an Excel file of the percent volume contributed by each sediment size class (in microns), as well as the mean grain size, median grain size, standard deviation, skewness, and kurtosis of each sample analyzed. Spatial variation analysis of surficial sediment was made using the samples collected on the NSF RAPID cruise in early August 2011. The top 6-12cm layer from the sediment cores collected on all 5 cruises (a total of 176 samples of 1-cm thick slices) were analyzed to determine temporal variability of sediment grain sizes down the sub-cores. The data generated from these temporal analyses will also be incorporated into a physical sediment transport model in the nGOM for future modeling studies.

2.3 Surficial Sediment Grain Size Spatial Variability

The spatial variation of surface sediment grain sizes was assessed for early August 2011 for most of the nGOM. Twenty seven stations (Fig. 2-2) were visited to retrieve sediment core samples for grain size analysis. Figure 2-5 shows the percent volume of grain size distributions of surficial sediment (0-1cm) for the 27 stations sampled in the nGOM. The average sediment grain size across the entire sample area is 6.31 Phi, which corresponds to the silt size class (Table 2-2). The grain size distributions are divided into three regions: East of Terrebonne Bay, Mid-shelf, West of Terrebonne Bay, and are shown to have relatively similar grain size distribution across the entire shelf area (Fig. 2-5). The highest peaks for percent volume for most of the sampled stations fall within the silt size class except for two stations, 10B and S39, which both have high percent peaks falling in the sand size class (finer sand) and are known to lie within areas that have sandier sediment environments. Box plots were used to compare median and range values for each of the stations sampled for surficial sediment grain size; there is not much difference between stations within each region sampled, except for two stations just mentioned, which have median values closer to 4 Phi corresponding to sandier compared to other stations with median values between 6 and 7 Phi (Figs. 2-6, 2-7, 2-8). Spatial distribution of 4 sediment size classes (Sand, Coarse Silt, Medium/Fine/Very Fine Silt, Clay) are illustrated in figure 2-9 and corresponds well with grain

size distribution results, here stations 10B and S39 are shown to have almost 50% of surficial sediment corresponding to sandy material. Overall, there is not much variability in grain size distributions among the stations sampled in this study, except for two of the 27 stations that lie within areas of sandy seabed environments.

The mean, median, standard deviation, skewness, and kurtosis values (in Phi scale) for each surficial sediment sample analyzed are presented in Table 2-2. The standard deviation of the grain size, which is a mathematical representation of surficial sediment sorting with verbal terms provided by Folk (1966) (Fig. 2-23) based on the standard deviation in the phi scale, indicates that all the samples collected across the nGOM are poorly sorted (Table 2-2). Skewness provides insight into the grain size distribution by determining the degree of asymmetry in a resulting histogram of percent volume of grain sizes. Positively skewed samples reflect grain sizes that are skewed to the positive end of the phi scale, which corresponds to smaller grain sizes. Conversely, negatively skewed samples are skewed to the negative end of the phi scale, corresponding to larger grain particles. Over half the stations sampled were negatively skewed (-0.2-0 phi) towards coarser sediment sizes, most occurring near or south of the Mississippi delta (Table 2-2). In addition, stations sampled have a relatively wide range of kurtosis values, which indicates how widely distributed the resulting grain size histogram is. Most samples fall within the mesokurtic range of values, which represents a fairly wide distribution with no distinct peaks, while the other samples, except for 2 (10B and 08C) which are platykurtic (relatively flat), increase in kurtosis values to the leptokurtic range which indicates that there is a distinct peak present within the grain size histogram (Blott and Pye, 2001).

2.4 Down-Core Sediment Grain Size Temporal Variability

Temporal variation of sediment grain size across the nGOM hypoxic zone is an important factor to account for when trying to fully understand how sediment resuspension might impact hypoxic events. Sediment transport dynamics vary from year to year depending on prevailing weather patterns which influence riverine discharge transport cross shelf and wave/current regimes for the nGOM. To produce accurate hind-cast models of the sediment transport that may affect hypoxic regimes in this region, researchers must analyze temporal variations in surficial sediment grain size across the entire model

domain. Time series analyses of surficial sediment changes in different areas of the hypoxic region are essential for developing accurate transport models that can reflect and correlate with observed field studies within the same area and time. Also, sediment core sampling of the top 10 cm of the seabed are necessary to determine what type of sediment materials may become exposed during high resuspension events, such as hurricanes and other major storms. For this project, sediment samples were collected at 4 of the 27 stations over 2 years during 5 cruises: AB5, 10B, 08C, and Atch (Fig. 2-2), with the exception of the NSF RAPID cruise, which did not visit the Atchafalaya station (Atch).Two year time series graphs were plotted for surficial sediments (0-1 cm) histograms (Fig. 2-11) and for down core samples (Figs. 2-12 through 2-19) from each of the 4 stations. The surficial sediment distributions at stations AB5, 10B, and Atch do not vary much over the two year sampling period (Fig. 2-11). The surficial sediment distribution at station 08C does change over the two year period from silty material in April and August 2011 to sandier material in April 2012 then back to silty material in August 2012 (Fig. 2-11). This time series analysis illustrates that the patterns of surficial sediment sizes are relatively stable across the nGOM.

The subsampled sediment cores (6-12cm long) were divided into 1 cm sections and analyzed to infer changes over time of grain size distribution and mean grain size variations with depth. The mean grain sizes at station AB5, just north of the Mississippi River southwest path, correspond to silty material ranging from 5 to 7 phi (Fig. 2-12). Ranges of grain size are lowest (~5.5phi to 6.5phi) near the surface and increase (~4.8phi to ~7phi) at the 10 cm depth of the subcore (Fig. 2-12). While the mean grain size is an important factor when analyzing grain size distributions, the other indicators such as median grain size and sorting derived from the standard deviation may also reveal other patterns from the distribution. The percent volume for each down core sample was color plotted to indicate how well or poorly sorted grain size samples are as they relate to depth below the seabed surface (Figs. 2-13, 2-15, 2-17, 2-19). The sorting of each subsampled core at station AB5 as it relates to depth (Fig. 2-13) seem to be poorly sorted as indicated in the figure. The warmer colors in figure 2-13 indicate layers of the core that have higher percentage of grain sizes, which is only present near the 10 cm depth during late August 2011 and April 2012. All samples show median grain sizes within the range of silt material, illustrated by the green colors running the length of the cores between the dashed white lines.

Station 10B, south of Terrebonne Bay along the 20 m isobath, shows a mean grain size that corresponds to sandier material at the surface then changing to silty material down the core; ranging from 3 to 8phi (Fig. 2-14). The range of sediment sizes near the surface are lower but correspond to larger sized particles (sandier); sediment size ranges increase down core and show fairly similar patterns of lamination over the two year period, and the overall pattern of all 5 subcore samples is relatively similar (Fig. 2-14). Although the mean grain size corresponds to sandy material only in upper 2 cm for some samples, the median grain size for most of the samples collected for this project at station 10B fall within the range of sandy material (Fig. 2-15). The samples at 10B also seem to be well sorted in more layers compared to the samples collected at other stations.

Mostly silty material was observed at station 08C, south west of the Atchafalaya bay between the 10 and 20 m isobath, for all of the cruises except the April 2012 cruise (Fig. 2-16). The median grain size seems to fall mostly within the range of silty material for most of the samples taken at station 08C, except for the April 2012 sample (Fig. 2-17). The upper 2cm of the core from this cruise are composed of much sandier material relative to the other cruise samples and are much better sorted (Fig. 2-17). All other intervals follow a similar pattern of silty material down the core for each cruise, ranging from 5 to 8 Phi (Fig. 2-16). Mean grain sizes down the core at the Atchafalaya Bay station represent silty material, ranging from 5 to 7 Phi (Fig. 2-18). The median grain size observed for different layers at this station fall mostly within the range of silt material; the degree of sorting seems to vary at different depths during different sampling dates (Fig. 2-19).

Over the 2 year period stations AB5 and Atch show similar lamination patterns throughout each subcore sampled (Figs. 2-12, 2-18).The lamination patterns at station 10B (while overall relatively similar, exhibit a wide range in mean grain size at certain depths) suggest there may be some physical conditions that affect sedimentation and resuspension over the 2 year period or may be an artifact of subtle differences in the actual position of where the sample was collected (Fig. 2-14). These suggestions may also explain the inconsistencies with samples collected at station 08C during the April 2012 research cruise.

2.5 Discussion

Influential factors affecting spatial sediment variability on the LATEX continental shelf appear to be proximity to the major river sources in the nGOM and historic delta lobe shifts. Data from this study (Fig. 2-5) show strong correlation between surficial grain sizes measured in early August 2011 with dominant bottom types mapped in the Gulf of Mexico Data Atlas provided by National Oceanic and Atmospheric Association (NOAA) (Fig. 2-20) (gulfatlas.noaa.gov). Similarly, comparison of grain sizes from samples collected during the August 2011 NSF RAPID cruise with samples from the usSeabed database showing mud percentages (Figs. 2-21, 2-22), also shows strong similarities with our dataset (Buczkowski et al., 2006). The term 'mud' refers to sediment size classes ranging from silty to clay material and the percent is the amount of these size classes compared to larger ones, such as sand or pebble. Each of these datasets, including the present study, illustrates those areas closer to the Mississippi and Atchafalaya River mouths are composed of a higher proportion of finer grained sediments compared to more distal areas such as the area south of Terrebonne and Atchafalaya Bay. While all these datasets seem to show the same dominant sediment types for different areas of the nGOM it should be noted that the methods used in this study allow for more precise sediment analysis both temporally and spatially. The methods used for the usSeabed database are a composite of a wide variety since the data is a compilation of many different studies, which may have used methods that only account for percent fractions of sand, silt, or clay or even percent mud (as is shown in Fig. 2-22). Some studies only analyze the bulk percent of mud for the entire upper 10-20 cm of sediment whereas the present study's methods analyze the whole grain size distribution for each centimeter of the top 10 cm, which allows for observations of lamination patterns.

It has been observed that almost 95% of the sediment load from the Mississippi River travels in suspension and consists of 65% clay and about 35% silt and fine sand particles (Johnson and Kelley, 1984; Orton and Reading, 1993; Coleman et al., 1998), which coincides with this study's observation of having mean grain sizes of greater than or equal to 6 phi near the Mississippi's southwest pass river mouth. Also, the presence of sandy sediments south of Atchafalaya and Terrebonne Bay are considered to be the remnants of ancient distributaries from pre-existing lobes of the Mississippi River deltaic system (Coleman and Gagliano, 1964). This historic lobe looks to represent a merger of two historic deltaic systems that deposited sands almost 7000 years before present (Coleman et al., 1998). Data gathered

from Briggs et al. (2009) indicates that sediments gathered from an area with frequent hypoxia near the Mississippi delta is generally comprised of poorly sorted silty clay material with a mean grain size of 8.1 phi. Surficial sediment samples taken from the same area (station AB5) were shown to be poorly sorted silty materials with mean grain sizes between 5 and 7 phi. While our dataset shows a range of values larger than those from Briggs et al. (2009), there is an overall pattern of poorly sorted silty material observed for this area of the nGOM.

Proximity to river mouths will influence the consolidation of these sediment materials; newly deposited sediment materials nearer to the mouth are less consolidated due to the short amount of time since initial deposition (Xu et al., in prep). From GUST experiments (to be elaborated on in subsequent chapters) conducted at each of the stations, results indicate that areas with freshly deposited materials (i.e. those closer to river mouths) will require less shear force to become resuspended versus consolidated materials or larger sized particles. The resuspension of these less consolidated materials along with associated organic matter that has accumulated from times of high productivity during the early spring could have major impacts on the occurrence and prevalence of hypoxic events due to the reintroduction of labile material into the lower water column (Rabalais et al., 2007). Thus the spatial significance of surficial sediment grain size distribution is an important factor to consider when analyzing resuspension events that occur within hypoxic areas of the nGOM. The physical and biogeochemical interactions that occur between floc material and the underlying sediment are influenced by the properties of sediment that are associated with grain size such as erodibility, porosity, and permeability, all of which may influence bottom water hypoxia formation, prevalence, and duration. Permeability of unconsolidated sediments has been related to grain size through many previous studies by a well-known formula, $k = cd^2$. It has been shown to be statistically significant that sediment permeability increases with larger sized particles (Shepard, 1989). The sediments across the nGOM hypoxic zone have been observed to have low levels of permeability due to fine sediment consolidation; sediment porosity across this area varies with the highest value occurring nearest to the southwest pass of the Mississippi delta (Briggs et al., 2009).GUST erosion microcosm system experiments conducted at the 4 temporal stations in this study indicate that areas closest to the Mississippi and Atchafalaya River mouths are composed of less consolidated material which allows for higher permeability and more easily eroded material (refer to 3.5.1).

No considerable temporal changes were observed in the percent volume of grain sizes across the shelf, with the exception of station 08C, which suggests the temporal variability of surficial sediment grain sizes across the Texas-Louisiana continental shelf remained static for many stations sampled over the 2 year period (Fig. 2-12 through 2-19). Analysis of down core sorting of sediments shows that the four stations analyzed have similar sorting patterns over the 2 years sampling period, which suggests that there is not much reworking of sediment materials below the top few centimeters of the sediment surface, or that newly deposited material area similar to old ones. Station 08C, in the western hypoxic zone, shows a shift from silty material to sandy material in the upper 2 cm of the April 2012 samples; but by August 2012, the down core profile had returned to a particle size distribution similar to those seen in the 2011 cruises (Fig. 2-16, 2-17). This fluctuation in sediment size class distribution could have arisen from increased resuspension and transport of smaller grain sizes in April 2012; such differential transport is predicted from simple transport models (McLaren and Bowles, 1984). Another explanation is that the temporal changes reflect spatial patchiness in the sediments across the western portion of the continental shelf or even within a smaller area such as that around the station itself. While every attempt was made to reoccupy the exact coordinates each time the station 08C was visited, the odds of sampling the exact same plot of seabed material at this station remains very low, lending to the notion that these changes may be an artifact of the sampling techniques used. In addition, the return to silt mean grain size in the August 2012 samples probably suggests the August 2011 anomaly may have resulted from the sampling methods. The temporal variability of surficial sediments is an important factor to include in physical models that simulate sediment transport across continental shelf systems for multiple years. With more observational data of temporal variability in surficial sediments, more comprehensive and realistic modeling systems can be developed for hind-casting physical oceanic conditions that may influence hypoxic events.

2.6 Conclusions

This study was able to conclude that spatial variability of surficial sediment across the nGOM is not very large, depending mostly on the historic changes in the position of major deltaic lobes. The temporal variability of the 4 stations sampled in this project is harder to distinguish for some areas compared to

others. Stations AB5 and Atch seem to have relatively static lamination patterns within the top 10 cm of the sediment layers. The lamination patterns observed at station 10B seem to be relatively similar down the core but the reasoning for such wide ranges in mean grain size values at layers below the top 2cm remains uncertain. One possibility is bed armoring, the process of winnowing of fine grained materials and thereby the protection from leftover coarse grained sediment near seabed. The changes in lamination patterns observed in April 2012 for station 08C is thought to be an artifact arising from differences in sampling techniques, i.e. exact location positioning, due to the return to similar lamination pattern in August 2012, which may also just be a reflection of spatial variability around the edge of the historically sandy area below Atchafalaya Bay. Overall the temporal stability of sediments at these four locations also seems to be static and with more sampling data the anomalies observed in this study may be rectified.

3 GUST Erosion Microcosm System Experiment for the Northern Gulf of Mexico

3.1.1 Sediment Impact on Hypoxia

There has been speculation, as stated earlier, that these annual hypoxic events are causing or have caused a change to an alternate state for this environment (Turner et al., 2008). Turner et al. (2008) explains that because the threshold for hypoxia has been decreasing continually, it may be reaching its geomorphological limit (>25,000 km^2) due to physical constraints of geometry of the northern LATEX shelf; the return to a previous state for this environment thus becomes much more difficult. Further explanation states that the longer nutrient loads into the gulf remain constant or increase overtime, the larger annual accumulation of OM will lead to an increase in sediment oxygen demand (SOD) (Turner et al., 2008). SOD is defined as the demand of oxygen due to biological respiration or chemical processes which take up oxygen. An increase in SOD is described to be caused from the large accumulation and delayed consumption of OM from previous years which may influence the dynamics of subsequent hypoxic events. Some studies have indicated that SOD attributes up to 73% of the total oxygen consumption in hypoxic bottom waters (Quinones-Rivera et al., 2007); however more recent studies have shown that SOD may only contribute up to 20% of the total below-pycnocline respiration (Murrell and Lehrter, 2010). SOD is exacerbating the effects of already excessive nutrient loads coming from the two river systems; this increased SOD is described to cause a greater sensitivity to hypoxic events in the years after 1999 with the same amount of nutrient loading as before 1988 (Turner et al., 2008). The focus of this study will be to evaluate how much accumulated OM and seabed sediment can be resuspended in different areas of the gulf region hypoxic zone. Studies modeling the relationships between frequencies of resuspension events and mineralization indicate that as resuspension events increase in frequency there is less mineralization in surficial and deep sediments and increased mineralization in the water column (Wainright and Hopkinson, 1997). Wainright and Hopkinson (1997) illustrate the important effects resuspension has on the sites and rates of OM processing on coastal shelf areas. Their study also demonstrates that the potential effects of resuspension on oxygen demand in the water column at the sediment-water interface are quite large during summer resuspension events because of increased respiration rates (Wainright and Hopkinson, 1997). These effects of resuspension events on bottom water

oxygen dynamics have not been studied extensively for this hypoxic region of the nGOM before. As stated earlier there have been studies on SOD in this area but none on the changes in oxygen consumption under the impacts of a resuspension event, especially with major emphasis on the floc layer observed at the sediment surface. Since the floc layer is mm to cm thick, regular sediment sampling techniques are unable to extract the floc layer appropriately. The purpose of this study is to quantify the amounts of organic material that may become reintroduced into the lower water column which may affect the respiration rates occurring within the BBL. Thus the effects of increased water column mineralization and increased respiration rates during summer coupled with resuspension events should be studied to help investigate the mechanisms that control bottom water hypoxia in the nGOM.

3.1.2 Field Studies of the Sediment-Water Interface

The BBL, as discussed in the previous chapter, is an important zone for the alteration, decomposition, and transport of sediments and organic materials across continental shelf systems. There are many physical factors that influence the BBL and control particle resuspension and transport across continental shelves such as waves, tides, currents, particle size, sediment density, seabed erodibility, biofilm, and OM content (McKee et al., 2004). The combination of these processes is what influences the frequency of resuspension events which can have impacts on the diagenetic reactions that occur in surficial sediments; thus physical sediment dynamics are extremely important for understanding geochemical reactions taking place in the BBL (McKee et al., 2004). Other studies using the GUST system by Dickhudt et al. (2009) have shown the presence of organic matter enrichment in material eroded at lower shear stresses compared to the material eroded at higher levels of shear stress. This lends credit to the assumption that studies of the physical and biogeochemical interactions at the sediment-water interface are critical for understanding what mechanisms may be controlling bottom water hypoxic regimes in the nGOM. Recently it has been observed that the concentration of organic material within the top 20cm of sediment is relatively low, less than 1.5% of total dry weight was organic carbon for the type of sediment environment being studied (silty material) (Reese et al., 2012). This study has also shown that there are distinctly different populations of bacteria occurring just above the sediment-water interface from those directly below the sediment-water interface; which lends to the notion that the organic material within the

floc layer and just below may not be the same type of material occupying the overlying BBL. Since 1) these low concentrations of organic matter are also observed for the top 5 cm of the sediment surface (Reese et al., 2012) and 2) sedimentation rates for areas just west of the SW pass of the Mississippi River are on the scale of around 0.62 cm $year^{-1}$ (Santschi et al., 2001), which is consistent with the 1993 modeled seabed elevation changes from Xu et al. (2011), having methods that allow for much smaller scaled studies (micro to millimeter scales) becomes vital for developing more accurate hypotheses for the roles of SOD and resuspension events in controlling hypoxic regimes. These observations indicated that sediment oxygen dynamics that may influence hypoxic events are confined to the top most 1-2 cm of the sediment surface; our study with the GUST erosional microcosm system allows for even greater refining of these observations to a millimeter scale. The biogeochemical processes occurring in the sediment-water interface and how they may change based on physical changes within the BBL have already been shown by previous studies to be of critical value when trying to model these interactions (Boudreau and Jorgensen, 2001).

3.1.3 The Need for Numerical Models

Analyzing each of the factors discussed above is essential in order to develop accurate and comprehensive physical oceanic modeling systems. These modeling systems are used by scientists to inform policy makers on the physical conditions of areas like the nGOM where there are important established fisheries that may be in jeopardy due to the increase of annual hypoxic events. Understanding the physical and biogeochemical dynamics that are necessary for the formation and maintenance of hypoxic events is critical to the efforts of mitigating the effects of these annual events in this region. Thus there is a need for modeling systems that can incorporate physical conditions with biological and geochemical dynamics occurring in these areas, which has become the focus of many research groups over the past decade. Separate models for physical oceanic conditions and biogeochemical dynamics occurring in this annually hypoxic region of the nGOM have already been developed by the Mechanisms Controlling Hypoxia (MCH) research group funded by the National Oceanic and Atmospheric Administration. A physical hydrodynamic model using the Regional Ocean Modeling System (ROMS) was developed by Hetland and DiMarco (2008) to study oxygen dynamics

within a physical modeling system for the nGOM where hypoxia is prevalent. Other studies have coupled this physical model with a simple biological model of nitrogen cycling to show that these coupled models are in agreement with observations and may predict rates of primary production and grazing that agree with experimentally determined rates (Fennel et al., 2011). The success of these coupled biological and physical models lends credit to research that has tried to further develop each type of these models to include more parameters such as sediment dynamics. One such development with this hydrodynamic model was made by Xu et al. (2011) which integrated sediment discharge from the Mississippi and Atchafalaya Rivers and sediment transport across the LATEX continental shelf. Other coupled models (Harris et al., 2013) are in development, one of which couples the Community Sediment Transport Modeling System (CSTMS), developed by Warner et al. (2008), with a biogeochemical model within the ROMS from Fennel et al. (2011); figure 3-1 illustrates the processes that are included in this coupled biogeochemistry-sediment transport model (Harris et al., 2013). There have been many simple models developed to hindcast, nowcast, and forecast the areal extent of hypoxia, as well other 3-D models used to study the physical, chemical, and biological mechanisms that may be associated with hypoxic events in the nGOM. The development and refinement of each of these types of models and their respective parameters is essential for a more complete picture of the mechanisms controlling hypoxia regimes in this area of the gulf.

3.2 Objectives and Hypotheses

The purpose of this part of the study is to develop and use methods to determine how much sediment and organic material is eroded from the seabed in certain regions of the nGOM using the dual core GUST erosion microcosm system for integration into future models that incorporate hydrodynamic-sediment transport with biogeochemistry. The main objective for these GUST experiments is to measure sediment erodibility and determine the amount of total suspended solids (TSS) eroded from sediment cores under increasing levels of shear stress that were collected from different sites in the nGOM hypoxic region; the resulting data will help to validate 3-D model simulations developed to hindcast, nowcast, and forecast annual hypoxic events. Erodibility refers to how easily material from the seabed surface may be eroded and resuspended into the water column under different levels of bed shear stress. The erodibility curves

produced from previous GUST experiments only account for TSS, which are then integrated in the coupled hydrodynamic-sediment transport models; the objective of the GUST experiments performed in this study is not only to determine the amount of TSS resuspended but also the amount of volatile suspended solids (VSS) resuspended, which can serve as a proxy for organic matter that may be reintroduced into the lower water column. Initial observations from previous GUST experiments (Xu et al., in prep) and literature (Dickhudt et al., 2009; Rowe et al., 2002) suggest that during resuspension under increasing levels of shear stress applied in sequence to a single core, concentrations of VSS will be higher at the lower shear stress levels, representative of a floc layer, than concentrations at higher shear stress levels. Therefore, determining how much organic material is present within the floc layer will be an important factor for future model development that couples sediment transport dynamics occurring at the BBL with biogeochemical processes occurring at the sediment-water interface.

3.3 Materials and Methods

3.3.1 Study Sites

Dual core GUST erosion microcosm experiments were carried out across the nGOM hypoxic zone over a 2 year period during 5 research cruises (Table 3-1). Experiments were conducted at 4 stations, AB5 (eastern hypoxic zone), 10B (middle hypoxic zone), 08C (western hypoxic zone), Atch (Atchafalaya Bay), across the nGOM during cruises in April and August of 2011 and 2012 (Fig. 3-2). In Mid-August of 2011, GUST erosion microcosm experiments were conducted at several other different locations across the nGOM for the NSF RAPID project but only data from the 4 stations previously stated were analyzed for this study. Although all of these experiments were performed for the same project, the other 22 GUST experiments from other stations are being analyzed and described in another publication in preparation by K. Xu et al.

3.3.2 Sediment Coring

The main challenge for the GUST experimental setup is to obtain sediment cores with preserved floc material at the sediment-water interface. Over the 2 year study period many different coring devices were used, methods include: *Hypox* corer, box corer, and multi-corer (Figs. 3-3, 3-4, 3-5). The same coring

method was used for the part of the study as those stated in section 2.2 and the challenges associated with capturing surface water are still present. Therefore, water in the upper part of the core might be representative of the surface or mid water column but water associated with the sediment-water interface is 'actual' bottom water retrieved within the core as indicated by salinity, temperature, and dissolved oxygen measurements (Table 3-2). This should not impact the erodibility measurement much as water is spun out of the core during the first two steps of shear stress application; however OM data from the first 2 steps of shear stress application might represent a mixture of water from the upper column and water from the actual sediment-water interface.

Two sediment cores, regardless of coring method, were collected once during a 24 hour period at each station for cruises in 2011 and collected twice during a 24 hour period at each station for cruises in 2012. The sediment cores were collected from the seabed, brought on deck, and fixed with a plastic plunger so that the sediment surface was 10 cm from the top of the plastic core (Fig. 3-7). The cores were then sealed on the bottom using the appropriate plunger and cap provided for the GUST system and then temporarily capped on top so that no water was lost while being transported from the deck to the ship's lab. Care was taken during transport so that there was little to no disturbance of the floc layer on top of the sediment surface. Once the sediment cores were in the lab, they were placed into the core holders of a modified bin (Fig. 3-6) so that the cores were held steady throughout the entire experiment.

3.3.3 GUST Erosion Microcosm System

The dual core GUST sediment erosion chamber system (Gust and Muller, 1997) was used at 4 stations in the nGOM to measure sediment erodibility. The entire GUST system (Fig. 3-6) consists of a laptop, power control box (Green Machine), two turbidimeters, Fluid Meter Inc.(FMI) pump controller, FMI pump, two rotating motors, two erosional heads, two sediment cores, source water, collection bottles, and a suction filtration system; a map of water and signal flow for the system is illustrated in figure 3-7. Two cores with motors, heads, hoses, and turbidimeters are used to ensure replicates in each experiment performed; this ensures that incase one core system malfunctions during the experiment the entire dataset is not lost or compromised. The laptop serves as the major controller for the entire system and is connected through a USB hub to the turbidimeters and the power control box. The pump, sediment cores, and turbidimeters

are connected through a series of water tubes which allow source water to be pumped through the sediment cores, then into the turbidimeters, and finally into collection bottles which will be filtered and analyzed for TSS and VSS. The rotating motors are attached to the erosional heads through magnetic-coupling disks which allow the erosional head to rotate at the same speeds as the rotating motors (Fig. 3-7). The rotating motors are controlled from the laptop and spin at rates that equal certain shear stresses when given a certain water temperature, measured in degree Celsius from thermometer placed in source water (temperature changes throughout experiment were minimal <1^{o}C). The spinning rate (rotations per minute) needed to reach a certain shear stress at a given water temperature is calculated by the Green Machine, which allows for precise control of spinning rates and therefore shear stresses applied to the sediment surface within the core. Source water for experiments conducted in April and August of 2011 was collected from the ocean surface using a bucket. After reevaluation of field methods used in the 2011 cruises changes were made to the methods in order to replicate more accurate field conditions; therefore source water for the experiments conducted in 2012 was collected using the Conductivity, Temperature, and Depth (CTD) Rosette recorder from 1 m above the seabed and transferred into several five gallon buckets for use in the lab. Once the sediment cores were retrieved and fixed, the entire system connected, and enough source water collected the experiment was conducted. The experiment requires that water be pumped into the sediment cores on the sides at a rate consistent with the shear stress being applied because the physical conditions developing inside the core cause water to be pumped out from the top center of the core (Fig. 3-9). As water is being pumped through the cores, the shear stress being applied from the rotating heads causes sediment to resuspend; this effluent material is carried out of the top center of the core and into the turbidimeters for a turbidity measurement, and then collected in a labeled plastic bottle. For these experiments there were a total of seven different shear stress levels (measured in Pascal, Pa) applied in succession to the sediment core: 0.01, 0.05, 0.1, 0.2, 0.3, 0.45, 0.6 Pa respectively; the experiment begins at the 0.01 Pa shear stress level and then after 20 minutes it is increased to the next level until the last level has completed. The amount of water and particles collected during the 20 minutes for each shear stress were measured in milliliters and then filtered, using the suction filtration system, onto a pre-weighed, numbered 142 mm wide binder-free borosilicate glass fiber filter with a 0.7 µm pore size. Before the cruises all filters were dried in an oven at 60^{o}C overnight then

weighed to get a blank filter weight (in grams). Once all collected water samples were filtered, the filters were wrapped in tin foil, labeled, and frozen for transport back to CCU. TSS analysis was performed on all samples by drying the wet filters in a drying oven at 60^{o}C overnight, weighing the filters, and then subtracting the blank filter weight, the net weight is then divided by the volume of water in the labeled plastic bottle to determine the amount of material resuspended at each shear stress level in milligrams per liter. Further analysis on these samples to determine the amount of VSS was performed through loss on ignition of the dried filter samples. Dry filter samples were burned in a muffle furnace at 500^{o}C for at least 4 hours, and then weighed again to determine how much material was lost on ignition; subtracting the burned weight from the dry weight and dividing by the volume determines the amount of VSS in terms of milligrams per liter. The VSS analysis only exist for samples from the April 2011, April 2012, and August 2012 cruises; time constraints immediately after the NSF RAPID and August 2011 cruise prevented VSS analysis.

3.3.4 VSS Background Removal

There are two types of background removal needed in this study. One for varying methods of source water sampling between cruises in April 2012 and August 2012 to account for background levels of VSS from the source water collected. In April 2012, only 1 L of source water was analyzed for VSS during each experiment at each station; whereas in August 2012, 1 L of source water was analyzed at 3 different times during each experiment: 0 min, 60 min, and 120 min. However, some background levels of VSS for source water samples were observed to have higher concentrations than some of the water samples collected throughout the experiment (Table 3-4; Figs. 3-19, 3-22, 3-25); this complication is thought to be due to the settling of TSS in the bucket throughout the GUST experiment, however uncertainties still exist. Therefore, the background level of VSS concentration in the source water was accounted for by subtracting the lowest concentration of VSS measured during the experiment from all other collected samples at the different shear stress levels. This method assumes since all shear stress water samples in each experiment are collected from the same source water, the lowest VSS concentration observed during the experiment should account for background VSS at all shear stress levels. The other method of background removal was used to account for some background VSS coming from the blank filters which

was averaged to be 0.01 grams from a total of 8 blank filter samples with a standard deviation of 0.0011g; the percentage of VSS weight from the blank filter accounts for an average of 35% of the total VSS weight with a standard deviation of around 16.5%. All data measurements reported in this study account for these background levels of VSS.

3.3.5 Turbidimeter Data Analysis

Erodibility profiles that plot the amount of eroded mass (kg/m^2) that become resuspended from the seabed under increasing levels of critical shear stress were developed by combining the TSS data and turbidity measurements using formulations and methods provided by Sanford and Maa (2001) and by Dickhudt et al. (2009). Formulations for determining the erosion rate of fine grained sediment in microcosm experiments, such as the GUST system, were developed by Sanford and Maa (2001) and Sanford (2006). The formulation used by Dickhudt et al. (2009; 2011) and in this study to determine E is written as:

$$E(m,t) = M(m)[\tau_b(t) - \tau_c(m)]$$

Where *E* is the erosion rate, *M* the depth-varying erosion rate ‘‘constant’’, $\tau_b$the stress applied to the bed, and τ_c the depth- varying critical stress for erosion. If one locally assumes τ_c increases linearly with the depth of erosion, this formulation allows a simple exponential decay of *E* with time to be fit to eroded mass observations for each period of constant applied shear stress, it is then straight forward to solve for τ_c (m) (Dickhudt, 2008; Dickhudt et al., 2011).

3.3.6 Statistical Analysis

Statistical analyses performed for this project to determine if the VSS concentrations measured at each shear stress are significantly different at 3 of the sites (AB5, 10B, 08C) sampled during this project. Orthogonal polynomial contrasts were used to determine if the log transformed mean VSS concentration measured at each shear stress are defined by a linear or quadratic fashion and are the concentrations significantly different at each site sampled. This contrast method was chosen, based on consultation with Dr. Geaghan of the Louisiana State University’s Experimental Statistics Department, because the factors tested (shear stress and VSS) are ordered in a sequential manner.

3.4 Results

3.4.1 Erodibility Profile from GUST Experiment

The GUST erosion microcosm system was used to determine the erodibility of seabed sediments at the 4 stations sampled in the nGOM. Erodibility profiles illustrate the amount of eroded material that becomes resuspended from the sediment surface within the GUST sediment core at different levels of shear stress. Since the shear stresses were applied in sequence, a cumulative curve of eroded mass is calculated and graphed to illustrate the erodibility profile for the station sampled (Figs. 3-14, 3-15, 3-16, 3-17).

Turbidity results from the GUST erosion microcosm experiments for each station in 2011 show that overall across the nGOM hypoxic zone seabed erodibility is higher in the April (spring) sampling period compared to the August (summer) sampling period (Fig. 3-12); these results are expected due to more energetic wind patterns observed for the April sampling period(Fig. 3-10). Similar turbidity results are observed for the 2012 spring and summer sampling periods (Fig. 3-13) due to the same observable wind patterns (Fig.3-11). There are much higher turbidity values and TSS concentrations when shear stress values reach above the 0.4 Pa as indicated by the high peaks around the 100 min mark of the experiment (Figs. 3-12, 3-13). The erodibility profile for Station AB5 in the eastern hypoxic zone of the nGOM illustrates that sediment in this area is fairly consolidated but considerable resuspension occurs during levels of shear stress greater than 0.4 Pa (Fig. 3-14). The profile for Station 10B (Fig. 3-15) in the middle hypoxic zone shows that sediments in this area are less erodible based on eroded masses compared to the sediments at the eastern (Fig. 3-14)and western stations (Fig. 3-16).The erodibility profile for Station 08C(Fig. 3-14) in the western hypoxic zone illustrates erodibility patterns similar to the eastern Station AB5.There were only a few data sets from the Station Atch within the Atchafalaya Bay but it was observed to have the highest range of eroded masses (Fig. 3-17) for resuspended seabed material compared to all other stations sampled.

3.4.2 Total and Volatile Suspended Solid Analysis from GUST Experiment

The TSS and VSS analyses were conducted for samples collected during the April 2011, 2012, and August 2012 cruises. The TSS analysis shows that the highest concentrations of eroded materials occur

during the highest applications of shear stress (Figs. 3-18, 3-21, 3-24). The highest concentrations of VSS occur during the application of the 0.01 Pa and 0.6 Pa shear strengths at all three stations but were not considered significantly different from each other for any of the stations sampled (Figs. 3-19,3-22,3-25). It was observed that the VSS concentrations at the three stations tested (AB5, 10B, 08C) followed a quadratic fashion based on orthogonal polynomial contrast. VSS concentrations at station AB5 were observed to be significantly different only between the lowest (0.01 Pa) and middle shear stresses applied (0.05-0.3 Pa), as well as for the highest (0.6 Pa) and the middle shear stresses (0.05-0.3 Pa) (Table 3-4). At Station 10B there was only a significant difference between VSS concentrations from the 0.01 Pa shear stress application and the shear stress applications of 0.1-0.45 Pa (Table 3-5). At Station 08C, VSS concentrations differed significantly between the 0.01 Pa shear stress application and the shear stress applications 0.05-0.45 Pa; the VSS concentrations at 0.6 Pa differed significantly only from the shear stress applications 0.2-0.3 Pa (Table 3-6).The overall highest TSS and VSS concentrations temporally are observed in August 2012 for all three stations, except for a high concentration (125 mg/L) at Station AB5 during April 2012. The percentage of VSS from TSS values indicate that the concentration of VSS is much higher during the applications of the lower shear stress levels at each of the stations, represented by higher percentage values (Figs. 3-19, 3-22,3-25). The VSS concentrations at Station AB5 during the lowest shear stress and highest shear stress are strikingly similar but the percentage of VSS is slightly higher at the lower shear stress level compared to the highest (Figs. 3-18, 3-19). This same pattern of similar VSS concentrations at the lowest and highest shear stress but with unequal percentages is also observed for both the middle hypoxic region and the western hypoxic region stations (Figs. 3-21, 3-22, 3-24, 3-25).

3.5 Discussion

3.5.1 Erodibility Profile Variability from GUST Erosion Microcosm Experiment

The erodibility profiles derived from the GUST erosion microcosm experiments conducted at the 4 sample stations indicate that there is temporal and spatial variability within the nGOM when analyzing sediment erodibility. The profiles from 4 sample stations (Figs. 3-14 through 3-17) illustrate that the middle hypoxic zone, Station 10B, is the area with the least erodible seabed overall both temporally and spatially. This is

expected due to the nature of sediments located in this area of the nGOM which is composed mostly of sandy material in the upper few centimeters of the seabed. The presence of sandy sediments south of Atchafalaya and Terrebonne Bay (middle hypoxic zone) are thought to be the remnants of ancient distributaries from pre-existing lobes of the Mississippi River deltaic system (Coleman and Gagliano, 1964), as discussed in Chapter 2. The erodibility profile of the eastern hypoxic zone station (Fig. 3-13) is indicative of an area with materials that are much more easily eroded compared to the middle hypoxic zone. Depending on proximity to river mouths the consolidation of these sediment materials will vary, newly deposited sediments closer to the mouth are less consolidated (Xu et al., in prep). The sediments in the eastern hypoxic zone and those within the Atchafalaya Bay are comprised of poorly sorted silty material that were freshly deposited from the southwest pass of the Mississippi River and Atchafalaya River respectively, compared to the center shelf areas of the nGOM. Due to shorter residence time since deposition these materials are not as consolidated as other areas and may require lower shear stress levels for resuspension; this is evident when comparing the range of eroded masses at the 0.4 Pa for the entire 2 year period of sampling (Figs.3-29).

The temporal variability in eroded mass values at 0.4Pa from Stations AB5 and Atch indicate that there may be a seasonal pattern of higher erodibility in the April cruises (spring) and lower erodibility in the August cruises (summer) (Figs.3-29). This seasonal pattern falls in line with the energetic wind patterns that occur during the April cruises in 2011 (Fig. 3-10) and 2012 (Fig.3-11), which had moderate waves that can induce a more energetic BBL and thus increase the number of resuspension events occurring at the sediment surface. These resuspension events agitate upper seabed material and thus make the seabed more prone to erosion during lower level resuspension events that may occur later. The eroded mass values at 0.4 Pa for the western hypoxic station (Fig. 3-29) have a similar seasonal pattern of erodibility when compared to the eastern hypoxic area and have a similar range of values for eroded masses calculated in April of 2011 and 2012; however the August ranges of values is not as similar even though the seabed material at this station is comprised of poorly sorted silty material, similar to the eastern hypoxic area. During other cruises, the NSF RAPID project in August of 2011 and process cruises in April 2010, researchers conducted GUST erosion microcosm experiments and showed that these and adjacent areas have high variability in erodibility spatially across the nGOM (Fig. 3-27) (Xu et

al. in prep). These two studies have datasets that were analyzed by K. Xu et al., the April 2010 data are from the MCH project for which this current study was done and data the NSF RAPID project will be used for another publication, Xu et al. in prep. The datasets from these previous and current studies of GUST experiments indicate that sediments nearer to major river deltas are less consolidated than those on the outer, central continental shelf where the majority of hypoxic events occur. The studies also indicate that sediment erodibility seems to be higher during the April (spring) period compared to August (summer) periods, which are related to the more energetic wind and wave conditions associated with the varying seasonal patterns. When comparing all of these data sets in the nGOM to other studies of sediment erodibility done in the York River estuary by Dickhudt et al. (2009) (Fig. 3-28 taken from Xu et al. in prep), it becomes observable that sediments in the nGOM are much more consolidated than those within the York River estuary. This is expected however due to the nature of the areas being sampled where our study looks at sediment erodibility of a continental shelf system versus looking at sediment erodibility within an estuarine system that would be composed of newly deposited sediment in the turbidity maxima of a shallow river estuary in Chesapeake Bay.

3.5.2 Volatile Suspended Solid Analysis from GUST Erosion Microcosm Experiment

The high concentrations of VSS during the lowest shear stress applied are thought to be indicative of a floc layer that is rich in organic material and extremely erodible (Wainright and Hopkinson, 1997; Rowe et al., 2002; Dickhudt et al., 2009); or indicative of OM-rich material from water column, a problem induced by the trapping of water during seabed penetration with the *HYPOX* corer. From initial observations it was hypothesized that the floc layer present above the sediment within these sampling areas would be indicated as a high VSS concentration in effluent samples collected during the 0.01 Pa shear stress applications as well as a higher percentage value of VSS from TSS. The results from our dataset show that this hypothesis is in line with the observations made during these GUST erosion experiments. It should be noted however that during core retrieval the amount of overlying water within the cores is only partially representative of bottom waters (Table 3-2); though because we remove all but the bottom 10 cm of overlying water from the sediment core it is assumed that the water present at the beginning of the experiment is actual bottom water or a mixture of bottom waters and upper column water.

The amounts of TSS that may be eroded from the seabed in the nGOM depend on the supply of organic material to the seabed (related to primary productivity) and the sediment environment on which they are deposited (sandy environment versus muddy environment). Mitra and Bianchi (2003) measured values for TSS in the lower water column during the month of April 1999 between the Mississippi River Southwest Pass delta and the 20m isobath southeast of Terrebonne Bay. They observed TSS concentrations in the bottom waters similar to those observed during the 0.1-0.3 Pa shear stress applications and from source water measurements (Figs.3-20, 3-23, 3-26; Table 3-3). The TSS values observed during these shear stress applications are thought to be mostly representative of background levels since there is very little material eroded from the sediment surface. Most of the other TSS values observed in this study are much greater than those observed by Mitra and Bianchi (2003) but this should be expected due to the resuspension of material in our experimental methods versus just looking at TSS values from the water samples within the lower water column used in their study; also differences in actual BBL conditions may account for some differences in values.

The VSS concentrations observed at these sample locations also seem to depend on the prevailing seasonal weather patterns, as was indicated in the erodibility profiles. During the April cruises, which occurred during times of energetic wave action, lower concentrations of VSS were observed at the lower shear stress levels overall compared to concentrations observed for August cruises (Figs. 3-21, 3-24, 3-27). This is expected due to the increased wave/current activity setup at the BBL which will increase the residence time of finer, less dense organic material within the water column. Less deposition of detrital material and fine particulate OM decreases the depth of the floc layer present above the sediment surface, which may be observed as the lower VSS concentrations when compared to the August cruises. The seasonality of changes in the amounts of VSS being deposited to the sediment surface is an important factor to account for when developing modeling systems that incorporate sediment transport mechanisms and biogeochemical dynamics occurring throughout the water column. Quantifying such changes has proven challenging but beneficial in the aspects of developing accurate modeling systems that can hind-cast physical/biogeochemical conditions observed before and during annual hypoxic events.

3.6 Conclusions and Future Work

Based on the data collected during this study there appear to be seasonal and spatial patterns influencing the composition and erodibility of seabed materials within the nGOM hypoxic zone. Overall seabed sediment across the northern LATEX continental shelf are fairly consolidated and erodibility appears to depend on proximity to major river deltas; where 'freshly' deposited materials nearer to the river mouth are less consolidated and more erodible compared to areas of the inner shelf. The sediment composition present in different areas of the nGOM also influence the erodibility of seabed material; such as areas like the sand sheets south of Terrebonne Bay which are less erodible than areas nearer to the Mississippi and Atchafalaya delta. The concentrations of organic material (VSS) that may be eroded seem to be highest within the floc layer of the seabed and then decrease until times when shear stress levels reach to or above 0.4 Pa; however, the percentage of VSS from TSS decreases by almost half, 20% during 0.01 Pa to 10% during 0.45-0.6 Pa. While observably there are higher concentrations of VSS within the floc layer, the lability of this material has yet to be determined. Conducting biochemical oxygen demand analysis on filters of TSS could give some indication on the lability of the organic material being resuspended from the seabed, with distinct focus on samples representing the floc layer. Performing these types of analysis will also shed some light on how much buried (within top 1-2 mm) organic material may play a role in SOD and hypoxic regimes of the lower water column. As stated earlier, other studies (Reese et al., 2012) have shown that there are very different microbial communities occurring just above the sediment-water interface from those just below the sediment surface, as well as low concentrations of organic material within the top few centimeters of the sediment surface. Our study will hopefully give some indication as to the amounts of organic material present at and just below the sediment water interface which may indicate whether this material is labile and processed by many different microbial communities or whether the material is refractory and therefore not a primary source of aerobic respiration by bacteria. Also, altering the *Hypox* corer with a firing mechanism to allow the collection of more overlying water from the BBL would better enhance the replication of accurate field conditions within the sediment core and give better representation of the amounts and composition of materials within the floc layer that may resuspended during low level resuspension events.

4 Hydrodynamic and Sediment Transport model for 2005 using Regional Ocean Modeling System

4.1 Introduction

4.1.1 Hypoxia for 2005 in Northern Gulf of Mexico

The nGOM has been prone to seasonal hypoxia for over 3 decades and is now thought to be an alternate state environment because of annual hypoxia (Turner et al., 2008). Influences by major storm events can drastically affect the extent and duration of hypoxic events by disrupting stratification and re-oxygenating bottom waters, therefore modeling systems that can appropriately hindcast these events and the biogeochemical dynamics that occur post storm are critical for a more complete understanding of hypoxic regimes in this area. During the hurricanes, buried organic matter can be resuspended and moved back to seabed for late usage of respiration. Both maximum erosional depth during the peak of hurricanes and deposition post storm are highly relevant to the reestablishment of subsequent hypoxic events. For the year 2005, the areal extent of hypoxia was just below the long-term mean with an estimated area around 11,000 km^2 (Fig. 4-1) (Rabalais et al., 2006), however this area was affected by many major storms during the summer months such as Hurricanes Katrina and Rita. The overall extent of the hypoxic area for the year 2005 (Fig. 4-2) was quite patchy compared to the areal extents of previous years that were not affected so much by major storms, allowing for more continuous coverage across the nGOM (LUMCON, gulfhypoxia.net). The largest area of hypoxia for the year 2005 was found off the southwestern coast of Louisiana in early July but was disturbed by a series of storm events (Hurricanes Cindy and Dennis). Hypoxia was reestablished and then disturbed again as Hurricane Katrina came through at the end of August; hypoxia was reestablished but mostly in shallow waters until storm fronts and Hurricane Rita came through the area to dissipate hypoxia for the rest of the year (Rabalais et al., 2006). While the main drivers of hypoxia in this region are the combined effects of nutrient loading and water column stratification, researchers have become more interested in observing/modeling the actual dynamics taking place that lead to hypoxia versus just analyzing historical nutrient loading trends. This has led to the diversion in research that is associated with observational/experimental studies and

modeling studies; therefore, collaboration efforts have been made and maintained overtime to lead to better understandings of the hypoxic regimes for this area.

4.1.2 Coupled Hindcast Models for the Northern Gulf of Mexico

Since these hypoxic events have become an annual occurrence over the past few decades, efforts to determine the mechanisms controlling the extent and duration of these events have become a major area of study. One of the most useful tools for studying these mechanisms, as stated earlier, are modeling systems that nowcast, hindcast, and forecast physical, chemical, and biological dynamics occurring in this area prone to annual hypoxia. The modeling systems are used to inform policy makers on what appropriate management actions should be taken in order to mitigate these annual hypoxic events. Three-dimensional simulation models and simple statistical models are the two main types of models that use physical conditions, biogeochemical dynamics, or a coupling of both, to determine what the areal extent for hypoxic events may be under certain conditions (Justic et al., 2007). Reviews of these many types of models have led researchers to the conclusion that both types are necessary for a complete view of the mechanisms that influence hypoxic events due to the different aspects of physics, chemistry, and biology of each model (Justic et al., 2007). Complex 3-D models have been developed in many ways by many different researchers to simulate different conditions that occur on the LATEX continental shelf. Both Wang and Justic (2009) and Hetland and DiMarco (2008) developed physical hydrodynamic simulation models to better understand the effects that stratification and circulation have on the development of hypoxia for the nGOM. Wang and Justic (2009) used the Finite Volume Coastal Ocean Model (FVCOM) system for their simulation and found that the model supports conclusions that wind forcing and buoyancy from riverine freshwater discharge are the dominant mechanisms affecting water column circulation and stratification in this area. Hetland and DiMarco (2008) using a different 3-D modeling system, ROMS as stated in chapter 3, found similar conclusions of local wind forcing and freshwater discharge as the main driver of water column circulation and stratification. The ROMS model developed by Hetland and DiMarco (2008) also sought to characterize the oxygen demand control structure by adding a simple respiration model into the physical model. While the physical conditions of the ROMS model were similar to those from Wang and Justic (2009), the ROMS model also led

researchers to the conclusion that water column respiration predominantly causes hypoxia east of Terrebonne Bay and benthic respiration being the main cause west of Terrebonne Bay (Hetland and DiMarco, 2008). Both of these models were validated using field observational and mooring data (Hetland and DiMarco, 2012). These types of models are helpful in identifying and prioritizing the different control mechanisms of hypoxia formation; however, forecasting of hypoxic events can be better achieved by statistical models such as those developed by Turner et al. (2006) and Forrest et al. (2011). Both of these models are statistical regression models that significantly correlate time and nitrogen loading with forecasted areal extent of hypoxic formation; though Forrest et al. (2011) used other variables such as wind forcing in their model which was found to be the best method for forecasting areal extent. Researchers have found that there is a need for both of these types of models, complex 3-D simulations and simple models (statistical), because each has their own advantages and disadvantages when it comes to understanding the mechanisms controlling hypoxia and the areal extent of the nGOM that will be affected. Simple models are advantageous because input requirements are much less extensive than those for complex models; because of this the simple models can use data from longer periods of record than complex models and thus provides a higher degree of robustness to forecast future conditions (Justic et al., 2007). These simple models, however, can only be valuable forecasting tools on a limited number of parameters, such as hypoxic area (Justic et al., 2007). Complex models are great tools for hindcasting hypoxic events but only for a limited time frame since these models require extensive amounts of data for input, calibration, and validation; nevertheless, these complex models can provide more complete understandings of cause-effect mechanisms that control hypoxia formation, maintenance, and spatial variability (Justic et al., 2007). Since both types of models have distinct advantages and caveats, researchers suggest refining both types of models in order to provide managerial agencies with a more complete understanding of what controls hypoxia formation and to what areal extent it may reach in future years.

Over the past few years, there have been increased efforts to develop complex 3-D modeling systems that couple physical conditions with biogeochemical dynamics, which can offer a more complete study of hypoxic regimes in the nGOM. Specifically within the MCH research group, there is a concerted effort to try and couple the hydrodynamic ROMS model for the nGOM developed by Hetland and DiMarco (2008)

with models for sediment transport, biological models, geochemical models, and a combination of all. A coupled physical-biological model for the nGOM was developed by Fennel et al. (2011) to simulate the complex interactions between riverine freshwater and nutrient discharge, water column stratification, vertical export of OM down the water column, and the microbial degradation of that OM. The results from this model simulation show that while primary production and phytoplankton biomass are positively correlated with nutrient input, phytoplankton growth is not, which suggests that accumulation of biomass in the nGOM is not controlled primarily by nutrient-stimulation but by systemic differences in the loss processes such as zooplankton grazing, mortality, and aggregation; which is thought to be caused by increased retention of river water during high discharge years (Fennel et al., 2011). This model was further developed to include 3 different sediment oxygen consumption (SOC; equivalent to SOD) parameters (1) instantaneous remineralization; which states all OM reaching the sediment is instantaneously remineralized accounting for the loss of fixed nitrogen due to denitrification. (2) Sediment oxygen uptake dependent on bottom water oxygen concentration and temperature based on Hetland and DiMarco (2008); this parameterization states OM essentially leaves the system when sinking out of the water column while a fraction of the nitrogen that sank out is returned to the water column as ammonium and (3) sediment oxygen uptake based on linear relationship between SOC and bottom water oxygen suggested by Murrell and Lehrter (2010); all three processes were simulated and studied for importance in determining areal extent of hypoxic bottom waters (Fennel et al., 2013).These simulations were found to be very sensitive to changes in the parameterization of SOC, which results from the fact that hypoxic conditions across most of the nGOM are restricted to a thin layer above the seabed (Fennel et al., 2013). Since these simulations have shown that SOC is extremely dependent on the input parameters related to the BBL, coupling this physical-biogeochemical model with one that simulates sediment transport across the continental shelf could become a powerful tool for illuminating the drivers of oxygen dynamics and hypoxia formation within the BBL.

A 3-D coupled hydrodynamic-sediment transport model for the year 1993 has been developed and tested by Xu et al. (2011). This model couples the ROMS hydrodynamic model from Hetland and DiMarco (2008) to the CSTMS sediment model developed by Warner et al. (2008). This coupled modeling system simulates the physical oceanic conditions that result from combinations of riverine discharge from the

Mississippi and Atchafalaya Rivers with wind and wave conditions that will allow for deposition, resuspension, and transport of sediment materials across the LATEX continental shelf. This coupled modeling system has been found to accurately simulate the near seabed physical conditions necessary for sediment resuspension and transport during the year 1993; and was validated from observational data. This coupled hydrodynamic-sediment transport model is in the process of being coupled with the Fennel et al. (2011) biogeochemical model and preliminary results were presented by Harris et al. (2013). The importance of coupling these models stems from the limitations of previous modeling efforts for geochemical processes as these rarely include the geochemical effects of resuspension sediment transport (Harris et al., 2013). Further development and validation of this coupled hydrodynamic-sediment transport-biogeochemical model will be essential for having simulations that can account for most of the parameters considered to be of first order importance in the formation and maintenance of hypoxic bottom waters in the nGOM.

4.2 Coupled Hydrodynamic-Sediment Transport Model for the nGOM in the year 2005

4.2.1Objectives

Developing a quantitative and comprehensive understanding of the spatial and temporal variations of sediment transport processes on the LATEX continental shelf is important when trying to fully understand the physical mechanisms that may be associated with the formation of hypoxic bottom waters in the nGOM. Strong waves and currents during hurricanes can disrupt pycnoclines and break down hypoxic conditions, however depending on the of the time hurricanes hypoxic conditions can be reestablished if the water column becomes stratified again. The deep and extensive seabed erosion during the extreme hurricanes can cause substantial sediment resuspension during which buried OM might be re-exposed on the seabed for later potential breakdown through respiration, which may affect those timescales for hypoxia reestablishment. While understanding the physical conditions that are necessary for hypoxia formation was the main driver for developing these 3-D modeling systems, other applications of the model systems for coastal management could also be considered. Analyzing model simulations for sediment dispersal during major storm events may become an increased area of study in order to monitor sediment exchange between shelf and wetland throughout the Louisiana and Texas coastlines.

The objective of this study was to use a high-resolution 3-D model to analyze sediment transport processes occurring on the LATEX continental shelf, with specific regards to major storm events such as hurricanes. The year 2005 was chosen to determine the degree of sediment reworking across this shelf system during fair weather and the occurrence of 2 major hurricanes during the late summer, Hurricanes Katrina and Rita. This study will first address the sensitivity of sediment dispersal from the Mississippi River, Atchafalaya River, and seabed by waves and currents during these major storm events under varying input values. Once all sensitivity model simulations have been tested and compared to observed data, the results from the most accurate model simulation will serve as the foundation for this study of sediment transport during major hurricanes. An accurate model of seabed interactions with extreme physical conditions associated with hurricanes, which have been known to disrupt water column stratification and dissipate bottom water hypoxia, will aid in determining the time scales for hypoxia reestablishment after a storm event. As stated earlier, the year 2005 was observed to have hypoxia dissipated after early summer storms but was able to reestablish hypoxia in the time leading up to Hurricane Katrina. Hindcast modeling of these conditions will aid future researchers in identifying the conditions and time necessary for hypoxia reestablishment.

4.2.2 Hurricanes Katrina and Rita

Both Hurricanes Katrina and Rita were very destructive storms for the Louisiana coastline, causing heavy damage to developed areas and major flooding. Overall both storms had similar tracks, starting in the Caribbean Sea and dissipating just south of the Great Lakes (Fig.4-3). Hurricane Katrina formed as a tropical depression on August 23, 2005 over the Bahamas Islands in the Caribbean Sea. After brushing past the southern tip of Florida, the hurricane moved westward into the Gulf of Mexico where it gained strength to become a category five hurricane by August 28 (csc.noaa.gov). Hurricane Katrina then moved northward and made landfall on August 29 over the birdfoot delta of the Mississippi River as a category four hurricane (Fig. 4-4). Hurricane Rita formed as a tropical depression in the Caribbean Sea on September 18, 2005 and headed westward into the Gulf of Mexico. On September 21 it became a category five hurricane and moved northwest towards the western Louisiana coastline, where it made landfall on September 24 on the Texas-Louisiana border as a category three hurricane (csc.noaa.gov).

After making landfall, Hurricane Rita pushed northward reaching Illinois as a tropical depression and finally dissipated after September 26, 2005 (Fig. 4-4).

4.3 Methods and Model Inputs

4.3.1 Coupled Hydrodynamic-Sediment Transport Model

This project simulates physical hydrodynamic conditions and sediment transport in the nGOM during the year 2005 by enhancing the hydrodynamic-sediment transport model developed by Xu et al. (2011), which focused on the year 1993. The 3-D, open-source ROMS formed the foundation of the numerical model and the CSTMS provides a mature sediment-transport module within the ROMS domain; BBL calculations were the same as those for the 1993 model (Xu et al., 2011). The model was initialized on February 1, 2005 and ran for an entire year with 20s time step and every 12hr outputs; this starting date was chosen based on available data from Wave Watch III (WWIII), which will be elaborated on in the subsequent section. The same latitudinal and longitudinal model grid (Fig. 4-5) used by Xu et al. (2011) was used for this model development but instead of having 20 vertical layers, the 2005 model incorporates 30 vertical layers. The addition of 10 vertical layers to the 2005 model increases the resolution of physical dynamics and conditions occurring within the BBL and at the sediment-water interface. The boundary conditions of temperature, salinity, and momentum used for the 1993 model domain were developed from horizontally uniform climatological fields obtained from regional hydrographic surveys; the monthly means were incorporated in the model domain as boundary conditions (Xu et al., 2011). For the 2005 model domain instead of using climatology data, daily Hybrid Coordinate Ocean Model (HYCOM) data from 2005 and 2006 were used for boundary conditions; the HYCOM system provides more accurate and higher resolution boundary conditions for deeper areas of the 2005 model domain (Zhang et al., 2012).

4.3.2 Input wind and waves

The 1993 model used spatially uniform but temporally variable winds based on measurements from the BURL 1 C-MAN weather station located near the mouth of the Southwest (SW) Pass of the Mississippi River (Xu et al., 2011). For 2005 model development, spatially variable wind forcing was derived and

integrated from the North American Regional Reanalysis (NARR) project dataset. The NARR project was created by the National Center for Environmental Prediction (NCEP) to develop a dataset to enable hindcast modeling; it provides a dataset of atmospheric conditions with a high resolution over the entire North American Region. The NARR model dataset was produced using the NCEP Eta Model combined with the Regional Data Assimilation System (RDAS) (esrl.noaa.gov). The NARR dataset used for the 2005 model was obtained from Zhang et al. (2012) and provides spatially and temporally variable winds with a 3-hr temporal resolution. The use of the NARR dataset was also necessary because there is no recorded data for wind speeds at the BURL 1C-MAN weather station after Hurricane Katrina due to sensor malfunction (Fig. 4-6).

The 1993 model used the Simulating Waves Nearshore (SWAN) model to provide wave inputs for the model domain but this model was not available for this project, instead wave input (height, period, direction; Fig. 4-7) were provided by WWIII from the NOAA Environmental Modeling Center website (http://polar.ncep.noaa.gov/waves/download.shtml?). The data used from NOAA's WWIII modeling system consisted of data files that went from February 1, 2005 to January 31, 2006; data for January 2005 were not available, which is the reason this model simulation begins on February 1, 2005. The field output data used and integrated into the ROMS sediment transport model were in the form of 4-arc minute coastal grid for the nGOM with 3-hr time step, which allows for the highest resolution output for this type of wave model. Before integrating wave inputs, the WWIII data had to be transformed from its original file type to the netCDF file type required for the ROMS model. The WWIII data were extracted and all data points with no values were filled in with values from adjacent grid cells to ensure the entire WWIII model domain would be complete. The WWIII model data were then interpolated into the nGOM ROMS model grid and transformed into the appropriate netCDF file type to be integrated as model input variables.

4.3.3 Fluvial Discharge

Fresh water and sediment discharge inputs from the initializing date (Feb. 1, 2005) to the end date (Feb. 1, 2006) for the Mississippi and Atchafalaya Rivers were incorporated into this model via the same methods used by Xu et al. (2011) (Fig. 4-8). These discharge measurements were taken from Tabert

Landing and Simmsport gauging stations maintained by the U.S. Army Corps of Engineers and U.S. Geological Survey.

4.3.4 Initial Sediment Bed

Initial seabed sediment layers for the 1993 model were composed of four 10 cm thick layers, however for the 2005 model the same number of layers were used but with a different initial thickness (Xu et al., 2011). For the 2005 model, four 2 m thick sediment layers were used to represent the initial sediment bed; the thickness of each layer was increased to ensure that all four layers do not become completely eroded under high resuspension events such as the two hurricanes (Katrina and Rita) observed during this year in the model domain. The bathymetry (obtained from R. Hetland) for the 2005 model grid is also not as smooth as the grid used for the 1993, which makes for a better representation of actual bathymetry observed for the area of the nGOM that encompasses the 2005 model domain, especially near Mississippi Delta Front and Mississippi Canyon. The 2005 model domain uses the same 50,000 historical surficial grain-size data archived by the usSEABED project (Buczkowski et al., 2006) to account for initial seabed sediment environments across the LATEX continental shelf (Figs.2-19,2-20).

4.3.5 Sediment Class Treatment

Like the 1993 model, these simulations use six sediment classes: two each for Mississippi River material, Atchafalaya River material, and the seabed (Xu et al., 2011). The model requires a settling velocity (W_s), critical shear stress for erosion (τ_{cr}), an erosional rate (E_{rate}), and fraction of sediment types for each sediment class within the model (Table 4-1, 4-2). As the objectives stated, this study ran a series of models that had varying settling velocities and erosional rates (Table 4-2), while the critical shear stress for erosion was held constant for each model run. The same assumptions of flocculation within the 1993 model were used in the 2005 model as well, where the model neglected aggregation and disaggregation of flocs and there was no exchange between the six sediment tracers in model runs (Xu et al., 2011). The 1993 model by Xu et al. (2011) ran model sensitivity tests and used observational data to determine that the values presented in table 4-1 for the 1993; which are still valid for the modeling of sediment transport in the year 2005 however some changes will be made to account for major resuspension events.

Sensitivity tests were performed to select the optimal E_{rate} and W_s that reflect actual field observational studies of erosional and depositional depths. For the sensitivity tests performed with this model, all parameters in table 4-1 were held constant except for changes made to the E_{rate} and W_s (Table 4-2). Four model simulations were performed to determine the sensitivity of changes to the amounts of sediment transported across the shelf system under varying conditions for seabed sediment settling velocity and erosional rate (Table 4-2).The conditions for the 4 simulations were: 1) *Low E_{rate} and high settling velocity*: the E_{rate} and W_s are the same as those from the 1993 model run. 2) *High E_{rate} and high settling velocity*: the E_{rate} for all sediment classes were increased by an order of magnitude (from $5x10^{-5}$ to $5x10^{-4}kg/m^2s$) and the W_s is the same as simulation 1. This simulation will increase the sensitivity for which particles will become eroded, and should therefore result in greater amounts of sediment being suspended and transported across the shelf system compared to simulation 1. 3) *Low E_{rate} and low settling velocity*: the W_s for the seabed sediment classes were changed from 10.0 and 1.0 mm/s to 1 and 0.1 mm/s for sand and mud, respectively. This simulation decreases the speeds at which seabed sediment particles settle out of the water column once resuspended and should also result in increased amounts of suspended sediment transport farther across the shelf system. 4) *High E_{rate} and low settling velocity*: this simulation is a combination of both the previous changes made to E_{rate} and W_s within the same simulation (i.e. high erosional rate and low settling velocity); overall, this model simulation should result in the greatest amounts of seabed sediment erosion and transport across the LATEX continental shelf.

4.3.6 Output and Analyses

In order understand and visualize the results of the 2005 ROMS sediment transport model simulation many different maps and graphs were made from modeling output data. Data from the ROMS model was outputted every 12hr into netCDF files and then extracted and analyzed using Matlab R2007a. To analyze the amounts of sediment being transported across the shelf, surface/bottom currents, shear stress, and surface/bottom suspended sediment concentrations (SSCs) will be mapped over the entire model domain for the times corresponding to Hurricanes Katrina and Rita. The contribution of each sediment class (Mississippi, Atchafalaya, seabed) to the SSC will also be examined to determine which areas of the model domain are prone to mixing. Calculating, mapping, and graphing of the maximum

erosional depths and depositional depths across the entire model domain and at specific stations will illustrate which areas of the model domain are more prone to seabed erosion/deposition and at what magnitude does the seabed erode. Analyzing each of the parameters will provide the study with an overall picture of when, where and how much sediment is eroded and transported across the nGOM during major storm events.

4.4 Results

4.4.1 Model Sensitivity Test

It was found that the most appropriate simulation performed for this study was the fourth simulation with a high E_{rate} and low W_s for seabed sediment types because it most matched the available observations of storm erosional and depositional depths provided from Goni et al. (2007). The maximum erosional depth was analyzed during both hurricanes for each of the four simulations to determine which simulation was the most sensitive to sediment erosion and transport, and is illustrated in Figs. 4-9 (Katrina) and 4-10 (Rita). Both figures illustrate that a change in the E_{rate} plays a much larger role on sediment erosional depth than changes to seabed sediment settling velocity, by almost an order of magnitude during both hurricanes. Through comparison of the depositional changes over time after each storm (Fig. 4-11) to the depth of hurricane layers as measured by Goni et al. (2007) (Fig. 4-12), simulation 4 best agreed with the observed data from the different areas analyzed. Therefore, all results further presented in this paper will be based on modeling results from simulation 4.

4.4.2 Annual and Hurricane Hydrodynamics

The annual means of salinity and temperature for both the surface (top grid cell) and bottom (bottom grid cell) waters within the ROMS model domain are illustrated in figure 4-13. The annual means for surface and bottom salinity are overall quite similar, between 30 and 35 ppt; however, surface salinities nearest to the Mississippi and Atchafalaya River deltas are much lower due to freshwater input creating buoyant river plumes (Fig. 4-13 A, B). The mean annual temperature differs between the surface (25^{o}C) and bottom waters (22-23^{o}C) by a few degrees; also the bottom temperature isotherms seem to contour to the deeper bathymetry (Fig. 4-13C, D). There is an overall westward flow for the mean annual surface and

bottom currents, mean bottom currents also seem to have a lower magnitude compared to the surface currents (Fig. 4-13). A transect plotted along the longitudinal grid cells through site 10B (Fig. 4-5), middle hypoxic zone, was used to generate a cross-shelf transect of water column density and current flow within the observed annual hypoxic zone (Fig. 4-2), which is illustrated in figure 4-14. The mean annual density increases from onshore to offshore, as well as increasing with depth (Fig. 4-14).

The means for salinity and temperature were also determined for Hurricanes Katrina (Aug. 26-Sept. 1, 2005) and Rita (Sept. 21-27, 2005); means were calculated over a 7-day period, 3 days before and after hurricane landfall, as well as the day of landfall. These 7-day periods were chosen to encompass the initial and residual hurricane conditions associated with pre/post landfall. The mean surface salinity during Hurricane Katrina ranged between 25-35ppt for most of the shelf area except close to the Mississippi and Atchafalaya River deltas; where freshwater plumes are present and transported west-southwest based on mean current flow to areas of mixed salinities on the inner western shelf (Fig. 4-15 A, B). The mean temperature for the surface waters during Hurricane Katrina were around 30^{o}C for the entire model domain; bottom water temperatures exhibited a much higher range of values and seemed to correlate with changes in depths on the shelf (Fig. 4-15C, D). A cross-shelf transect of mean density and current flow during Hurricane Katrina at 10B is illustrated in figure 4-16, which shows a stratified water column along the transect at water depths >10m; figure 4-15 supports this as well with lower salinities and higher temperatures in surface waters compared to bottom waters. The cross-shelf transect (Fig. 4-16) also indicates offshore surface currents which result from changes in wind direction as Hurricane Katrina made landfall over the Mississippi Delta; figure 4-15(C) also shows surface currents in the offshore southwesterly direction. During the peak of Hurricane Katrina within the model domain, offshore winds west of the Mississippi Birdfoot delta drive westward offshore surface currents (Fig. 4-17).

The mean surface salinity during Hurricane Rita was between 25-35ppt for most of the shelf area except close to the Mississippi and Atchafalaya River deltas due to freshwater input and transport west based on mean current flow; the areas of mixed salinities on the inner western shelf is not as large compared to Hurricane Katrina (Fig. 4-18 A). The mean westerly surface current seems to be much greater on the inner shelf during Rita, which is consistent with the hurricane's path (Fig. 4-4). The mean temperature for

the surface waters during Hurricane Rita were between 25-30^{o}C, which is slightly lower than temperatures observed during Katrina; bottom water temperatures were observed to have a lower range of values compared to Katrina temperatures and seem to correlate with changes only in bathymetry depths on the outer shelf (Fig. 4-18 C, D). A cross-shelf transect of mean density and current flow during Hurricane Rita at 10B is illustrated in figure 4-19, which shows a mixed range of speeds and direction of current flow; the density transect during Rita seems to be well mixed across the entire shelf. During the peak of Hurricane Rita over the model domain, onshore winds dominate to the right of the hurricane path causing large westward surface currents across the shelf (Fig. 4-20).

The driver of shear stress for sediment erosion and transport in this model for the entire year of 2005 is the result of wave generated shear stress (Tau_W) and current generated shear stress (Tau_C) combining to generate the total applied shear stress (Tau_{CW}). Sediment erosion and transport for the model year 2005 was found to be wave dominated (Fig. 4-21); this wave dominated shear stress was also observed during the two hurricanes Katrina (Fig. 4-22) and Rita (Fig. 4-23). The mean modeled shear stress for the hurricanes is far greater, up to one order of magnitude, compared to the mean shear stress model outputs for the entire year. These results agree with the statements by Goni et al. (2007) that interaction between storm waves and the seabed result in the hurricane deposits their study observed.

4.4.3 Hurricane Sediment Dynamics

As shown in figure 4-24, SSCs were highest immediately following the hurricanes, so only the times of the two hurricanes were mapped for SSC and seabed elevation changes. Additional analyses were made to determine the amounts of each sediment class (Mississippi, Atchafalaya, seabed) that composed the entire amount of suspended sediment; which gives some indication as to the areas in which suspended and discharged sediments from the Mississippi River mix with those from the Atchafalaya River and those resuspended from the seabed. Figure 4-25A illustrates the total SSC (kg/m^3) within the surface layer of the water column during Hurricane Katrina; figure 4-25 B, C, and D illustrate the concentrations and locations of the 3 different sediment tracers: seabed, Mississippi, and Atchafalaya, respectively (Tables 4-1, 4-2). The same setup is made for the map of bottom water column SSC during Hurricane Katrina (Fig. 4-26). The same two types of maps were made to analyze SSCs within the surface and bottom layers of

the water column during Hurricane Rita (Figs. 4-27, 4-28). During the peaks of both hurricanes over the model domain, there is highly elevated shear stress levels associated with the east side of both hurricanes which corresponds to high SSCs (Figs. 4-17C, 4-20C).

The changes to seabed elevation over time, i.e. net results of erosion and deposition, are illustrated in figure 4-29 for August to November 2005 to incorporate the two hurricanes. The five stations (Fig. 4-5) depicted in this figure were chosen to give some indication as to which seabed areas of the LATEX shelf are most affected by major storm events. Seabed depth above/below the initial seabed height at the peak and post Hurricanes Katrina (Fig. 4-30) and Rita (Fig. 4-31) show stations on the eastern shelf (AB5 and River) are more impacted by Hurricane Katrina with erosional depths of 31.5cm and 75.9cm and depositional depths of 12.7cm and 14.5cm, respectively (Fig. 4-29, 4-11). During Hurricane Rita these two stations were also heavily impacted, AB5 more so with an erosional depth of 37.7cm and depositional depth of 36.8cm, while at the River the erosional depth was 52.7cm (while this depth is less than that during Katrina, it is still the largest erosional depth hind casted during Hurricane Rita from these 5 stations) and the depositional depth only 2.12cm (Fig. 4-29, 4-11). The middle station (10B) is affected by both hurricanes on a similar scale, with erosional and depositional depths during/post Katrina of 16.3cm and 17.0cm; and during Rita an erosional of 22.5cm and depositional depth post Rita of 14.0cm (Fig. 4-29, 4-11). The western stations (08C and Atch) were both not affected greatly by Hurricane Katrina with erosional and depositional depths of 0.72cm and 0.77cm at 08C, respectively, and 1.29cm and 1.2cm at Atch, respectively. However during Hurricane Rita the erosional and depositional depths observed at 08C were much greater, 36.3cm and 27.2cm, compared to the Atch station just outside Atchafalaya Bay (Fig. 4-5) where the erosional depth was observed to be 4.54 cm and the depositional depth 5.64cm. The greatest amount of erosion occurred at the River station, right at the opening of the Mississippi SW pass, during both hurricanes with erosional depths >50cm (Fig. 4-11). This station seems to have a depositional depth (about 15cm) after Katrina similar to stations 10B and AB5 but after erosion from Rita the following deposition is much less (about 2cm) (Fig. 4-11).

4.5 Discussion

4.5.1 Model Seabed Sensitivity

The maximum erosional depths calculated during the hurricanes from simulation 4 (Figs. 4-9, 4-10) were observed to generate the best results when compared to observed data collected by Goni et al. (2007) (Fig. 4-12). Their study found that up to 8 cm of the surficial sediment was eroded from the seabed as a result of both storms, but are considered conservative estimates (Goni et al., 2007); their data also show hurricane depositional layers (Fig. 4-12) that correspond well the changes in seabed elevation over time for 5 different spots shown in figure 4-29. The comparison of the depositional changes over time after each storm (Fig. 4-11) to the depth of hurricane layers as measured by Goni et al. (2007) are in agreement for the different areas analyzed in both studies. Areas on the western shelf are much more impacted by Hurricane Rita; resulting only one storm layer (Goni et al., 2007) and a very small fall in the time series data during Katrina (Fig. 4-29 stations Atch and 08C). Areas on eastern shelf, just west of the Mississippi Birdfoot delta, were much more impacted by Hurricane Katrina but also show some sensitivity to Rita; reflecting the actual hurricane's intensity and path as it passed toward the east of the modeled and sampled domain.

4.5.2 Hurricane Sediment Transport

Many factors can influence the amounts of sediment that may become eroded and transported across continental shelf systems and understanding the dynamics between physical conditions and the environments on which they act is essential for proper model simulation and analysis. The maximum annual changes to seabed elevation across the model domain seems to be sensitive to factors such as seabed environment and major changes in physical conditions such as those associated with major storms or hurricanes. The total observed changes in seabed elevation for the entire 2005 simulation seem to derive from a combination of the elevation changes occurring during and following the two major hurricanes simulated, Katrina and Rita (Fig. 4-32). For the 5 different areas studied, it was found that Hurricane Rita had greater impacts on the amounts of sediment being eroded and deposited at these 5 different stations (Fig. 4-30, 4-31). The 5 different sampled stations show that some areas are affected differently by different hurricanes, which is related to the path and size of the hurricane. Overall, the area nearest to the mouth of the Mississippi River SW pass was the most heavily impacted area during the storm events with erosional depths greater than 50cm, however post storm deposition was much less

than the other areas analyzed and varied between storms (Fig. 4-29, 4-11). These model observations connect well with those depositional depths measured by Goni et al. (2007) that show large depositions after Katrina but not Rita for areas close to the Mississippi River mouth (Fig. 4-12). This also supports claims from Chapter 3 that state areas closer to a major river mouth have more erodible surficial sediments than those on the inner shelf, which is thought to be due to less consolidation of seabed material that has been 'freshly' deposited (Fig. 3-27). The Atch station just outside Atchafalaya Bay was observed to be the least impacted area during both hurricanes which is surprising considering the track of Hurricane Rita's path. However, based on model animations (Fig. 4-17, 4-20) it would appear that wave dissipation (0-2m wave height) occurs just outside of the Atchafalaya Bay in areas <10m deep, which could explain why this area had such little erosion of surficial sediments. Other areas of the nGOM analyzed for maximum erosional depths seem to be influenced by another factor, sedimentary environment and sediment grain size, which were discussed in the previous chapters. The area just south of Atchafalaya and Terrebonne Bay within the 10-20m isobath is considered a sandy area (Fig. 2-22), which would require more energy to erode more sediment, thus resulting in a smaller maximum erosional depth in this area (Fig. 4-29: 10B) compared to areas of the shelf with more erodible sediments such as those directly off the SW pass of the Mississippi Birdfoot delta or outside of Atchafalaya Bay (Fig. 4-29: River & 08C; Fig. 2-22). These differences in grain size across the shelf, as discussed in chapter 2, support the hypothesis that areas with smaller grain sizes will have increased amounts of erosion during storm events (Fig. 4-32; Fig. 2-22).

This simulation study also sheds light on areas of the nGOM where mixing of Mississippi and Atchafalaya River sediments occurs. During these major hurricanes the scale of sediment dispersal becomes much larger and thus can result in the erosion and subsequent deposition of riverine sediment hundreds of miles away from their source (Figs. 4-25 through 4-28). The amounts of SSC observed over the entire year remains very low except during the two hurricane storm periods (Fig. 4-24). The bottom water column SSCs are much higher than in the surface and the area of elevated SSCs covers a much larger area than the surface concentrations. This is likely due to the increased levels of shear stress applied to the sediment bed, as indicated in figures 4-21, 4-22, 4-23, and 4-24 through 4-28. The elevated SSC in the surface and bottom layers are shown to cover a much larger area of the model domain during

Hurricane Rita compared to Katrina. This is due to the different paths of landfall that each hurricane took; Rita covering more of the LATEX continental shelf and model domain than Katrina. During Rita it also seems that there was a much larger dispersion of surface water column sediments from the Mississippi and Atchafalaya Rivers; most likely due to the same reasons of the path taken by Rita versus the path taken by Katrina (Figs. 4-25, 4-27). More of the model domain falls within the affected area of Hurricane Rita's path than by Katrina's path, which is likely the reason for greater dispersion of sediment classes during Rita (Figs. 4-25 through 4-28).

Modeling the transport of high SSCs during hurricane events could be an important tool used to aid other researchers who study the amounts of sediment deposition occurring in low lying wetlands and coastal areas in southern Louisiana. Tweel and Turner (2012) conducted a survey to determine the amounts of storm derived sediment deposition in areas known to have hurricane depositional surfaces (Fig. 4-33); their study found that during Hurricanes Katrina and Rita, storm surge deposits were estimated to be 67.8±8.6 and 48.2 ±8.3 million metric tons (MMT) of inorganic sediment on coastal wetlands respectively (Tweel and Turner, 2012). The major areas of deposition for these two hurricanes are illustrated in Fig. 4-34, and show that for Katrina most deposition occurred along the storm track onto the northeastern Deltaic Plain; during Rita most of the inland deposition occurred to the east of the hurricane path onto the Chenier Plain (Fig. 4-34). By analyzing areas of high SSC for the two hurricanes (Figs. 4-25 through 4-28) during and immediately following landfall, some indication as to the inland areas that may receive large amounts of storm sediment deposits become observable. By being able to compare model data with observed data, like Tweel and Turner (2012), storm modeling researchers and wetland conservation researchers may have a better understanding as to the effects and scale to which storm deposited-sediments could impact wetland restoration efforts. While there is still a lot of debate on the magnitude of the effects that storm deposits have on wetland accretion, ongoing research into these impacts should not be dismissed and should be incorporated into wetland management strategies (Turner et al., 2006; Tornqvist et al., 2007).

4.5.3 Impacts to Hypoxia

The refinement of the 3-D hydrodynamic sediment transport model for the nGOM is essential tool for better hindcasting efforts and understanding the different physical dynamics that occur before, during, and after hypoxic events in this area. The observed hypoxic water distribution for the year 2005 was well documented but was greatly affected by these two major hurricanes. The area of hypoxic water during the weeks before Katrina was considered patchy but still present in the mid-hypoxic region, which is supported by the water column stratification observed in Fig. 4-35 (Rabalais et al., 2006). While Katrina did disrupt hypoxic waters in depth less than 25m, hypoxia was able to reform in the time leading up to Hurricane Rita, which is also supported by stratified water columns on the inner shelf (Fig. 4-36) (Rabalais et al., 2006).

Coupling a more refined physical model, with biological, chemical, or biogeochemical models will lead to a more comprehensive understanding of the physical, biological, and chemical interactions occurring at the sediment water interface and within the BBL. Most of the seasonal hypoxia in the nGOM occurs in the bottom waters, 1-2m above seabed, thus having models that can accurately simulate conditions within the BBL becomes essential (Fennel et al., 2013). While this model study shows that the annual overall shear stress being applied to the seabed (Fig. 4-24) is usually less than 0.1 Pa, which as discussed in Chapter 3 results in very little material being eroded, the values observed during the hurricanes are at least one order of magnitude higher; the maximum shear stress at station 10B observed during Hurricanes Katrina and Rita were 5.49 Pa and 5.33 Pa, respectively. These large changes in shear stress lead to the same type of pattern where bottom SSC during hurricanes are an order of magnitude higher versus the rest of the year and between 3-5 times greater than surface sediment concentrations (Fig. 4-24). This leads to the understanding that there is definitely an erosionally active BBL resulting from both hurricanes while they were positioned on the LATEX continental shelf. Along the mid-hypoxic zone transect used in this study, a BBL with higher sediment concentrations is hindcasted to have resulted from Hurricane Katrina (Fig. 4-37). During and after Hurricane Rita the BBL was hindcasted to have not been as sediment laden; although a thin layer of elevated SSC is present around the 20m and 25-40m depths just above the seabed (Fig. 4-38). The thin layer (<1m) of highly elevated SSC predicted to be present in contact with the seabed supports the presence of an energetic BBL. Recent modeling by Fennel et al. (2013b) has shown that the position of the major pycnocline (major referring to closest and

most distinct pycnocline observed above seabed) has a significant impact on the percentage of oxygen consumption from the seabed relative to oxygen uptake in rest of the water column. If the major pycnocline is located around 1-2m above the seabed, SOC can account for up to 60% of the below major pycnocline oxygen consumption, while if the pycnocline is higher in the water column (>10m) SOC only accounts for up to 25-30% of the below pycnocline oxygen consumption (Fennel et al., 2013b). These observations support the conclusion that the physical dynamics at the sediment water interface and within the BBL play a large role in influencing biological and chemical regimes affecting hypoxia. For this modeling study the BBL is only observable during the storm events; however it is observed that shear stress levels throughout the entire year are usually less than 0.2 Pa and these are strengths great enough to affect the floc layer material and therefore may influence hypoxic regimes during calmer weather when hypoxia may establish.

4.5.4 Ongoing and Future Work

The coupled 3-D hydrodynamic and sediment transport model used in this study has been refined and validated to provide researchers with an important tool for hindcasting coastal marine physical conditions on the LATEX continental shelf. Future modeling efforts with this LATEX model domain will involve running the model for extended periods of time (multiyear studies). Further model validation and enhancement will come from the integration of observed GUST erodibility derived erosional rates, as discussed in Chapter 3, into the numerical model. These integrated profiles should provide the models with more appropriate input/output values associated with the sediment-water interface.

There is ongoing work, as stated earlier, being done to combine this hydrodynamic and sediment transport model with biological/biogeochemical models by Courtney Harris (Harris et al., 2013). This research focuses on developing and enhancing hindcast modeling of hypoxic regimes and the coastal marine dynamics that may play a role in hypoxia formation and maintenance, which has become an invaluable tool when advising local, state, and federal agencies on coastal management decisions. Another important application of this coupled hydrodynamic sediment-transport model would be to extend the model from shelf to tidal marsh/wetland areas, which would require developing and adding ‘wet and drying’ modules into the model system. By extending the model domain to include marshes, coastal

inundation and storm surge models could be combined with the sediment-transport model to examine the effects of hurricane and major storm events on coastal wetland accretion.

4.6 Conclusion

There are many conclusions that derive from this study of modeling sediment transport on the LATEX continental shelf during major hurricane events. This study showed the highly episodic nature of sediment transport in the nGOM and illustrated that major hurricanes greatly impact sediment erosion and deposition. The sensitivity tests performed on the 2005 model have shown that the maximum erosional depth seemed to be more sensitive to changes in erosional rate than to settling velocity. The mechanisms for eroding sediment material from the seabed is almost entirely derived from waved generated shear stress; the degree of which is an order of magnitude greater during hurricanes than the means for the entire year. Estimated sediment erosion was localized and mainly located along the eastern side of the hurricane tracks. During both hurricanes major erosion occurred between the 5m and 50m isobath and net sediment transport was landward. Modeling the transport of the large suspended sediment loads and comparing the results with storm surge models and wetland sediment layers post hurricane may serve as a new tool for coastal wetland management. The refinement of the physical conditions occurring at the sediment water interface as described in this modeling study will become essential for future modeling efforts that combine physical models with biogeochemical models. This study sought to replicate and understand the sediment transport dynamics that occur during and after major hurricanes for areas of LATEX continental shelf; the results of this study will provide insight into BBL characteristics that are present before and during hypoxic events but also sediment transport scales which could be used to better understand wetland elevation changes after major hurricane events.

5 Final Discussion and Conclusions

Examination of grain size analyses from samples across the nGOM suggest that there is relatively little spatial variability of surficial sediment across the nGOM, except for those two sites (10B and S39) associated with the area known to be the sandy shoals of a major historic deltaic lobe shift. There does not appear to be much temporal variability of grain sizes at the four surveyed stations, except for the absence of lamination patterns observed in April 2012 at station 08C, which is thought to be an artifact arising from differences in location positioning. However this observed variability at station 08C may also indicate that the areas surrounding the historic sandy lobe have increased grain size variability very short distances. Overall the sediments at the stations seem to be stable in time and space, and the anomalies observed in this study may be rectified with more sampling data in the future.

The GUST core experiments illustrated that there appear to be seasonal and spatial patterns influencing the composition and erodibility of suspended seabed materials within the nGOM. It also appears that the varying sedimentary environments across the nGOM have a major influence on the erodibility of seabed material; specifically the sand shoals south of Terrebonne Bay are less erodible than areas nearer to the Mississippi and Atchafalaya delta. The GUST and modeling results indicated that areas closer to the mouth of the two major river deltas are more prone to erosion, compared to areas of the inner and middle shelf which have more consolidated sediments. Temporal variability in seabed erodibility seems to be most associated with seasonal weather patterns occurring in the nGOM. Energetic conditions observed in the months leading up to the April sampling periods may have increased BBL activity which can cause the upper seabed material to be more erodible, thereby resulting greater erodibility measurements in April compared to those from the August sampling period. The quiescent period during several months before August sampling periods allow sediment to consolidate and dewater, leading to less erodible sediment in August. These changes in wave characteristics that are associated with seasonal weather may then lead to the observed results and illustrate a seasonal erodibility pattern of surficial sediments across the nGOM.

Measurements of organic material (VSS) eroded at the lowest shear stress were found to be significantly higher than those measured at other higher shear stress levels except the highest. Illustrating the

difference in the percentage of OM being eroded during the lowest and highest, the greater percentage occurring during the lowest shear stress application, gives an very clear indication that there is a an organically enriched flocculent layer present at the sediment water interface. Measuring the amounts of resuspended OM and determining how labile that material is through biochemical oxygen demand experiments are urgently needed to determine if these organic materials being reintroduced into the water column are of primary importance to oxygen dynamics leading to hypoxia.

Determining how much material, organic and inorganic, that is reintroduced into the water column and the time spent in suspension will be essential to future models that incorporate sediment transport and biogeochemical processes. As stated earlier, the time scale for which major erosion and deposition occur during storms is fairly short, and sediment and oxygen dynamics post storm play a major role in hypoxia reestablishment. This study has shown that the amount of material that may become resuspended during major storms can be up to 5 times greater than what occurs during fair weather events. During these intense erosion events the materials that become resuspended may then be sorted based on their particle size due to differences in settling velocity. With OM occupying the smaller particle size class, one may speculate that the materials remaining in the water column post storm has a higher proportion of OM than materials that settle out fairly quickly. Other researchers (Reese et al., 2012) have found low amounts of OM present in the top 5cm of the seabed the direct influences of the top 5 cm seabed sediment to hypoxia may or may not be significant; therefore, the impact of resuspension during major storm events on reintroducing labile material into the water column is still uncertain. However, this study showed that the floc layer may become resuspended at fairly low shear stress levels (0.01 Pa). This floc layer seems to contain a higher percentage of OM than the sediments just below the floc layer. The greater percentage of OM in the flocculent layer compared to 5cm below sediment surface suggests that, when respired, OM associated with the sediment water interface may play the largest role in SOD compared to other biological activities occurring in the sediment. Due to intense seabed erosion and deposition over a short period; seabed sediment becomes very loose, allowing for more pore water diffusion of soluble gases and nutrients into the deeper parts of the sediment (as seen in Fig. 3-1), which could have major influences on the amount of SOD occurring post storm. While this modeling study has been shown to accurately simulate physical hurricane conditions of increased wind, wave, and current

activities, coupling this model with a biogeochemical model will provide much more insight into the mechanisms occurring post storm during which hypoxic waters may become reestablished.

The modeling efforts put forth by researchers to better understand the physical, chemical, and biological dynamics associated with the formation of hypoxic events have led to the development of sophisticated tools that will allow for more informed mitigating policy decisions. The challenge of identifying, quantifying, and understanding the interactions and mechanisms that control hypoxia formation is a highly complex task for any researcher, hence concerted efforts on all aspects (physical, biological, geological, and chemical) to develop 3-D modeling systems are needed. This study has provided a portion of insight into how sediment transport dynamics may interact with other physical processes to influence biological and chemical regimes associated with hypoxia formation, but one must have all the pieces to a puzzle in order to solve it. The refinement of these complex models to include more parameters will enrich the ability for other researchers to incorporate modeling parameters that may have once not been associated with the study of hypoxia formation in the nGOM. This study illustrates the need for more field, laboratory, and modeling efforts to help validate, complement, and enhance current theories and concepts being put forth by the scientific community involved in studying these hypoxic events.

References

Blott, S.J., Pye, K. 2001. Gradistat: A Grain Size Distribution and Statistics Package for the Analysis of Unconsolidated Sediments. Earth Surface Processes and Landforms. 26. 1237-1248.

Boudreau, B.P., Jorgensen, B.B. 2000. The Benthic Boundary Layer: Transport Processes and Biogeochemistry. New York: Oxford University Press.

Briggs, K., Watkins, J., Shivarudrappa, S., Hartman, V. 2009.Effects of hypoxia on sediment properties in the northern Gulf of Mexico. Naval Research Laboratory Public Records.

Buczkowski, B.J., Reid, J.A., Jenkins, C.J., Reid, J.M., Williams, S.J., and Flocks, J.G., 2006, usSEABED: Gulf of Mexico and Caribbean (Puerto Rico and U.S. Virgin Islands) offshore surficial sediment data release: U.S. Geological Survey Data Series 146, version 1.0.Online at http://pubs.usgs.gov/ds/2006/146/

Coleman, J.M., Gagliano, S.M. 1964. Cyclic sedimentation in the Mississippi River deltaic plain. Transactions—Gulf Coast Associationof Geological Societies. XIV. 67-80.

Coleman, J.M., Roberts, H.H., Stone, G.W. 1998. Mississippi River Delta: an Overview. Journal of Coastal Research.14 (3). 698-716.

Dagg, M., Sato, R., Liu, H., Bianchi, T., Green, R., Powell, R. 2008.Microbial Food Web Contributions to Bottom Water Hypoxia in the Northern Gulf of Mexico. Continental Shelf Research. 28. 1127-1137.

Dickhudt, P.J., Friedrichs, C.T., Schaffner, L.C., Sanford, L.P. 2009. Spatial and temporal variation in cohesive sediment erodibility in the York River estuary, eastern USA: A biologically influenced equilibrium modified by seasonal deposition. Marine Geology. 267. 128-140.

Fennel, K., Hetland, R., Fend, Y., DiMarco, S. 2011. A coupled physical-biological model of the Northern Gulf of Mexico shelf: model description, validation and analysis of phytoplankton variability. Biogeosciences Discussions. 8. 121-156.

Fennel,K., Hu, J., Laurent, A., Marta-Almeida, M., Hetland, R.D. 2013. Sensitivity of hypoxia predictions for the Northern Gulf of Mexico to sediment oxygen consumption and model nesting. American Geophysical Union.10.1002/jgrc.20077.

Fennel,K., Hu, J., Laurent, A., M., Hetland, R.D. 2013b. Pattern of phytoplankton limitation and hypoxia in the northern Gulf of Mexico: Observations, simulations and predictability. Presentation at Louisiana State University, April 2013.

Folk, R.L. 1966.A review of grain-size parameters. *Sedimentology* 6. 73–93.

Forrest, D.R., Hetland, R.D., DiMarco, S.F. 2011. Multivariable statistical regression models of the areal extent of hypoxia over the Texas-Louisiana continental shelf. Environmental Research Letters. 6.

Friedman, G.M., Sanders, J.E. 1978. Principles of Sedimentology. John Wiley & Sons, Inc. 138-139.

Gardner, W.S., McCarthy, M.J., Carini, S.A., Souza, A.C., Lijun, H., McNeal, K.S., Puckett, M.K., Pennington, J. 2009. Collection of intact sediment cores with overlying water to study nitrogen- and oxygen-dynamics in regions with seasonal hypoxia. Continental Shelf Research. 29. 2207-2213.

Goni, M.A., Alleau, Y., Corbett, R., Walsh, J.P., Mallinson, D., Allison, M.A., Gordon, E., Petsch, S., Dellapenna, T.M. 2007. The effects of Hurricanes Katrina and Rita on the seabed of Louisiana shelf. The Sedimentary Record 5. No. 1.

Grant, W.D., Madsen, O.S. 1986. The Continental-Shelf Bottom Boundary Layer.Annual Review of Fluid Mechanics. 18. 265-305.

Gulf of Mexico Data Atlas.NOAA.http://gulfatlas.noaa.gov/

Gust, G., Muller, V. 1997.Interfacial hydrodynamics and entrainment functions of currently used erosion devices. Cohesive Sediments.149-174.

Harris, C.K., Fennel, K., Hetland, R.D. 2013. Effects of resuspension on sediment bed oxygen consumption: a numerical modeling study. American Society of Limnology and Oceanography (ASLO) Aquatic Sciences Meeting, Abstract 11435, New Orleans, LA.

Hetland, R., DiMarco, S. 2007. How does the character of oxygen demand control the structure of hypoxia on the Texas-Louisiana continental shelf? Journal of Marine Systems. 70. 49-62.

Hetland, R.D., DiMarco, S.F. 2008. How does the character of oxygen demand control the structure of hypoxia on the Texas-Louisiana continental shelf? Journal of Marine Systems 70. 49-62.

Hetland, R.D., DiMarco, S.F. 2012.Skill assessment of a hydrodynamic model of circulation over the Texas-Louisiana continental shelf. Ocean Modeling. 43-44. 64-76.

Hjulstrom, F., 1935, Studies of the morphological activity of rivers as illustrated by the River Fyris: Bulletin Geological Institute, University Uppsala. 25. 221-527.

Johnson, A.G., Kelley, J.T. 1984. Temporal, spatial, and textural variation in mineralogy of Mississippi River suspended sediment. Journal of Sedimentary Petrology. 54. 1. 0067-0072.

Jones, N.W. 1999. Laboratory Manual for Physical Geology. McGraw-Hill Companies, Inc. 2nd ed. 45-46.

Justic, D., Bierman, V.J., Scavia, D., Hetland, R.D. 2007. Forecasting Gulf's Hypoxia: The next 50 years? Estuaries and Coasts. 30. 5. 791-801.

Kirchner, J.W., Dietrich, W.E., Iseya, F., Ikeda, H. 1990.The variability of critical shear stress, friction angle, and grain protrusion in water-worked sediments. Sedimentology. 37. 647-672.

McKee, B.A., Aller, R.C., Allison, M.A., Bianchi, T.S., Kineke, G.C. 2004. Transport and transformation of dissolved and particulate materials on continental margins influenced by major rivers: benthic boundary layer and seabed processes. Continental Shelf Research. 24. 899-926.

McLaren, P., Bowles, D. 1984. The Effects of Sediment Transport on Grain-Size Distributions. Journal of Sedimentary Petrology. 55. 4. 0457-0470.

Meade, R.H., Moody, J.A. 2010. Causes for the decline of suspended-sediment discharge in the Mississippi River system, 1940-2007. Hydrological Processes 24. 35-49.

Mehta, A.J., Hayter, E.J., Parker, W.R., Krone, R.B., Teeter, A.M. 1989. Cohesive Sediment Transport. I: Process Description. Journal of Hydraulic Engineering. 115. 8. 1076-1093.

Mitra, S. Bianchi, T.S. 2003. A preliminary assessment of polycyclic aromatic hydrocarbon distributions in the lower Mississippi River and Gulf of Mexico. Marine Chemistry. 82. 273-288.

Murrell, M.C., Lehrter, J.C. 2010.Sediment and Lower Water Column Oxygen Consumption in the Seasonally Hypoxic Region of the Louisiana Continental Shelf. Estuaries and Coasts. 34. 5. 912-924.

Orton, G.J., Reading, H.G. 1993. Variability of deltaic processes in terms of sediment supply, with particular emphasis on grain size. Sedimentology. 40. 475-512.

Quinones-Rivera, Z.J., Wissel, B., Justic, D., Fry, B. 2007. Partitioning oxygen sources and sinks in a stratified, eutrophic coastal ecosystem using stable oxygen isotopes. Marine Ecology Progress Series 342. 69-83.

Rabalais, N.N., Turner, R.E., Sen Gupta, B.K., Boesch, D.F., Chapman, P., Murrell, M.C. 2006. Characterization and Long-Term Trends of Hypoxia in the Northern Gulf of Mexico: Does the Science Support the Action Plan? Presentation Handout at Hypoxia In the Northern Gulf of Mexico: Assessing the State of the Science symposium. <http://water.epa.gov/type/watersheds/named/msbasin/upload/2006_10_16_msbasin_symposia_laa_session1.pdf>

Rabalais, N.N., Turner, R.E., Sen Gupta, B.K., Boesch, D.F., Chapman, P., Murrell, M.C. 2007. Characterization and Long-Term Trends of Hypoxia in the Northern Gulf of Mexico: Does the Science Support the Plan to Reduce, Mitigate, and Control Hypoxia? Estuaries and Coasts 30(5). 753-772.

Reese, B.K., Mills, H.J, Dowd, S.E., Morse, J.W. 2013.Linking Molecular MicrobialEcology to Geochemistry in a Coastal Hypoxic Zone.Geomicrobiology Journal. 30:2. 160-172.

Rowe, G.T., Cruz Kaegi, M.E., Morse, J.W., Boland, G.S., Escobar Briones, E.G. 2002. Sediment Community Metabolism Associated with Continental Shelf Hypoxia, Northern Gulf of Mexico. Estuaries 25. 1097-1106.

Sanford, L.P., Maa, J.P.Y. 2001.A unified erosion formulation for fine sediments.Marine Geology. 179. 9-23.

Santschi, P.H., Presley, B.J., Wade, T.L., Garcia-Romero, B., Baskaran, M. 2001. Historical contamination of PAHs, PCBs, DDTs, and heavy metal in Mississippi River Delta, Galveston Bay and Tampa Bay sediment cores. Marine Environmental Research. 52. 51-79.

Shepard, R.G. 1989. Correlations of Permeability and Grain Size. GROUNDWATER. 27. 5. 663-668.

Stanley, S.M. 1999. Earth Systems History. W.H. Freeman and Company. 41-43.

Tornqvist, T.E., Paola, C., Parker, G., Liu, K., Mohrig, D., Holbrook, J.M., Twilley, R.R. 2007. Comment on "Wetland Sedimentation from Hurricanes Katrina and Rita. Science. 316. 201b.

Turner, R.E., Baustian, J.J., Swenson, E.M., Spicer, J.S. 2006.Wetland Sedimentation from Hurricanes Katrina and Rita. Science. 314. 449-452.

Turner, R.E., Rabalais, N.N., Justic, D. 2006. Predicting summer hypoxia in the northern Gulf of Mexico: Riverine N, P, and Si loading. Marine Pollution Bulletin 52, Issue 2, 139-148.

Turner, R.E., Rabalais, N.N., Justic, D. 2008. Gulf of Mexico Hypoxia: Alternate States and a Legacy. Environmental Science and Technology 42, 2323-2327.

Tweel, A.W., Turner, R.E. 2012. Landscape-Scale Analysis of Wetland Sediment Deposition from Four Tropical Cyclone Events.PLoS ONE 7(11): e50528. doi:10.1371/journal.pone.0050528.

Wainright, S.C., Hopkinson Jr., C.S. 1997. Effects of sediment resuspension on organic matter processing in coastal environments: a simulation model. Journal of Marine Systems 11. 353-368.

Wang, L., Justic, D. 2009. A modeling study of the physical processes affecting the development of seasonal hypoxia over the inner Louisiana-Texas shelf: Circulation and stratification. Continental Shelf Research 29. 1464-1476.

Warner, J.C., Sherwood, C.R., Signell, R.P., Harris, C.K., Arango, H.G. 2008.Development of a three-dimensional, regional, coupled wave, current, and sediment-transport model. Computers& Geosciences. 34. 1284-1306.

Wentworth, C. 1922. A Scale of Grade and Class Terms for ClasticSediments.The Journal of Geology. 30. 5. 377-392.

Wright, J., Open University. 1999. Waves, Tides and Shallow-Water Processes. Elsevier Science & Technology Books. 96-116.

Xu, K., Briggs, K., Cartwright, G., Corbett, D.R., Friedrichs, C.T., Harris, C.K., Mickey, R.C., Walsh, J.P. Seabed Erodibility on the Louisiana Continental Shelf Before and After 2011 Mississippi River Great Flood. In prep for submission to Geophysical Research Letters.

Xu, K., Harris, C.K., Hetland, R.D., Kaihatu, J.M. 2011. Dispersal of Mississippi and Atchafalaya sediment on the Texas-Louisiana shelf: Model estimates for the year 1993. Continental Shelf Research 31. 1558–1575.

Zhang, X., Marta-Almeida, M., Hetland, R.D. 2012.A high-resolution pre-operational forecast model of circulation on the Texas-Louisiana continental shelf and slope. Journal of Operational Oceanography. 5. 1. 19-34.

FIGURES:

Table 2-1
Summary of cruise dates and number of samples taken from each station during each cruise.

Year	**2011**	**2011**	**2011**	**2012**	**2012**
Month	April	Early August	Mid August	April	Mid August
Cruise	**MCH**	**NSF Rapid**	**MCH**	**MCH**	**MCH**
No. of stations	4	28	4	4	4
Sediment Cores	4	28	4	4	4
Sub core length(cm)	12	10	10	12	11
No. of GS analyses	48	56	40	48	44

Table 2-2. Station name and region sampled during August 2011. Grain size measurements (Phi): mean, median, standard deviation, skewness, and kurtosis.

Station Location	Phi scale				
East of Terrebonne Bay	**Mean GS**	**Median GS**	**SD (Sorting)**	**Skew**	**Kurt**
S68	6.51	6.64	2.13	-0.08	1.07
S50	6.62	6.81	2.27	-0.13	1.09
S64	6.44	6.76	2.50	-0.15	0.93
S1	6.72	6.74	2.04	-0.03	1.19
S60	6.42	6.51	2.11	-0.02	0.95
S54	6.19	5.92	2.07	0.19	0.92
S12	6.82	6.81	1.92	0.0047	1.08
S15	6.85	6.87	1.93	-0.05	1.25
S7	6.13	6.39	2.38	-0.12	0.98
S3	6.88	6.92	1.90	-0.05	1.20
S11	5.68	5.81	2.20	-0.03	0.93
S18	6.17	6.18	1.86	0.04	1.05
S5	6.72	6.80	2.07	-0.08	1.26
S20	6.52	6.93	2.45	-0.20	1.12
S22	6.13	6.30	2.26	-0.07	0.98
AB5	6.35	6.24	1.98	0.12	1.04
Mid-shelf					
S46	6.35	6.34	2.24	0.01	0.98
10B	4.99	4.11	2.56	0.50	0.74
S45	6.29	6.38	2.05	-0.0005	0.94
S44	6.28	6.30	1.95	0.0038	1.10
South and West of Atchafalaya Bay					
S29	6.03	6.01	2.24	0.03	0.96
08C	5.93	5.89	2.38	0.10	0.83
S34	6.83	6.77	1.80	0.06	1.13
S41	6.73	6.81	2.08	-0.09	1.24
S37	6.66	6.93	2.31	-0.17	1.17
S39	4.98	4.21	2.10	0.53	0.90
S35	6.23	6.39	2.14	-0.09	1.14
Average	**6.31**	**6.32**	**2.14**	**0.01**	**1.04**

Table 2-3. Salinity, DO, and Temperature comparison of overlying water in sediment cores after retrieval and CTD profiles. Data collected in August 2012.

CTD			Hach Sensor in sediment core		
AB5			AB5		
Height above sediment (m)	1	1	Height above sediment (cm)	24	4
Salinity (ppt)	25.25	36	Salinity (ppt)	25	35
DO (mg/L)	5	0.5	DO (mg/L)	na	na
Temperature ^{o}C	31	26.5	Temperature ^{o}C	na	na
10B			10B		
Height above sediment (m)	1	1	Height above sediment (cm)	20	3
Salinity (ppt)	29.8	36	Salinity (ppt)	30.8	35.2
DO (mg/L)	4.75	1.5	DO (mg/L)	7.56	1.99
Temperature ^{o}C	31	26.5	Temperature ^{o}C	29.8	27.6
08C					
Height above sediment (m)	1	1	Height above sediment (cm)	24	3
Salinity (ppt)	31.8	36	Salinity (ppt)	33	35.6
DO (mg/L)	4.2	1.8	DO (mg/L)	7.69	2.77
Temperature ^{o}C	31	28	Temperature ^{o}C	28.3	28.2

Millimeters	μm	Phi (ϕ)	Wentworth size class	
		-20		
4096		-12	Boulder (-8 to -12ϕ)	
1024		-10		
256		-8	Pebble (-6 to -8ϕ)	
64		-6		
16		-4	Pebble (-2 to -6ϕ)	Gravel
4		-2		
3.36		-1.75		
2.83		-1.50	Gravel	
2.38		-1.25		
2.00		-1.00		
1.68		-0.75		
1.41		-0.50	Very coarse sand	
1.19		-0.25		
1.00		-0.00		
0.84		0.25		
0.71		0.50	Coarse sand	
0.59		0.75		
1/2 — 0.50	500	1.00		
0.42	420	1.25		
0.35	350	1.50	Medium sand	Sand
0.30	300	1.75		
1/4 — 0.25	250	2.00		
0.210	210	2.25		
0.177	177	2.50	Fine sand	
0.149	149	2.75		
1/8 — 0.125	125	3.00		
0.105	105	3.25		
0.088	88	3.50	Very fine sand	
0.074	74	3.75		
1/16 — 0.0625	63	4.00		
0.0530	53	4.25		
0.0440	44	4.50	Coarse silt	
0.0370	37	4.75		
1/32 — 0.0310	31	5		
1/64 0.0156	15.6	6	Medium silt Fine silt	
1/128 0.0078	7.8	7	Very fine silt	
1/256 — 0.0039	3.9	8		Mud
0.0020	2.0	9		
0.00098	0.98	10		
0.00049	0.49	11	Clay	
0.00024	0.24	12		
0.00012	0.12	13		
0.00006	0.06	14		

Figure 2-1. Wentworth grain size scale (Wentworth, 1922).

A

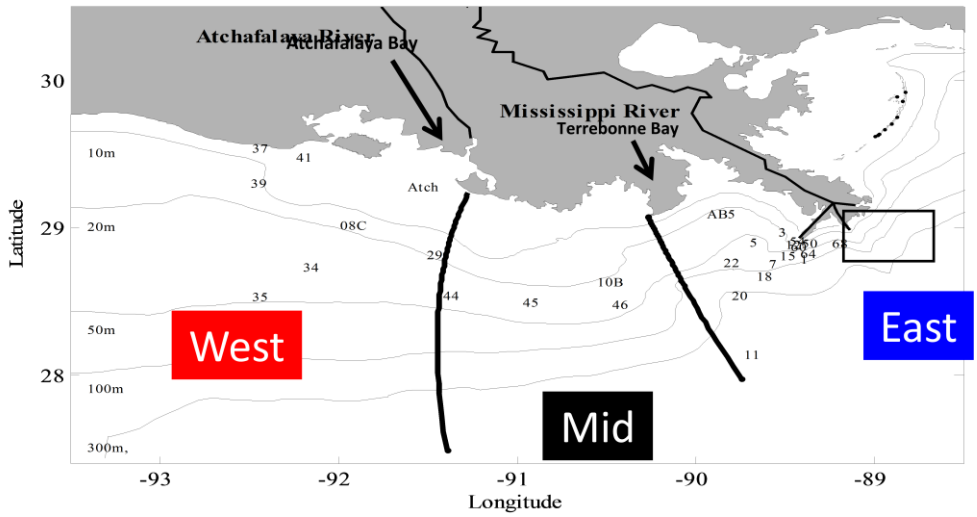

B

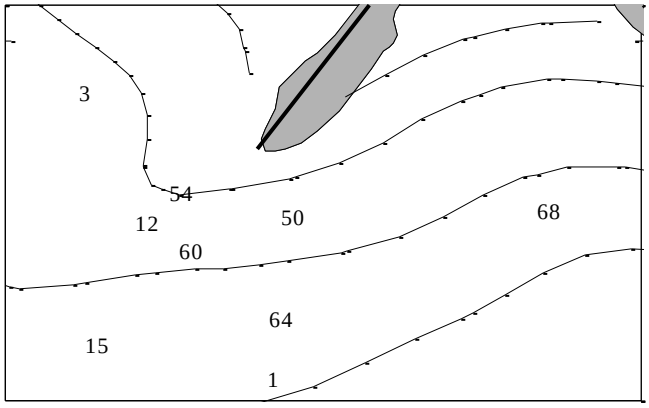

Figure 2-2. (A) Map of sampling locations, indicated by station labels, across northern Gulf of Mexico. All sites used in spatial variability analysis; only AB5, 10B, 08C, Atch were used in temporal variability analysis. Black lines indicate different regions (West of Atchafalaya Bay, Mid-shelf, East of Terrebonne Bay). (B) Zoom in of stations located near SW Pass of Mississippi Delta (box).

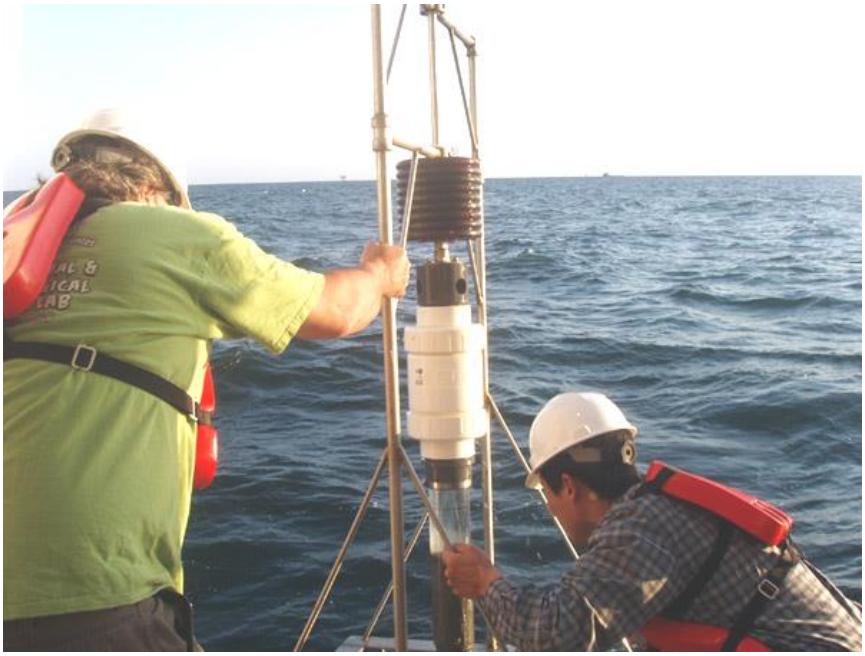

Figure 2-3. Hypox coring device used to retrieve seabed sediment samples.

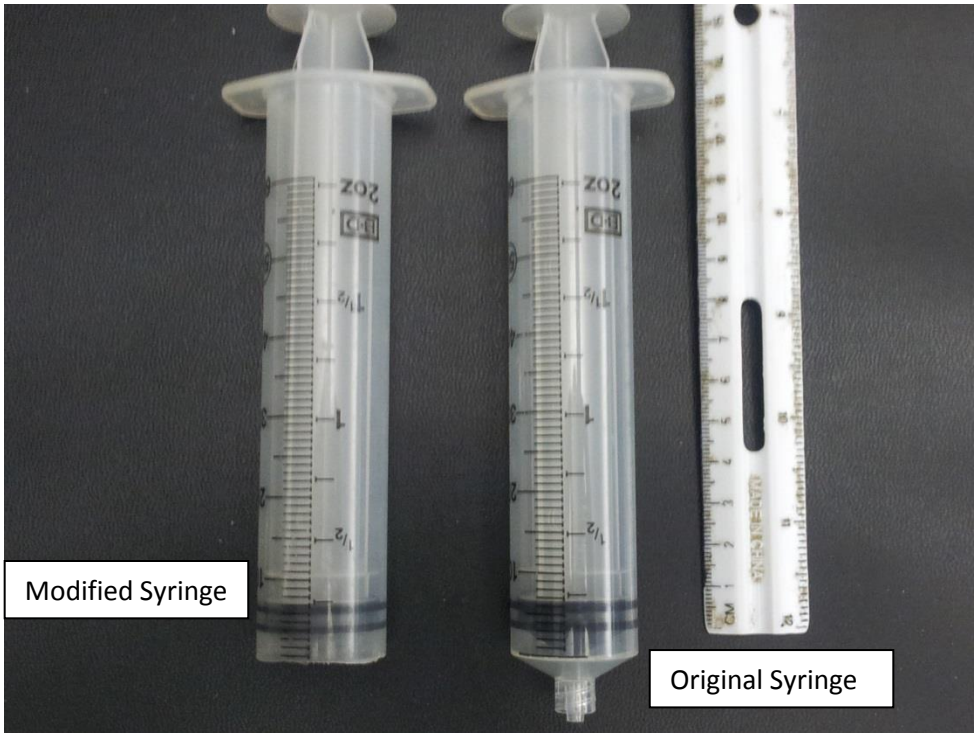

Figure 2-4. Modified syringe used to take sub-cores of sediment (10-12cm).

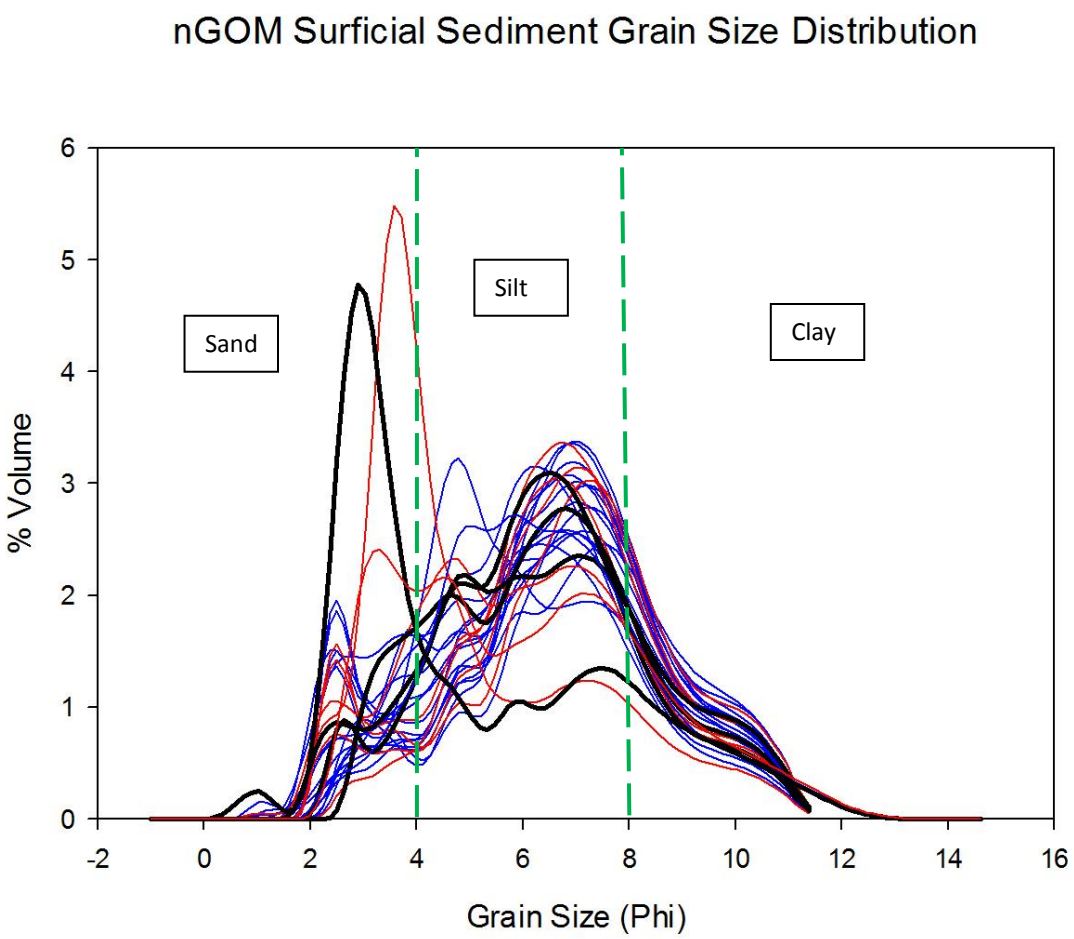

Figure 2-5. Grain size (Phi) distribution by percent volume for all surficial sediment samples taken in August 2011 on the RAPID Cruise.Blue: East of Terrebonne Bay, Black: Mid-shelf, Red: West of Terrebonne Bay. Green dashed lines indicate changes in sediment size class.

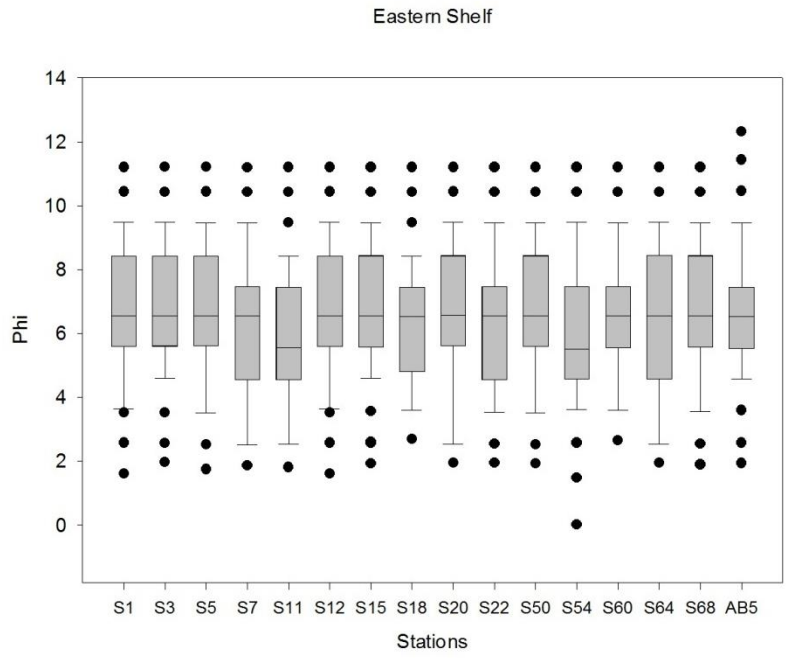

Figure 2-6. Grain size distribution box plots for stations on the eastern shelf. Median indicated by the black center line, first and third quartiles are the edges of gray boxes, upper and lower quartile are edges of lines, and dots indicate outliers.

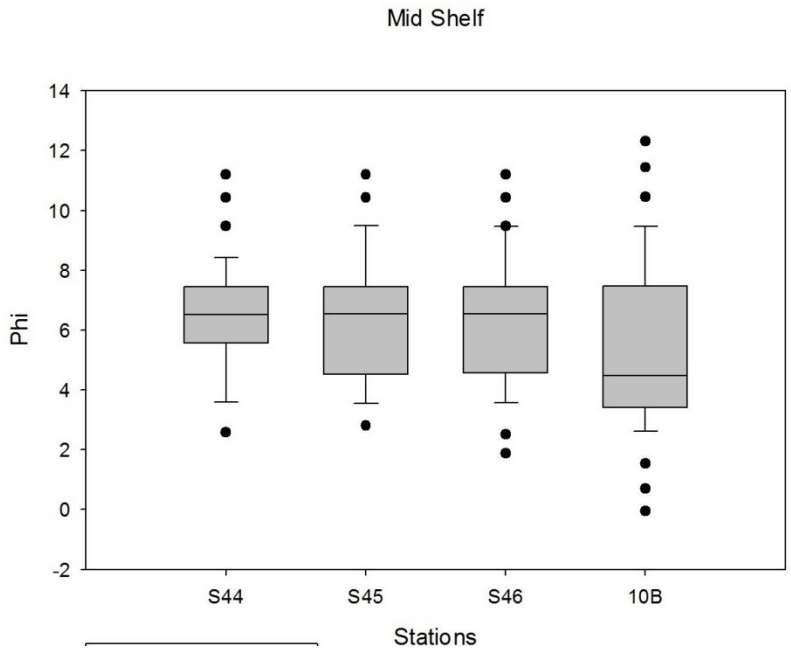

Figure 2-7. Grain size distribution box plots for stations on the mid shelf. Median indicated by the black center line, first and third quartiles are the edges of gray boxes, upper and lower quartile are edges of lines, and dots indicate outliers.

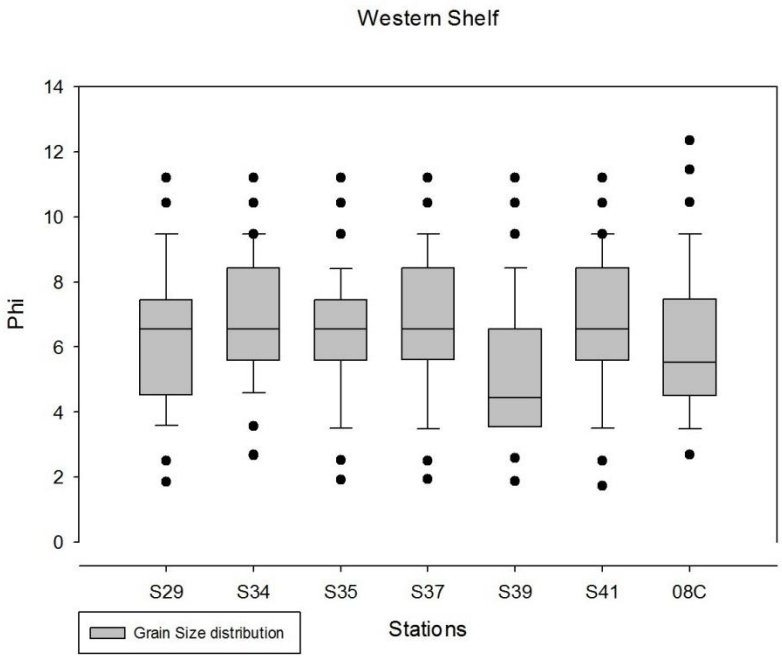

Figure 2-8. Grain size distribution box plots for stations on the western shelf. Median indicated by the black center line, first and third quartiles are the edges of gray boxes, upper and lower quartile are edges of lines, and dots indicate outliers.

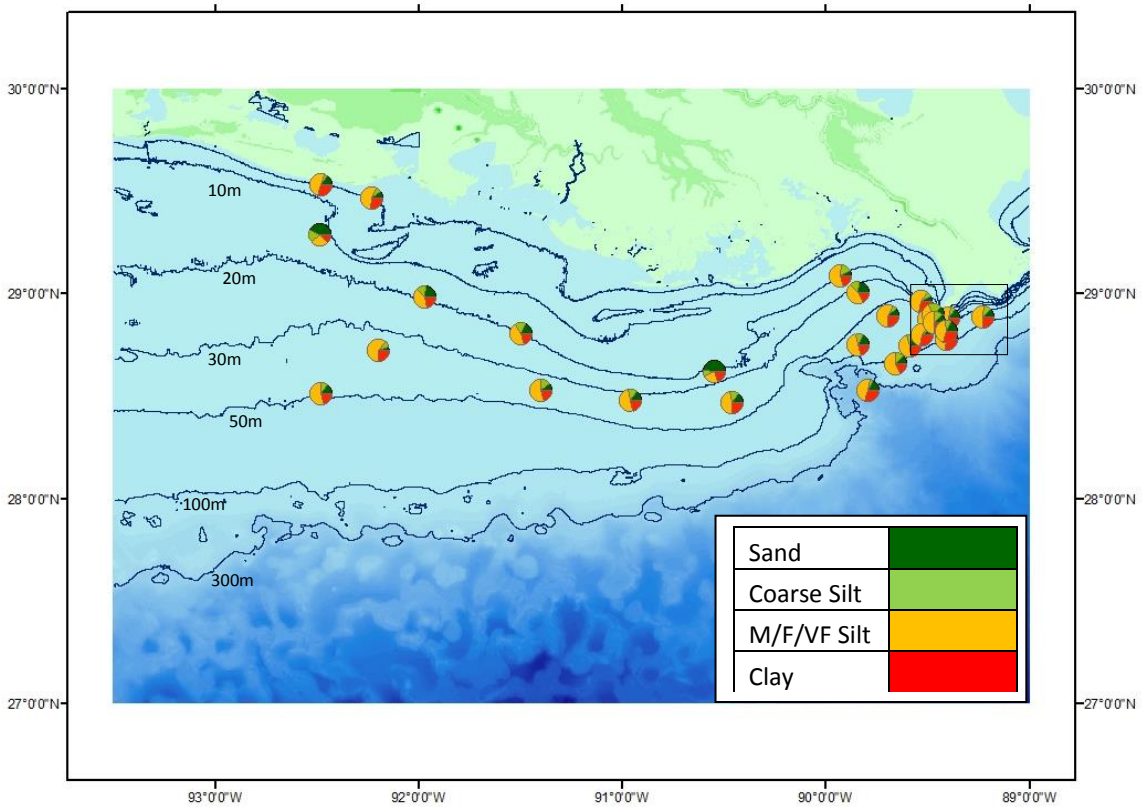

Figure 2-9. Plot of pie charts representing percentage of 4 different sediment types (Sand, Coarse Silt, Medium/Fine/Very Fine Silt, Clay). Each pie chart is plotted at the station location to indicate grain size percentages. Small black box represents inset corresponding to Figure 2-10.

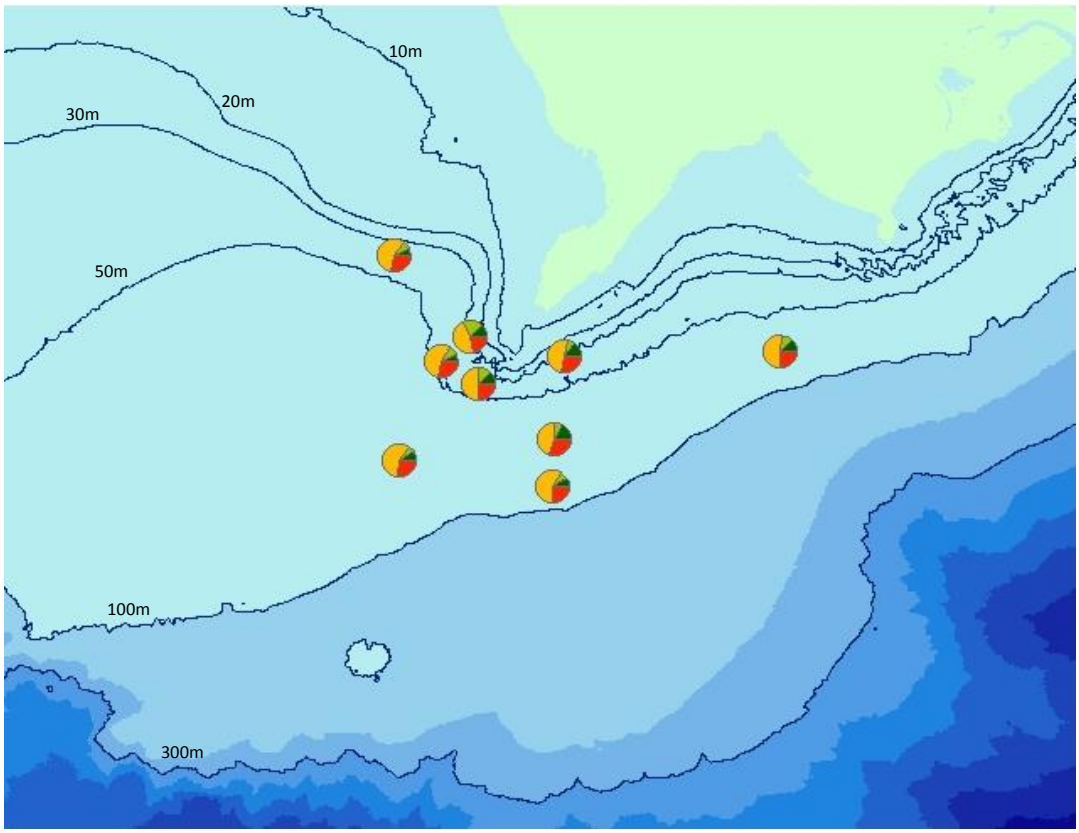

Figure 2-10. Plot of pie charts representing percentage of 4 different sediment types (Sand, Coarse Silt, Medium/Fine/Very Fine Silt, Clay) near the mouth of the SW pass of Mississippi River.

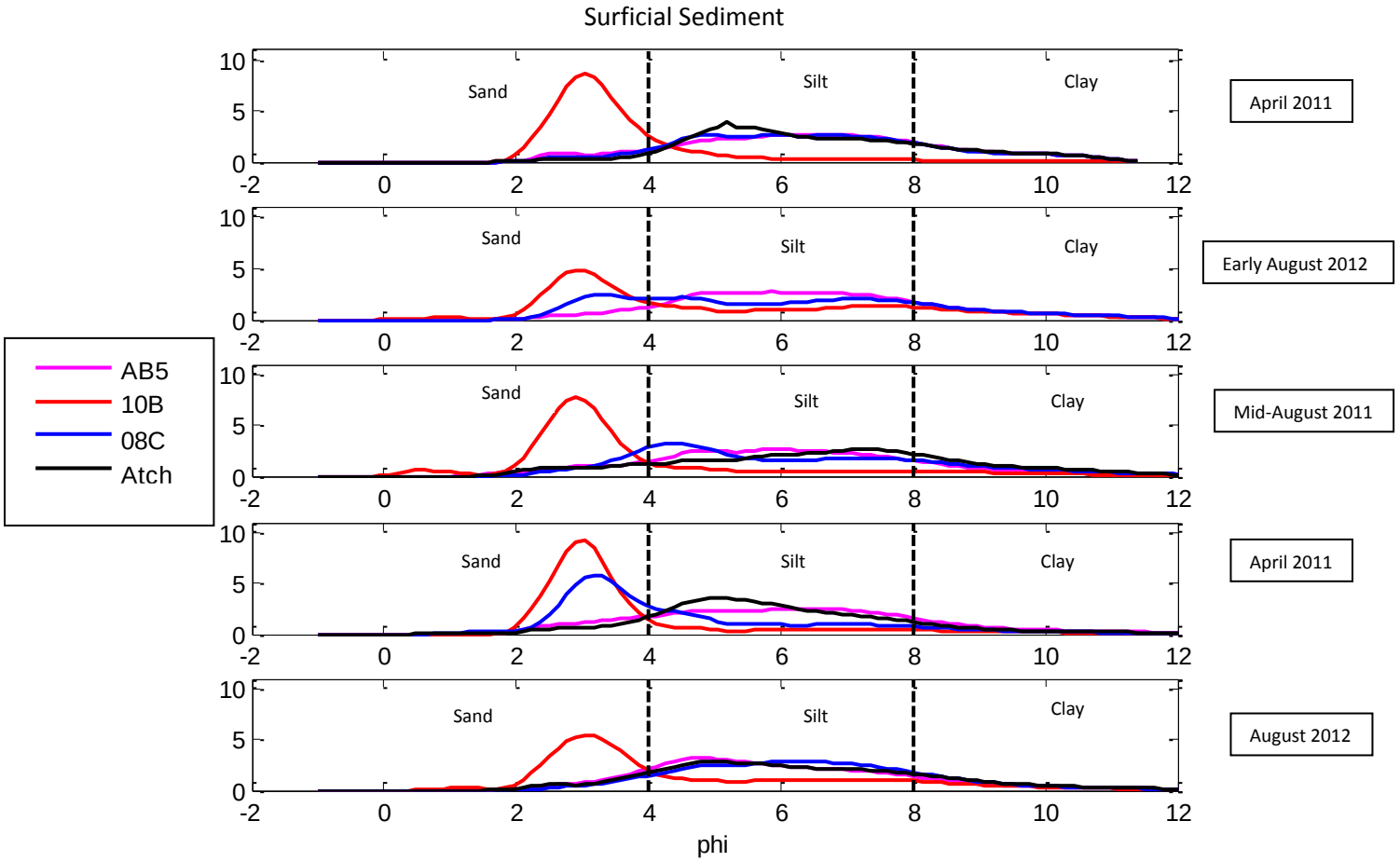

Figure 2-11.Time series subplot of volume percent of mean grain size in phi scale for 4 stations surficial sediment (0-1cm) samples over 2 year period. Solid vertical lines indicate sediment size class based on Wentworth scale.

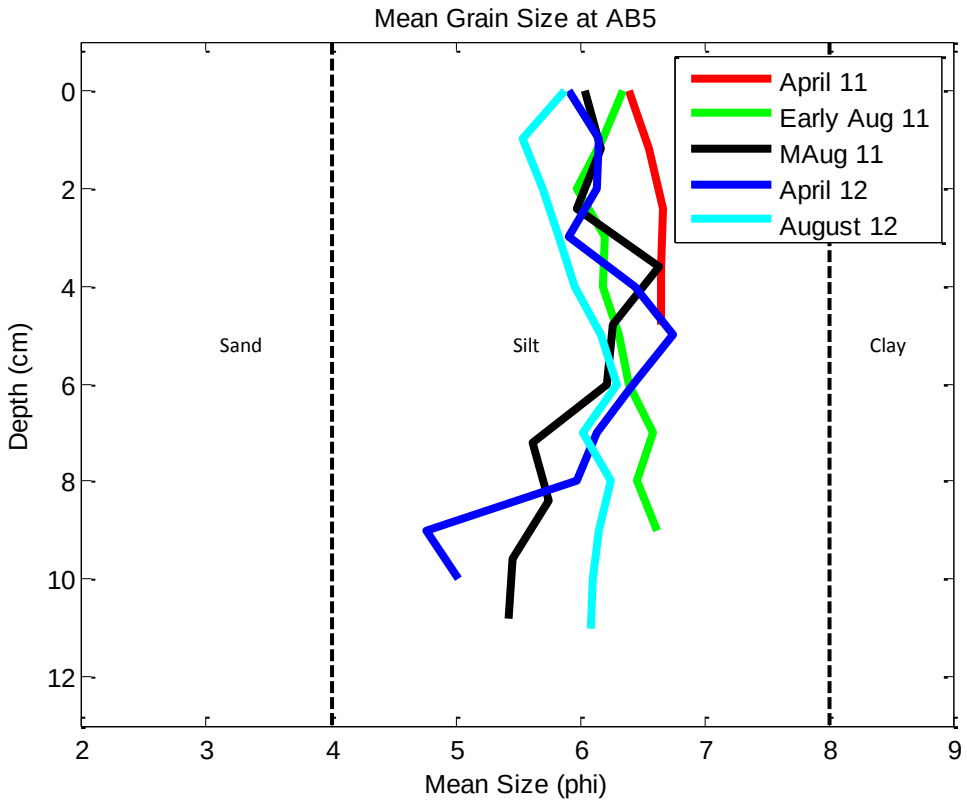

Figure 2-12. Mean grain size related to depth of 10-12cm core taken on each cruise at station AB5. Solid vertical lines indicate sediment size class based on Wentworth scale.

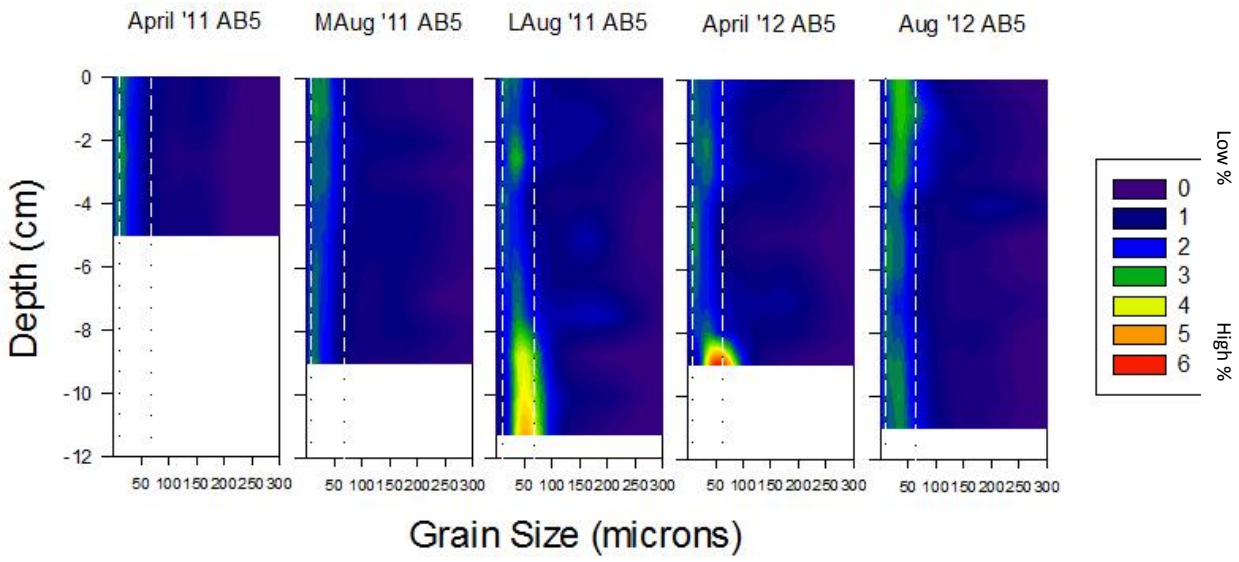

Figure 2-13. Contour plot of down core sediment grain size percent volume for each subsample at station AB5. White dashed lines indicate changes in sediment size classes (Sand>63µm>silt>4µm>clay).

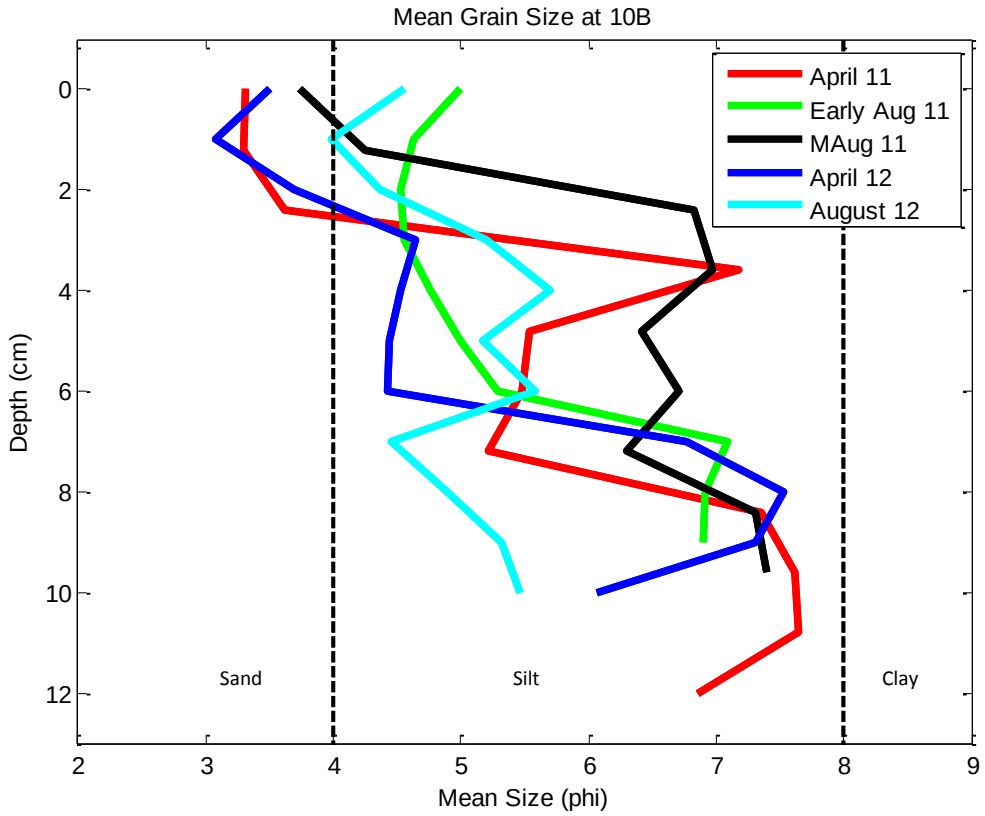

Figure 2-14. Mean grain size related to depth of 10-12cm core taken on each cruise at station 10B. Solid vertical lines indicate sediment size class based on Wentworth scale.

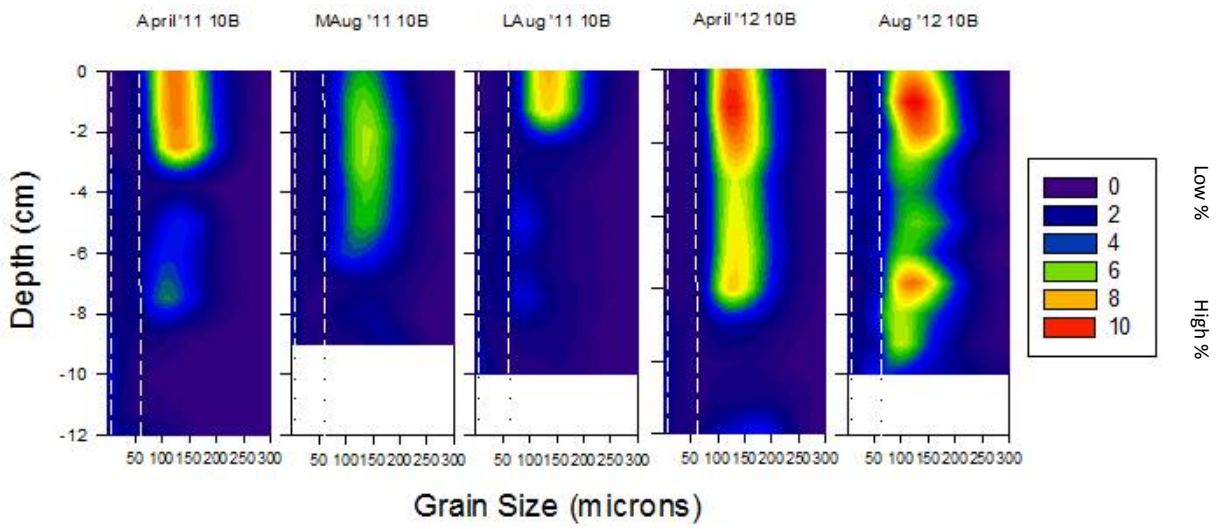

Figure 2-15. Contour plot of down core sediment grain size percent volume for each subsample at station 10B. White dashed lines indicate changes in sediment size classes (Sand>63µm>silt>4µm>clay).

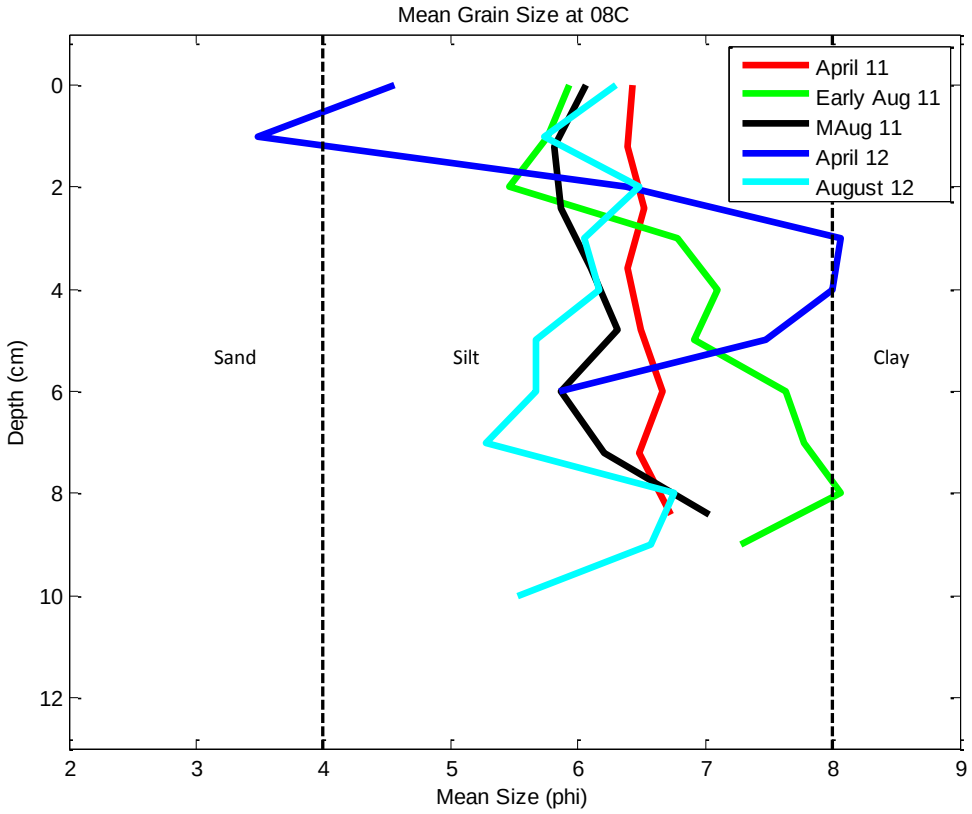

Figure 2-16. Mean grain size related to depth of 10-12cm core taken on each cruise at station 08C. Solid vertical lines indicate sediment size class based on Wentworth scale.

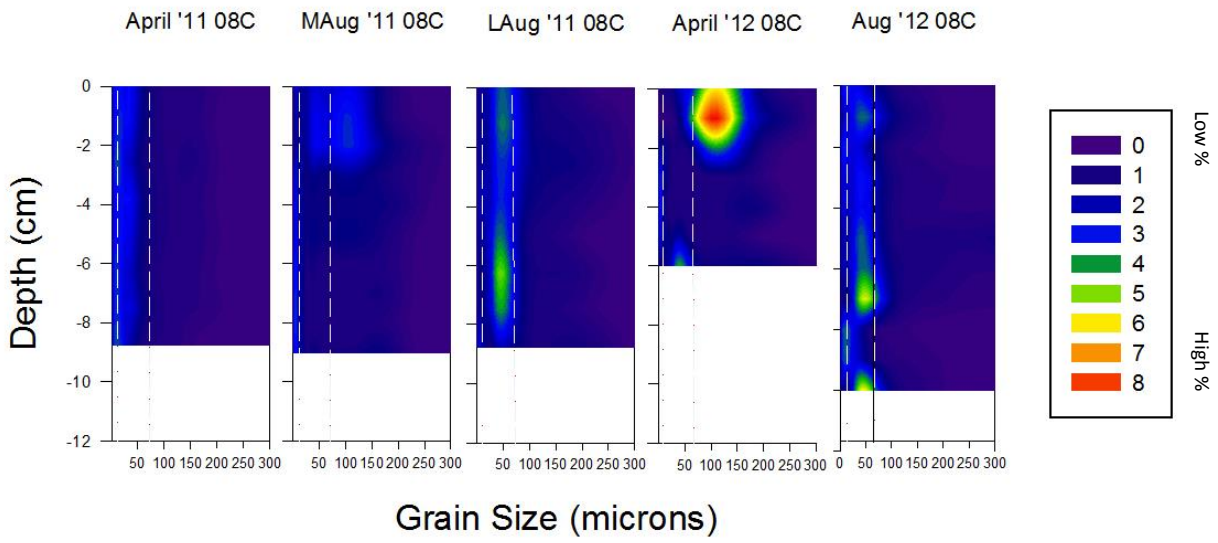

Figure 2-17. Contour plot of down core sediment grain size percent volume for each subsample at station 08C. White dashed lines indicate changes in sediment size classes (Sand>63µm>silt>4µm>clay).

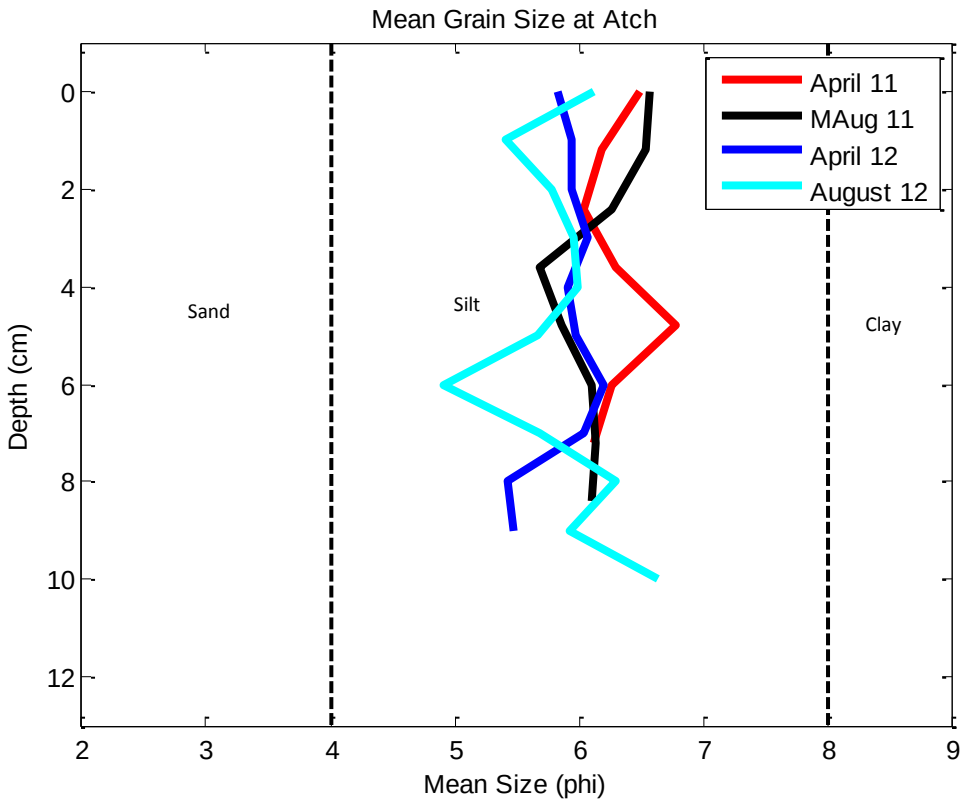

Figure 2-18. Mean grain size related to depth of 10-12cm core taken on each cruise at station Atch. Solid vertical lines indicate sediment size class based on Wentworth scale.

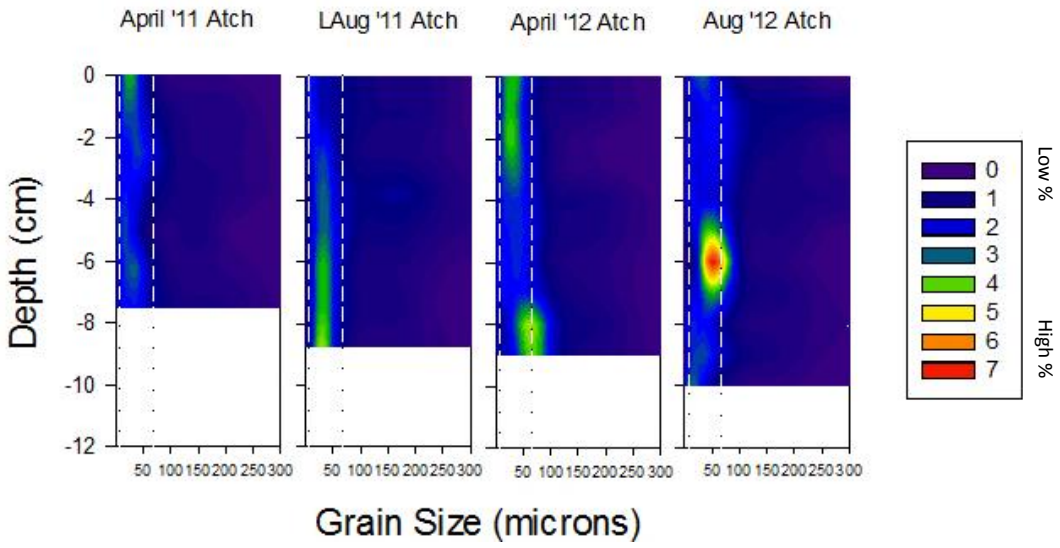

Figure 2-19. Contour plot of down core sediment grain size percent volume for each subsample at station Atch. White dashed lines indicate changes in sediment size classes (Sand>63µm>silt>4µm>clay).

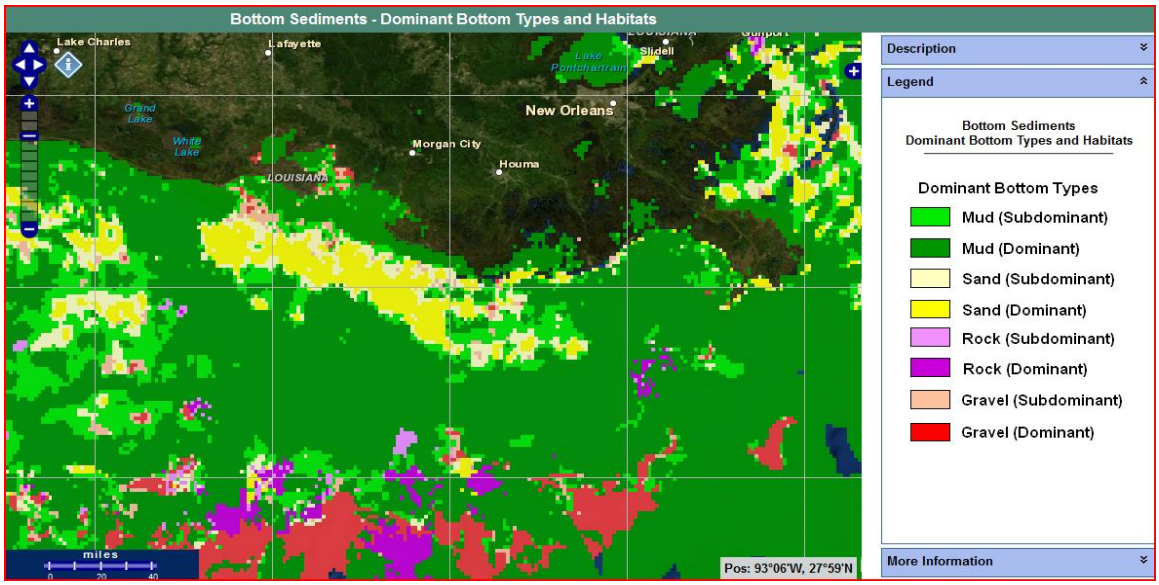

Figure 2-20. GIS map of dominant bottom sediment types from the Gulf of Mexico Data Atlas provided by NOAA (gulfatlas.noaa.gov).

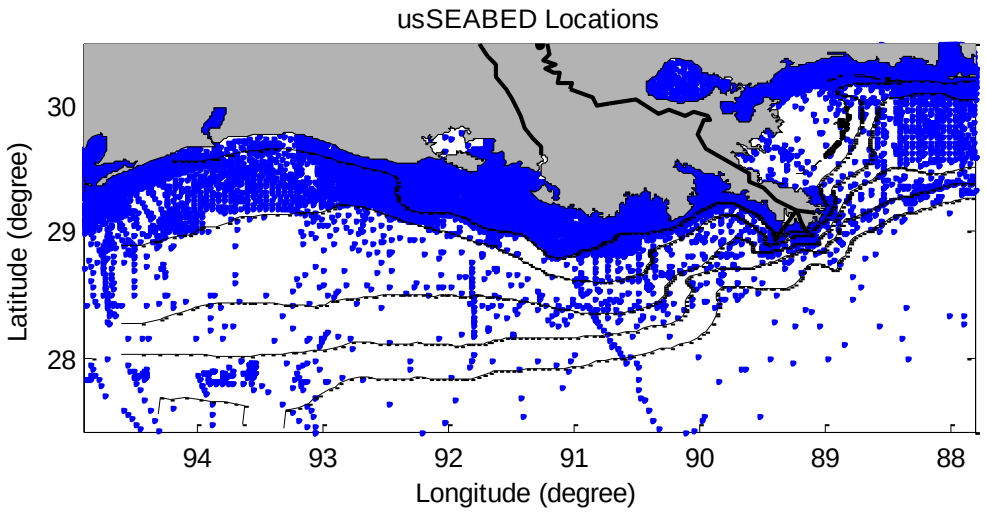

Figure 2-21. Locations of >50,000 grain size data points from usSEABED in the northern Gulf of Mexico from the USGS (Buczkowski et al., 2006).

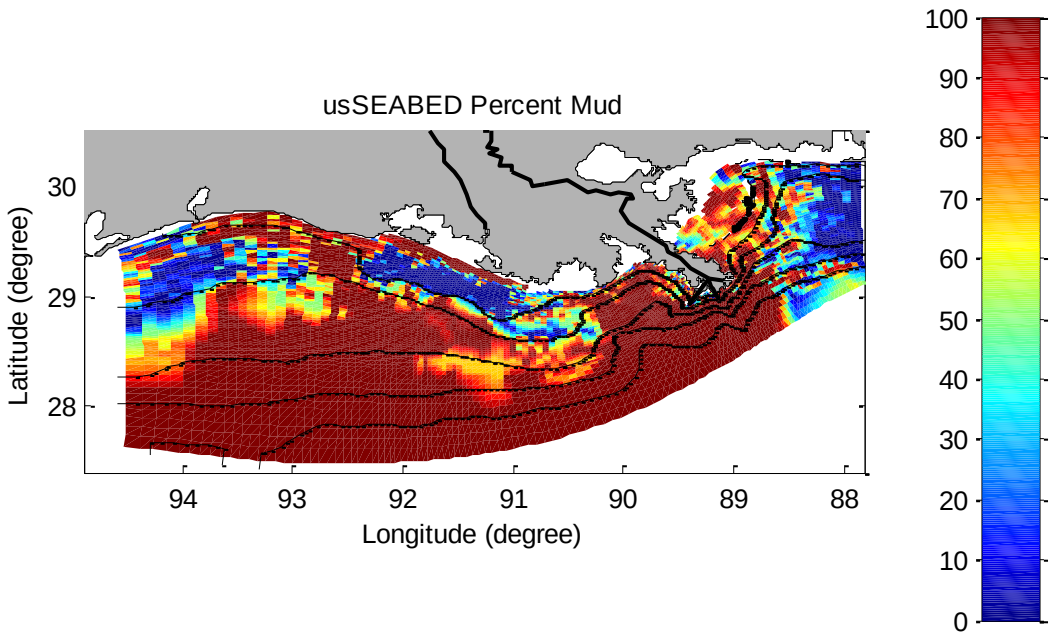

Figure 2-22. Interpolated mud fraction within the model grid based on usSEABED data. Isobaths contoured at 10, 20, 50, 100, 300m. Shoals shallower than 10m south of Atchafalaya Bay are sandy (Buczkowski et al., 2006).

SCALES FOR SORTING

Sorting term	σ, φ *units*	
	FOLK *and* WARD *(1957)*	FRIEDMAN *(1962b)*
Very well sorted	0.35	0.35
Well sorted	0.50	0.50
Moderately well sorted	0.71	0.80
Moderately sorted	1.00	1.40
Poorly sorted	2.00	2.00
Very poorly sorted	4.00	2.60
Extremely poorly sorted		

Figure 2-23. Folk and Ward (1957) and Friedman (1962) scales for sorting based on phi scale standard deviation.

Table 3-1. Cruise information, coring method used during cruise, number of stations visited during each cruise, number of Gust experiments conducted on each cruise, number of sediment cores retrieved on each cruise.

Project	P.I.	Month/ Year	Research Vessel	Coring Device	Stations	Gust Experiments	Cores
NOAA NGOMEX (MCH)	DiMarco, Bianchi et al.	**Apr-11**	**Pelican**	**Box and *Hypox***	**4**	**4**	**8**
NSF RAPID	Walsh et al.	**Aug-11**	**Cape Hatteras**	**Multi-core**	**28**	**28**	**56**
NOAA NGOMEX (MCH)	DiMarco, Bianchi et al.	**Aug-11**	**Pelican**	**Box and *Hypox***	**4**	**4**	**8**
NOAA NGOMEX (MCH)	DiMarco, Bianchi et al.	**Apr-12**	**Pelican**	***Hypox***	**4**	**8**	**16**
NOAA NGOMEX (MCH)	DiMarco, Bianchi et al.	**Aug-12**	**Pelican**	***Hypox***	**4**	**8**	**16**

Table 3-2. Salinity, DO, and Temperature comparison of overlying water in sediment core and CTD profiles. Data collected in August 2012.

CTD (raw)			Hach Sensor in core		
AB5	Surface		AB5		
Height above seabed (m)	20	1	Height above seabed (m)	0.24	0.04
Salinity (ppt)	25.25	36	Salinity (ppt)	25	35
DO (mg/L)	5	0.5	DO (mg/L)	na	na
Temp ^{o}C	31	26.5	Temp ^{o}C	na	na
10B	Surface		10B		
Height above sediment (m)	20	1	Height above sediment (m)	0.20	0.03
Salinity (ppt)	29.8	36	Salinity (ppt)	30.8	35.2
DO (mg/L)	4.75	1.5	DO (mg/L)	7.56	1.99
Temp ^{o}C	31	26.5	Temp ^{o}C	29.8	27.6
08C	Surface		08C		
Height above sediment (m)	20	1	Height above sediment (m)	0.24	0.03
Salinity (ppt)	31.8	36	Salinity (ppt)	33	35.6
DO (mg/L)	4.2	1.8	DO (mg/L)	7.69	2.77
Temp ^{o}C	31	28	Temp ^{o}C	28.3	28.2

Table 3-3. TSS concentrations (mg/L) for source water taken from 1 m above seabed with CTD Rosette. Time indicates when throughout the experiment the sample was taken (0=begin, 60=mid, 120=before 0.6Pa application). The last three rows are for duplicated cores during the August 2012 cruise.

Cruise	AB5	10B	08C	Time (min)
Apr-12	94.44	135.38	110.02	0
Aug-12	105.5	112.3	150.6	0
Aug-12	138	173.3	169.2	60
Aug-12	154.7	297.3	188.3	120
Aug-12		65.52	49.5	0
Aug-12		49.57	56.22	60
Aug-12		47.68	34.75	120

Table 3-4. VSS Concentrations (mg/L) for source water samples collected at the beginning, middle, and near the end of the Gust experiments.

	Cruise date	Begin	Middle	End
AB5	Apr-12	15.39		
	Aug-12	22.39	27.99	36.09
10B	Apr-12	17.80		
	Aug-12	17.79	31.59	61.49
08C	Apr-12	11.99		
	Aug-12	20.19	28.59	39.39

Table 3-5. Results of orthogonal polynomial contrast to test linear or quadratic trend of the mean of VSS between different critical shear stress (CSS) levels at Station AB5. Effect=CSS Method=Tukey-Kramer (P<0.01) Set=1.

Obs	CSS	Estimate	Standard Error	Alpha	Lower	Upper	Letter Group
1	0.01	2.8090	0.2337	0.05	2.3346	3.2835	A
2	0.6	2.7615	0.2337	0.05	2.2871	3.2360	A
3	0.45	2.3187	0.2584	0.05	1.7941	2.8433	AB
4	0.1	1.0688	0.2337	0.05	0.5943	1.5432	BC
5	0.05	1.0192	0.2337	0.05	0.5448	1.4937	C
6	0.3	0.8044	0.2337	0.05	0.3299	1.2789	C
7	0.2	0.4470	0.2337	0.05	-0.02747	0.9215	C

Table 3-6. Results of orthogonal polynomial contrast to test linear or quadratic trend of the mean of VSS between different critical shear stress (CSS) levels at Station 10B. Effect=CSS Method=Tukey-Kramer (P<0.01) Set=1.

Obs	CSS	Estimate	Standard Error	Alpha	Lower	Upper	Letter Group
1	0.01	2.9538	0.3123	0.05	2.3190	3.5885	A
2	0.6	2.0593	0.3325	0.05	1.3835	2.7351	AB
3	0.05	1.6845	0.3123	0.05	1.0498	2.3193	AB
4	0.2	1.5278	0.3123	0.05	0.8931	2.1626	B
5	0.45	1.4253	0.3325	0.05	0.7495	2.1011	B
6	0.1	1.4218	0.3123	0.05	0.7871	2.0565	B
7	0.3	0.7592	0.3123	0.05	0.1245	1.3940	B

Table 3-7. Results of orthogonal polynomial contrast to test linear or quadratic trend of the mean of VSS between different critical shear stress (CSS) levels at Station 08C. Effect=CSS Method=Tukey-Kramer (P<0.01) Set=1.

Obs	CSS	Estimate	Standard Error	Alpha	Lower	Upper	Letter Group
1	0.01	3.3041	0.2720	0.05	2.7518	3.8563	A
2	0.6	2.5270	0.2899	0.05	1.9386	3.1155	AB
3	0.45	1.8368	0.2720	0.05	1.2845	2.3890	BC
4	0.1	1.6745	0.2720	0.05	1.1223	2.2268	BC
5	0.05	1.4603	0.2720	0.05	0.9081	2.0126	BC
6	0.2	0.7125	0.2720	0.05	0.1603	1.2648	C
7	0.3	0.6833	0.2720	0.05	0.1310	1.2355	C

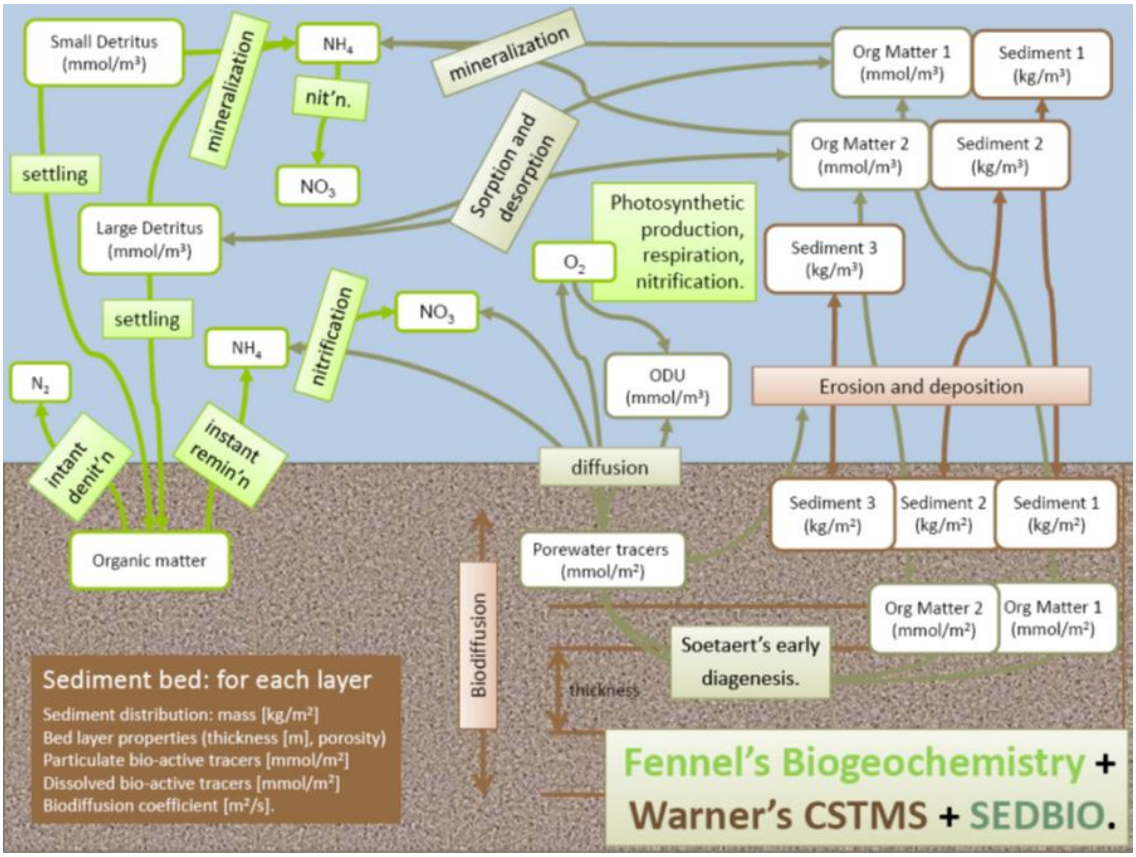

Figure 3-1. Schematic showing processes included in the linked sediment transport – biogeochemistry model. Green and brown, respectively, shows processes included in Fennel et al.'s (2011) biogeochemistry and Warner et al.'s (2008) sediment transport models. (Harris et al., 2013).

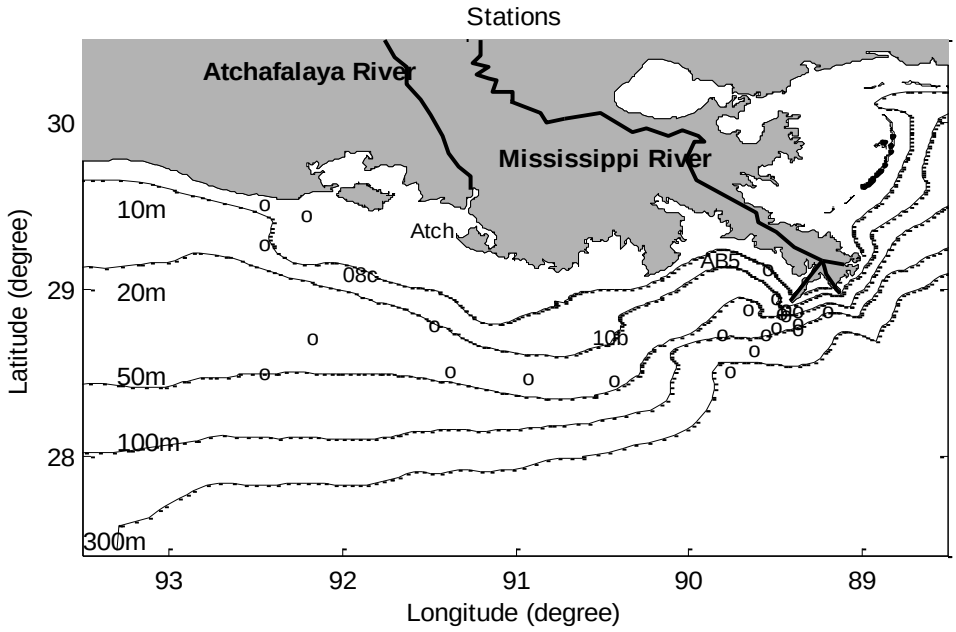

Figure 3-2. Map of sample station locations across northern Gulf of Mexico.

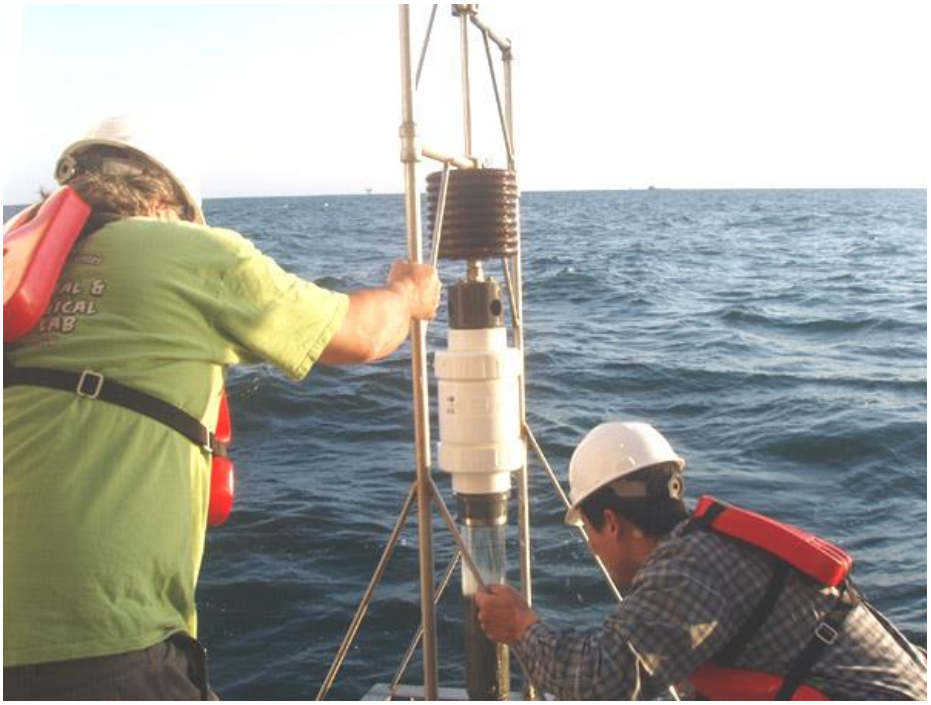

Figure 3-3. *Hypox* corer on R/V Pelican.

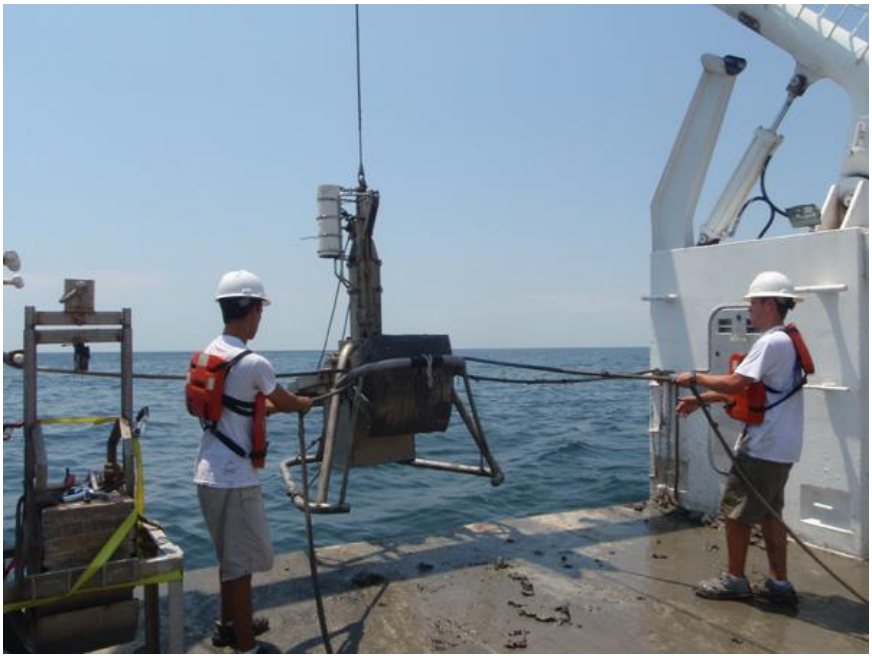

Figure 3-4. Box corer on R/V Pelican.

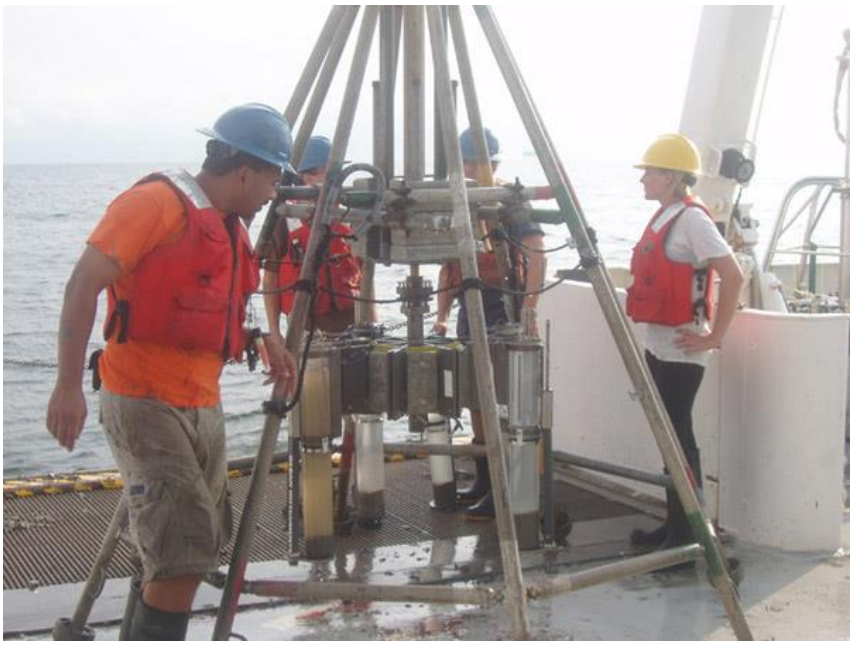

Figure 3-5. Multi-corer on R/V Cape Hatteras.

Figure 3-6. Dual-core Gust Erosion Microcosm System and Filtration System.

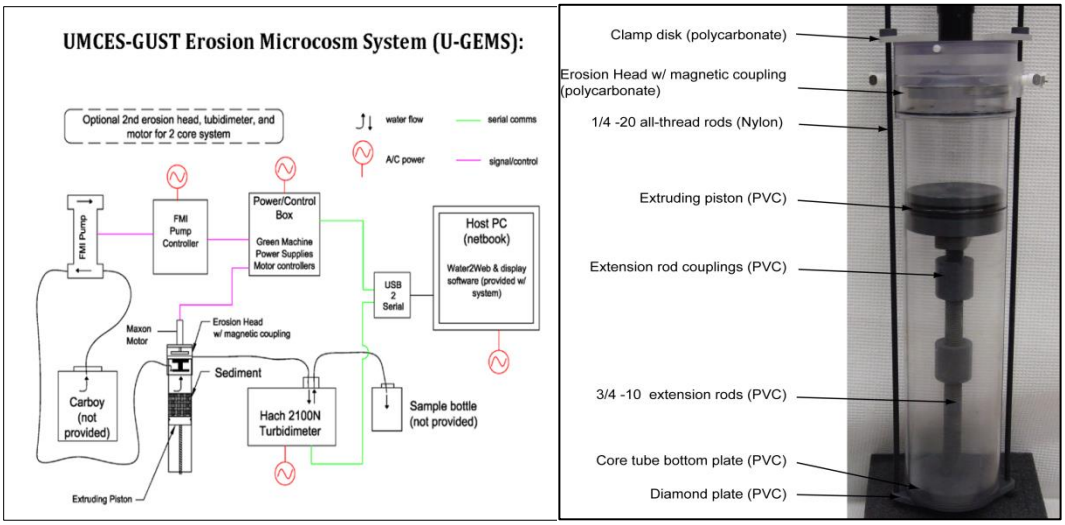

Figure 3-7. Flow schematic of Gust Erosion Microcosm System and Core accessory description (from Green Eyes: Environmental Observing Systems).

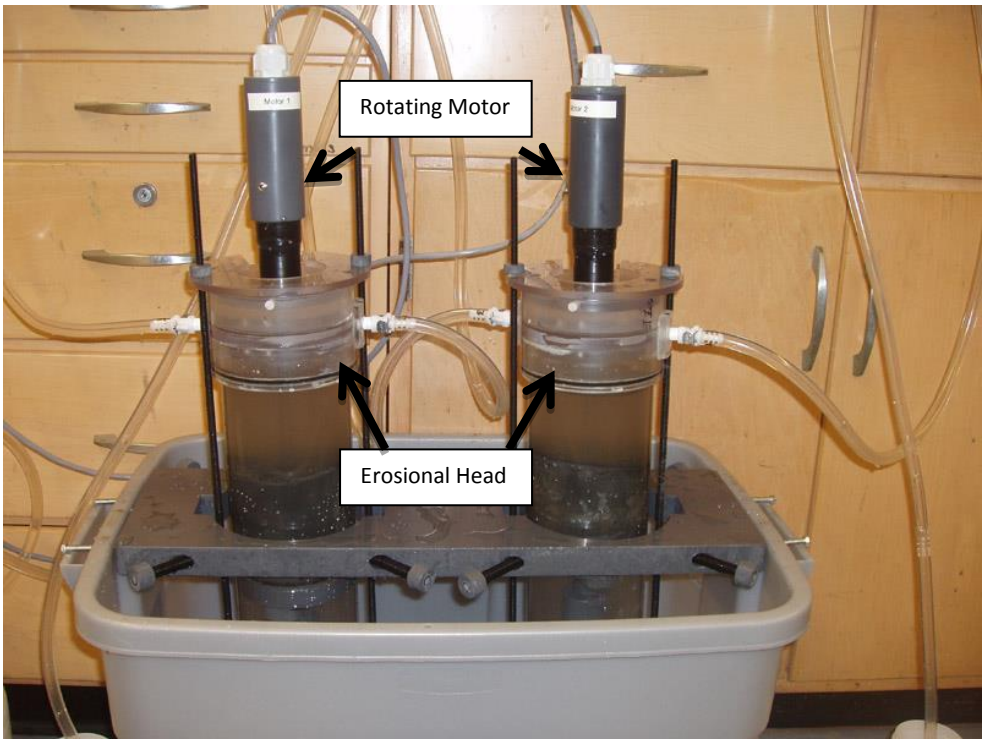

Figure 3-8. Gust rotating motors and erosional heads.

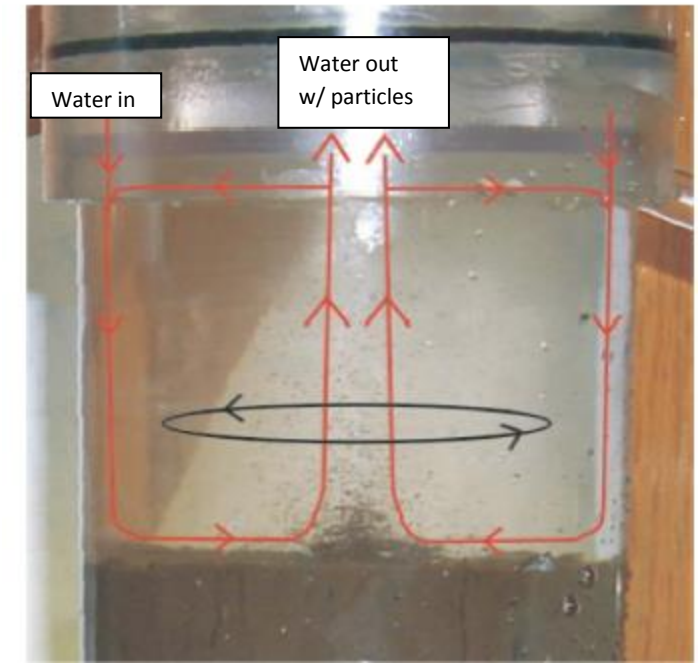

Figure 3-9. Physical dynamics inside active erosional sediment core (from Green Eyes: Environmental Observing Systems).

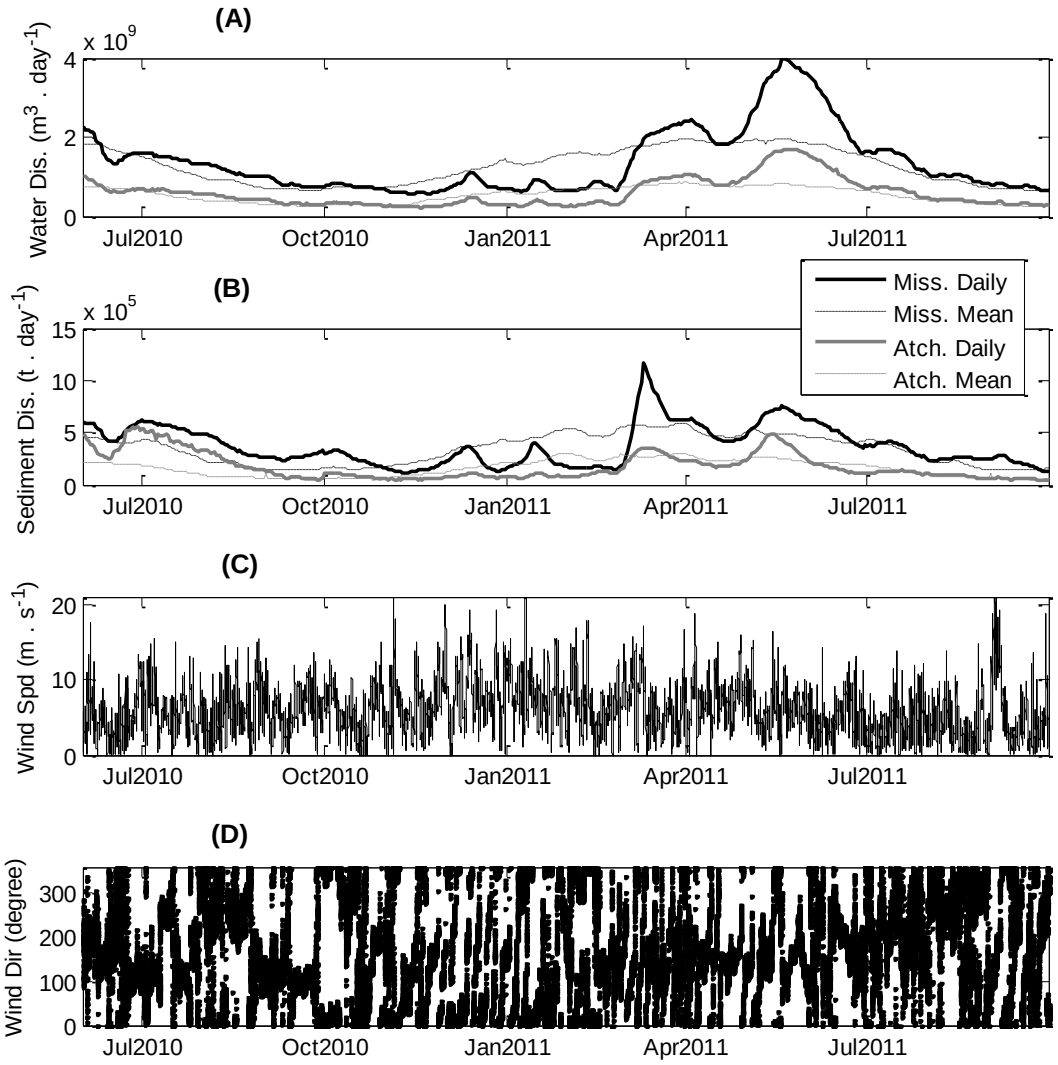

Figure 3-10. A) Daily and mean water discharge of the Mississippi (at Tarbert landing) and Atchafalaya (at Simmesport) Rivers from June 2010 to September 2011. Mean discharge is the averages of discharge from 1991 to 2010. B) Daily and mean sediment discharge of the Mississippi and Atchafalaya Rivers from June 2010 to September 2011. C) and D), Wind speed and direction from BURL1C-MAN weather station near the Southwest Pass of the Mississippi Delta. (from Xu et al., in prep)

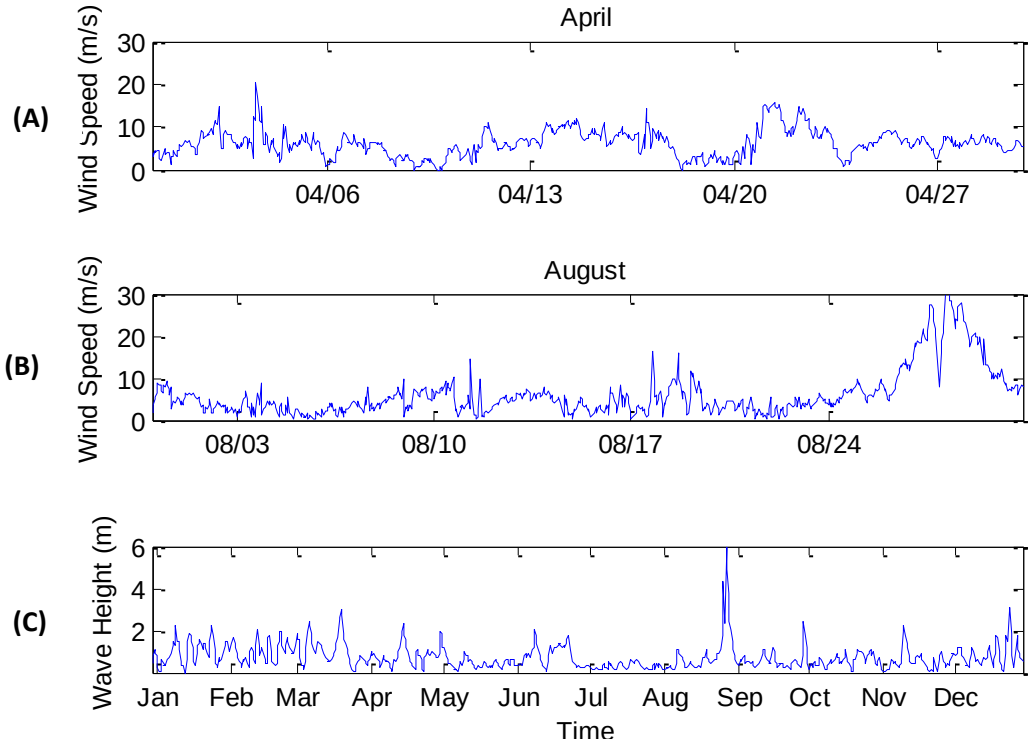

Figure 3-11. Time series wind speed from BURL 1 C-MAN weather station for April (A) and August (B) of 2012. (C) WaveWatchIII modeled wave height at BURL weather station for 2012.

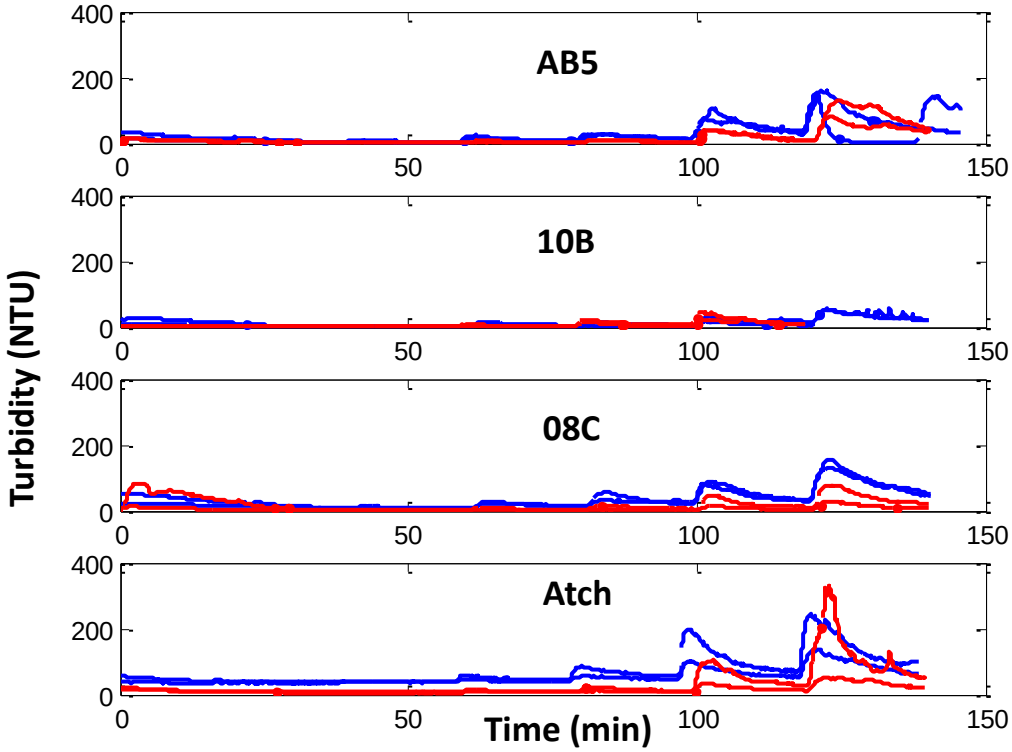

Figure 3-12. Gust Erosion Microcosm Turbidity for April and August 2011 (NTU: Nephelometric Turbidity Units).

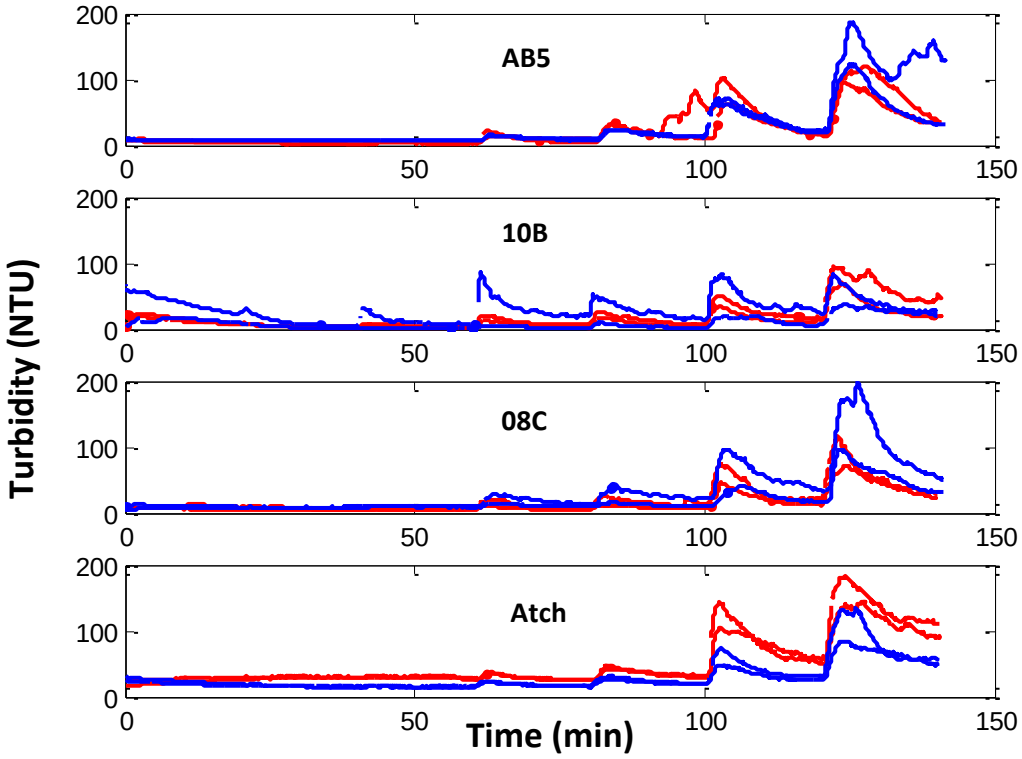

Figure 3-13. Gust Erosion Microcosm Turbidity for April and August 2012 (NTU: Nephelometric Turbidity Units).

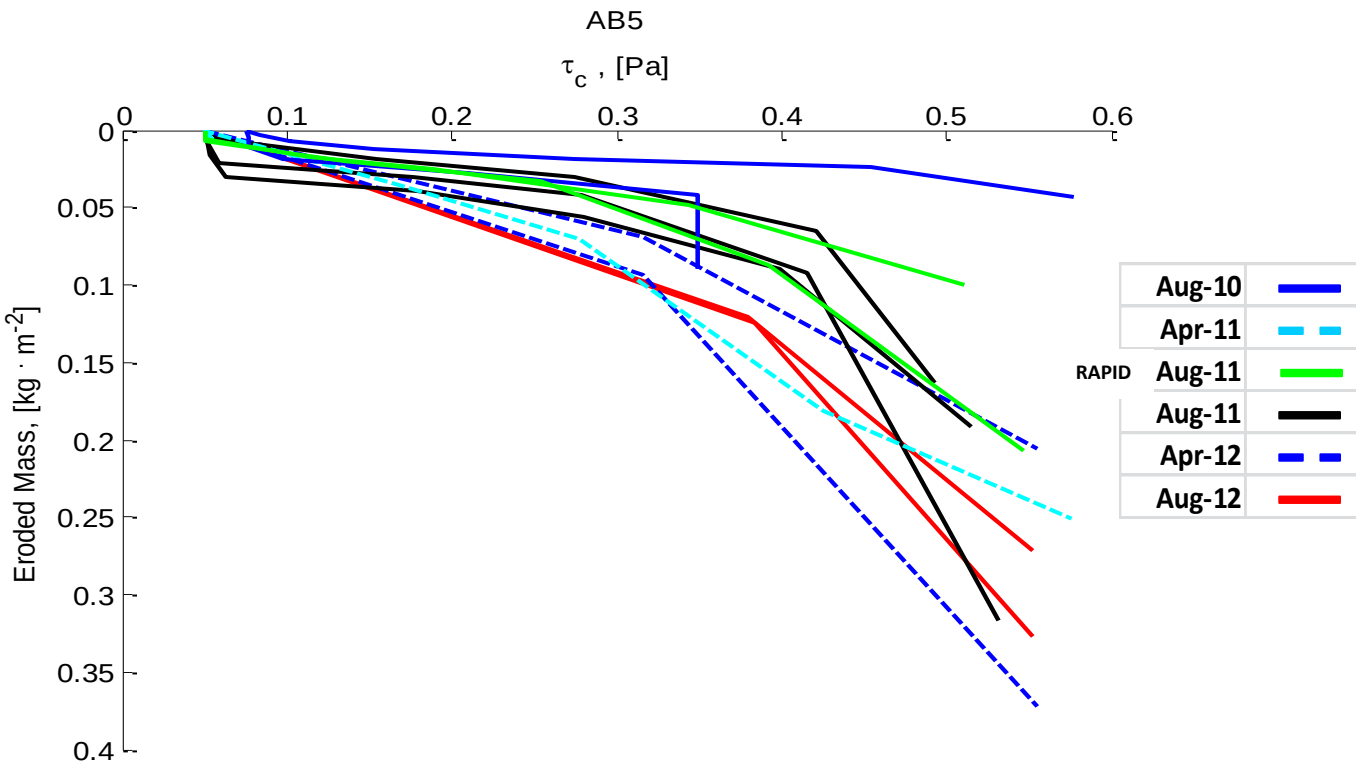

Figure 3-14. Erodibility profile for each GUST experiment over the 4 year period for Station AB5 (eastern hypoxic zone) (other data taken from cruises in August 2010 by K. Xu).

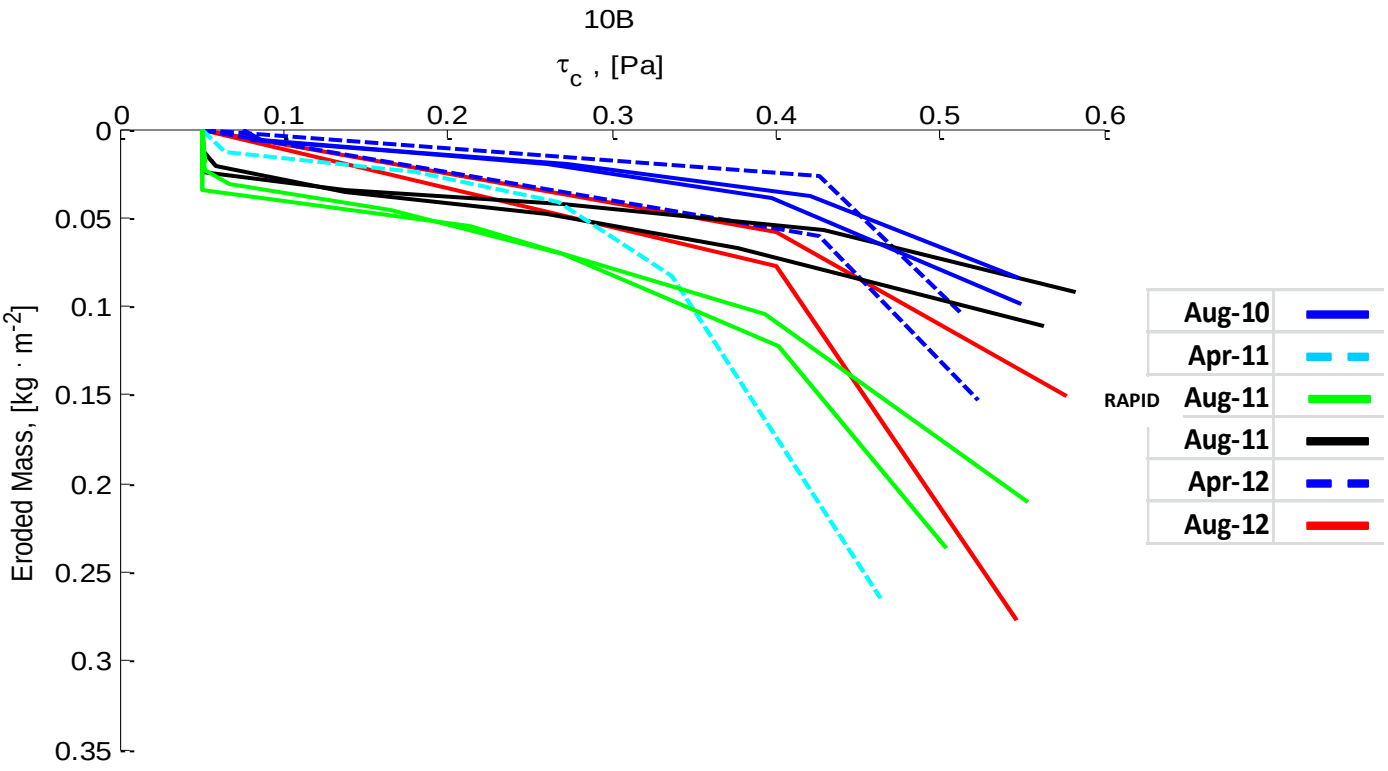

Figure 3-15. Erodibility profile for each GUST experiment over the 2 year period for Station 10B (middle hypoxic zone) (other data taken from cruises in August 2010 by K. Xu).

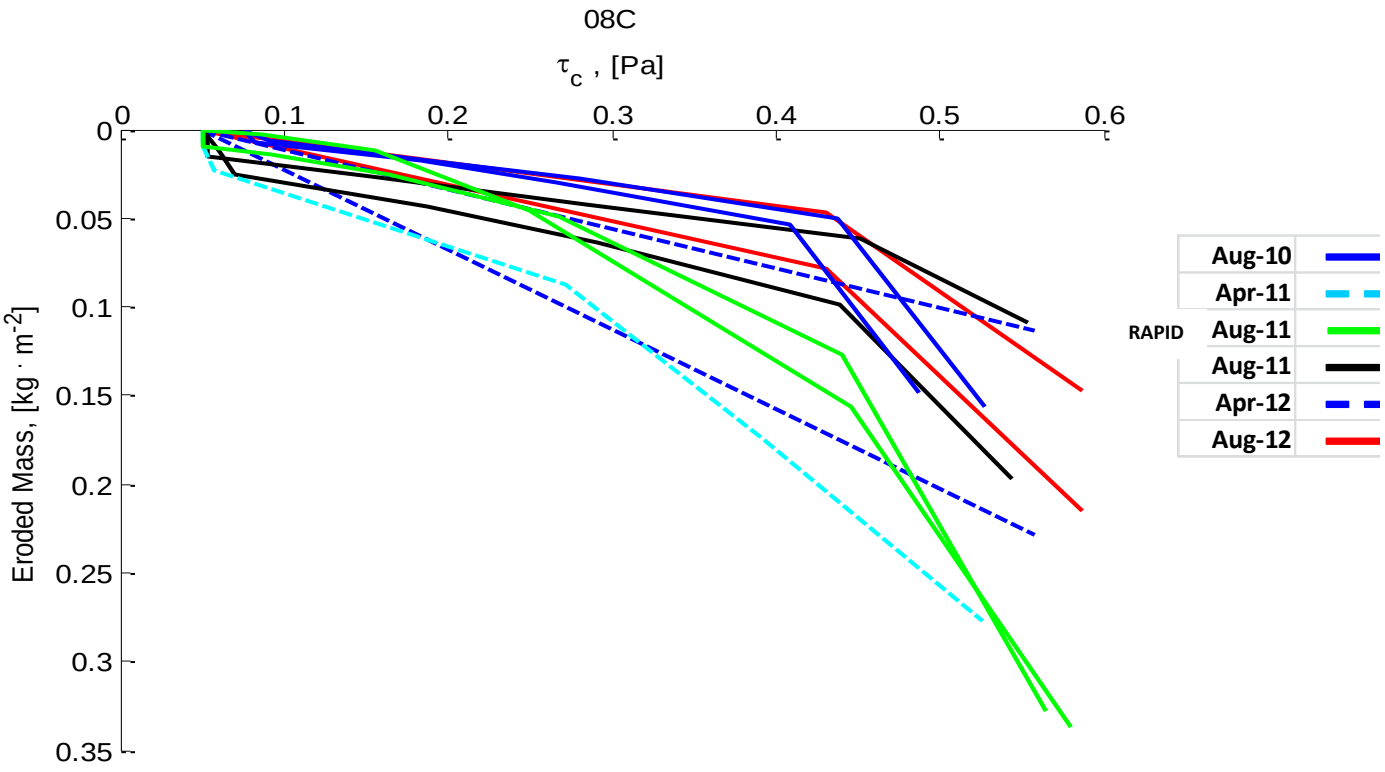

Figure 3-16. Erodibility profile for each GUST experiment over the 2 year period for Station 08C (western hypoxic zone) (other data taken from cruises in August 2010 by K. Xu).

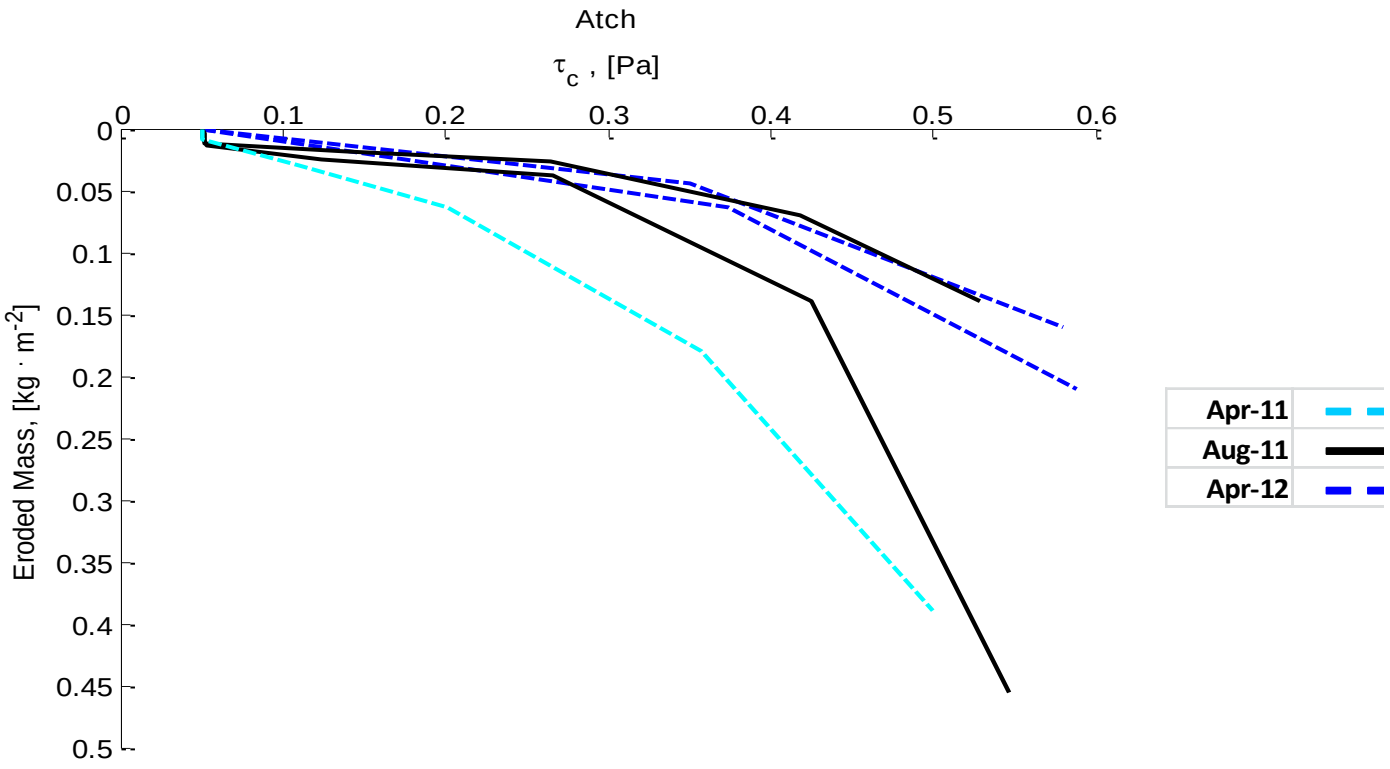

Figure 3-17. Erodibility profile for each GUST experiment over the 2 year period for Station Atch (Atchafalaya Bay).

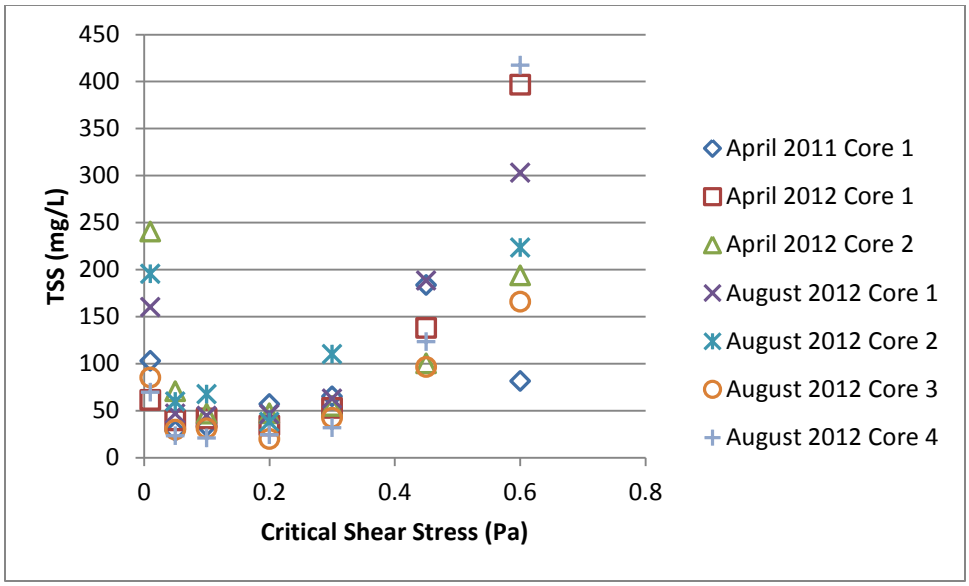

Figure 3-18. Total suspended solid measurements from each shear stress level in mg/L for all cores collected in April 2011, 2012 and August 2012 at Station AB5 (eastern hypoxic zone).

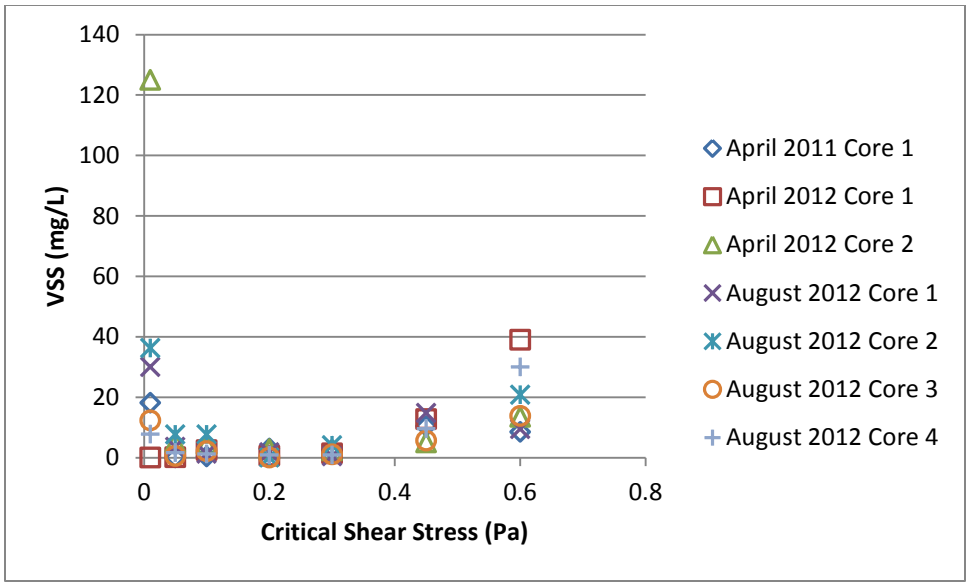

Figure 3-19. Volatile suspended solid measurements from each shear stress level in mg/L for all cores collected in April 2011, 2012 and August 2012 at Station AB5 (eastern hypoxic zone).

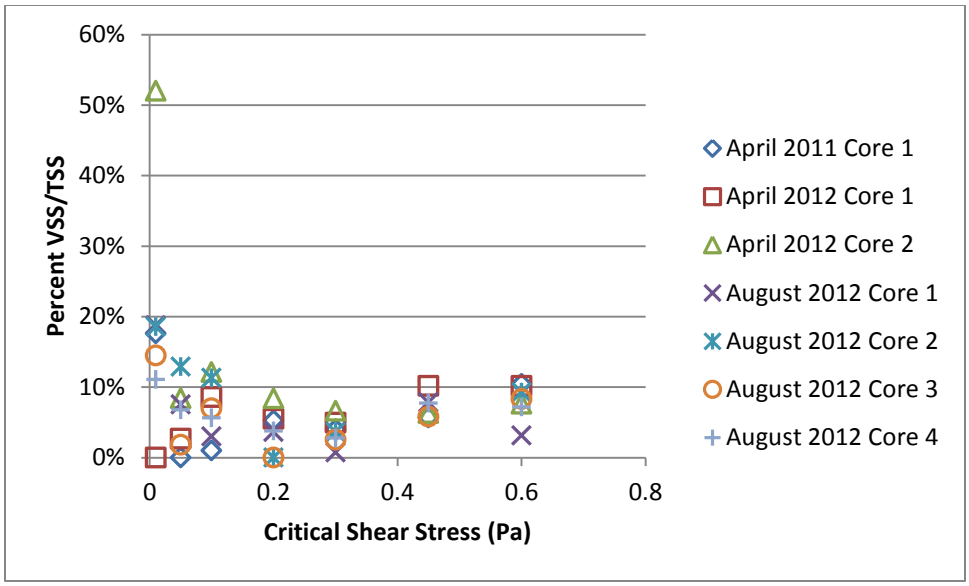

Figure 3-20. Percent value of VSS/TSS (mg/L) at each shear stress level measured for all cores collected at Station AB5.

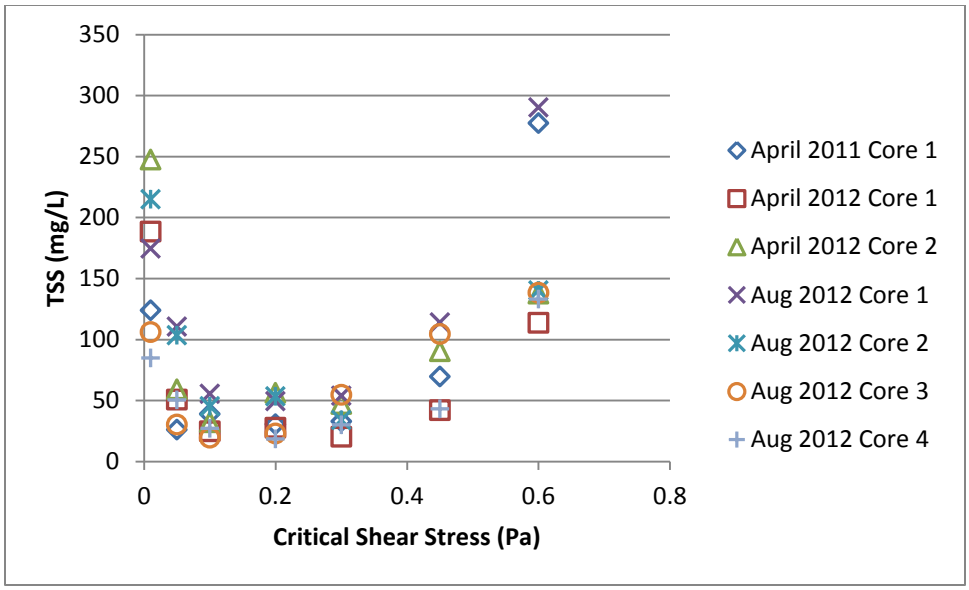

Figure 3-21. Total suspended solid measurements from each shear stress level in mg/L for all cores collected in April 2011, 2012 and August 2012 at Station 10B (middle hypoxic zone).

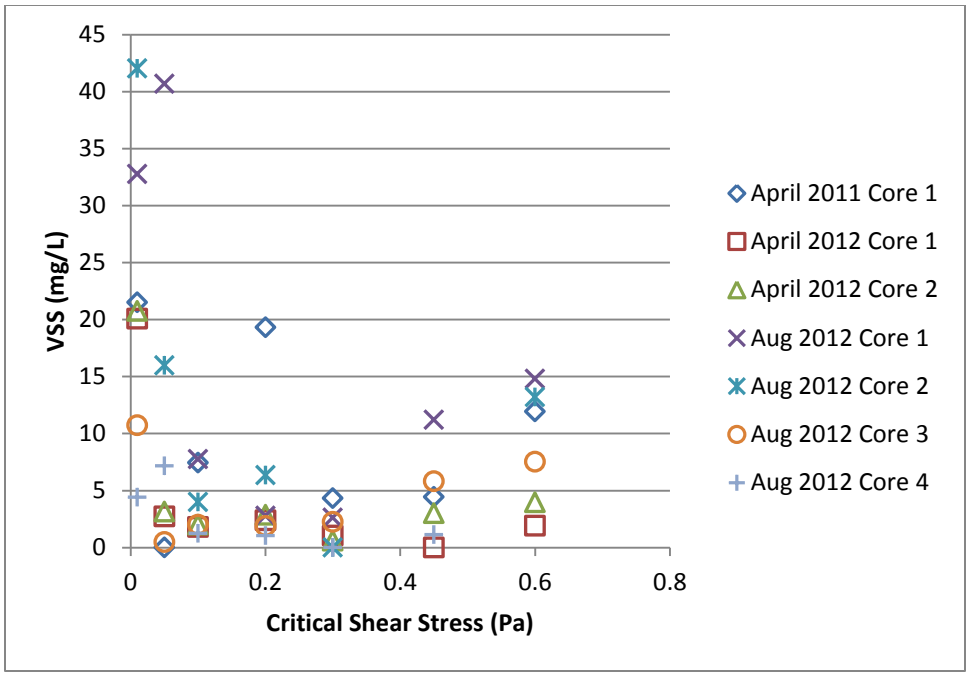

Figure 3-22. Volatile suspended solid measurements from each shear stress level in mg/L for all cores collected in April 2011, 2012 and August 2012 at Station 10B (middle hypoxic zone).

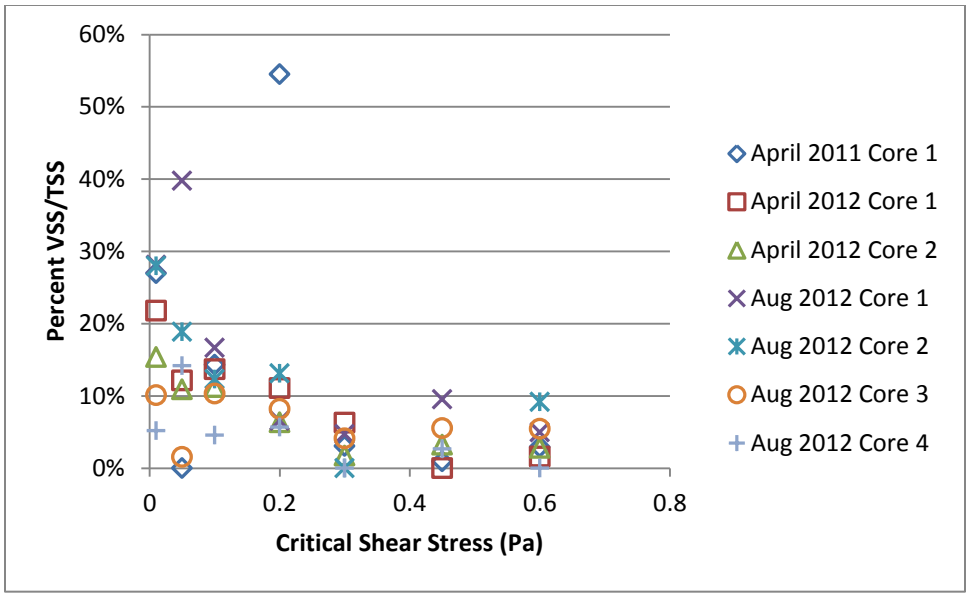

Figure 3-23. Percent value of VSS/TSS (mg/L) at each shear stress level measured for all cores collected at Station 10B.

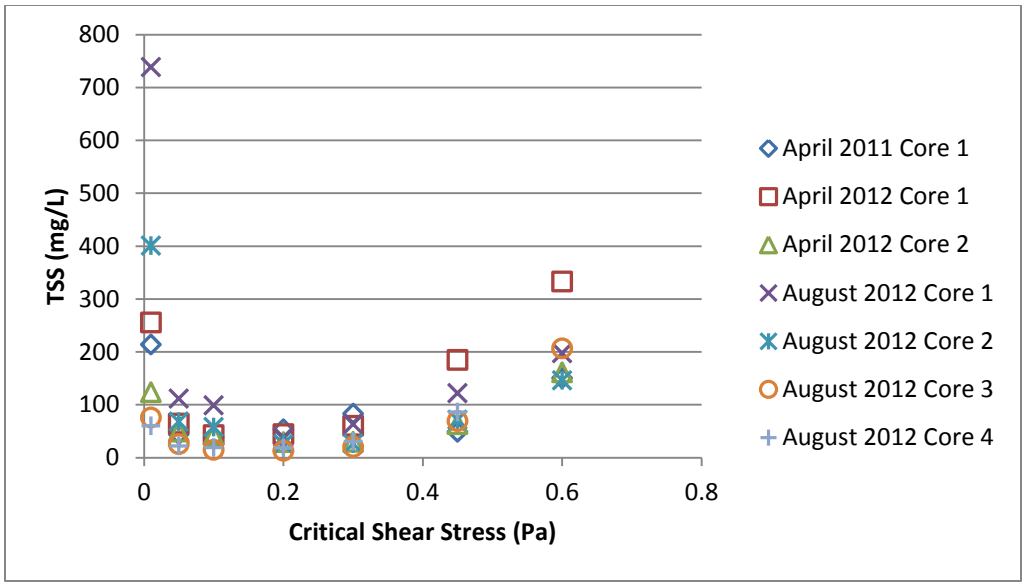

Figure 3-24. Total suspended solid measurements from each shear stress level in mg/L for all cores collected in April 2011, 2012 and August 2012 at Station 08C (western hypoxic zone).

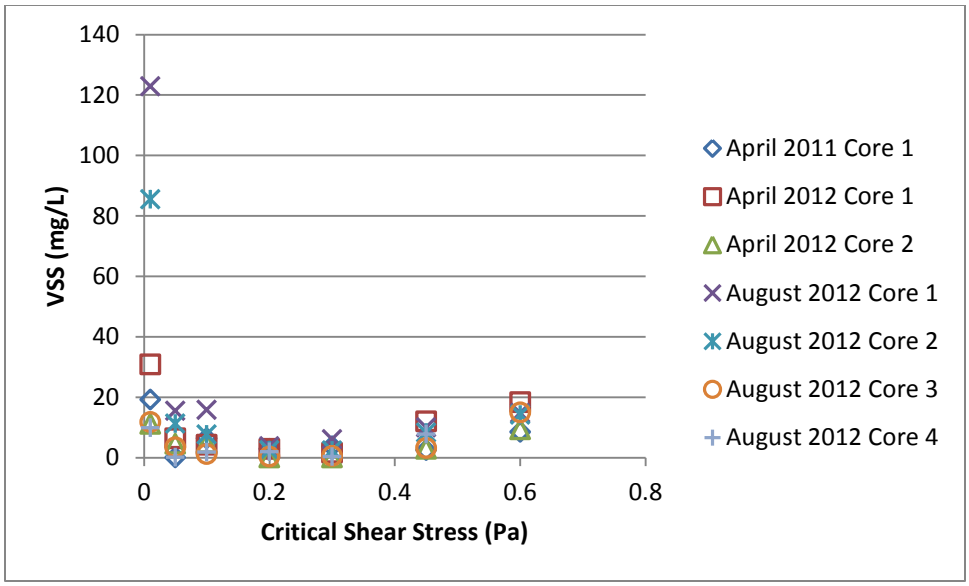

Figure 3-25. Volatile suspended solid measurements from each shear stress level in mg/L for all cores collected in April 2011, 2012 and August 2012 at Station 08C (western hypoxic zone).

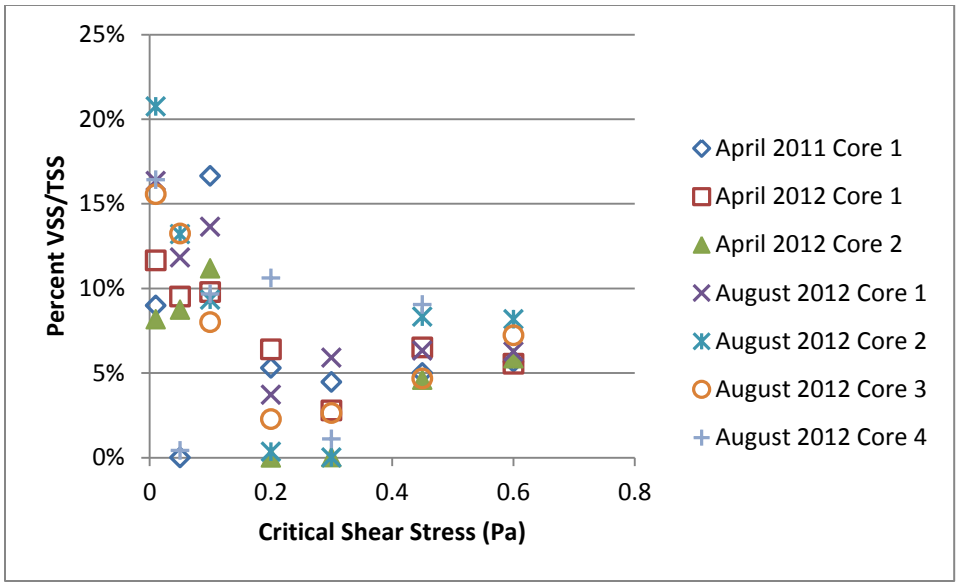

Figure 3-26. Percent value of VSS/TSS (mg/L) at each shear stress level measured for all cores collected at Station 08C.

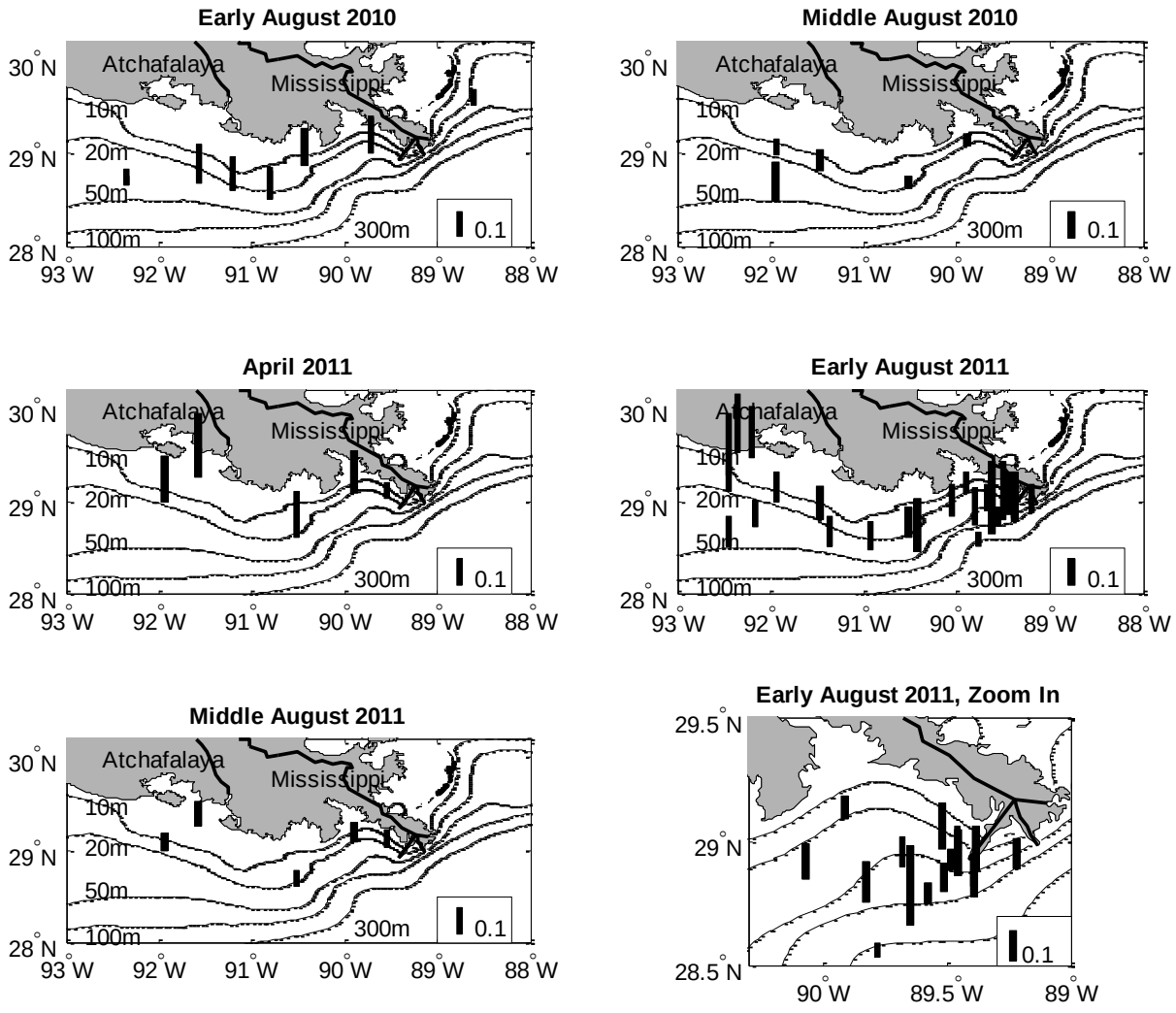

Figure 3-27. Eroded mass (kg/m^2) at 0.4 Pa of sea bed in the Louisiana shelf in early August 2010, middle August 2010, April 2011, Early August 2011, and middle August 2011. (from Xu et al. in prep).

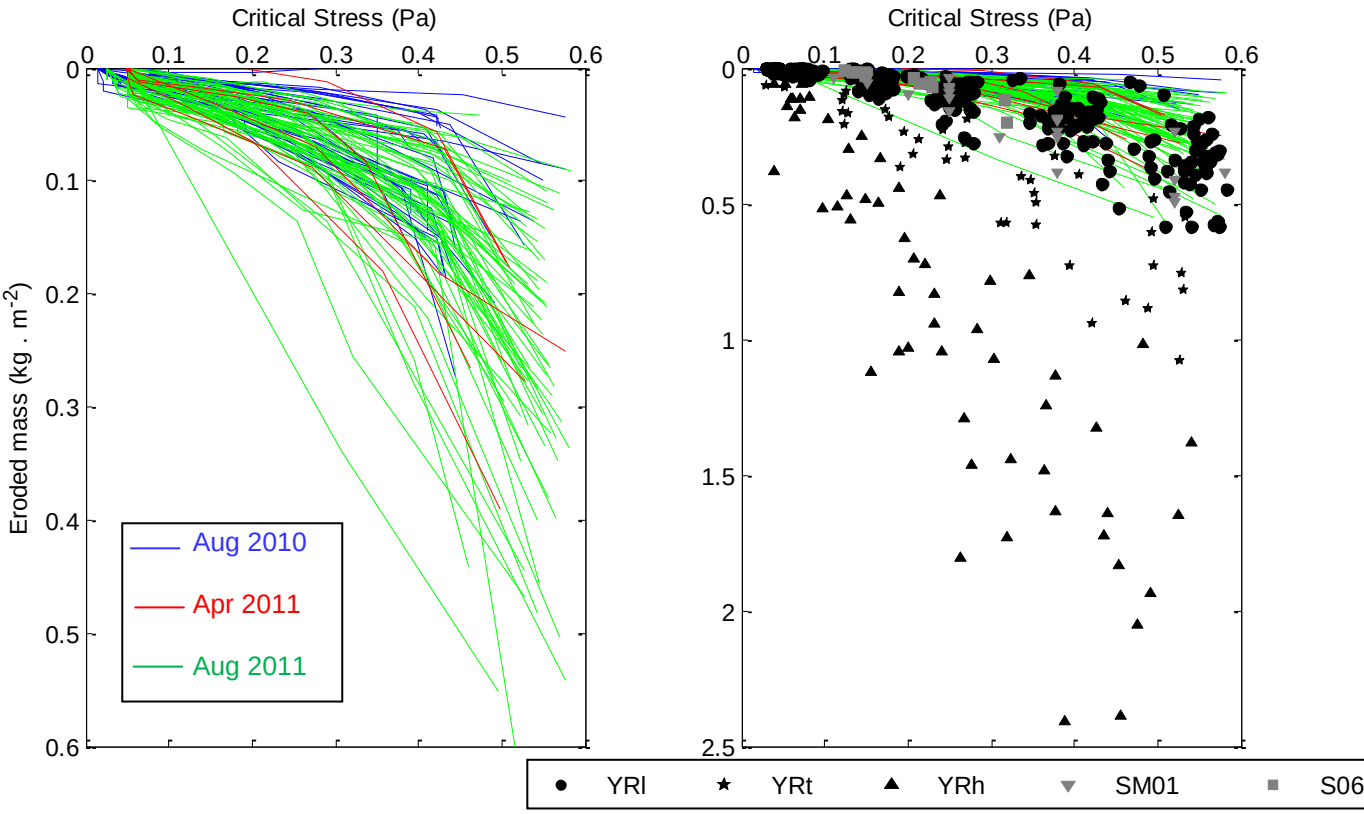

Figure 3-28. A) Profiles of critical shear stress (Pa) versus eroded mass (kg•m-2) for August 2010, April 2011 and August 2011. B) Comparison of erodibility profiles from northern Gulf of Mexico to erodibility profile points analyzed for the York River Estuary by Dickhudt et al., 2009. YRI=York River low erodibility, YRt=York River transitional erodibility, YRh=York River high erodibility, SM01=Sanford and Maa (2001), S06=Sanford (2006) (from Xu et al. in prep).

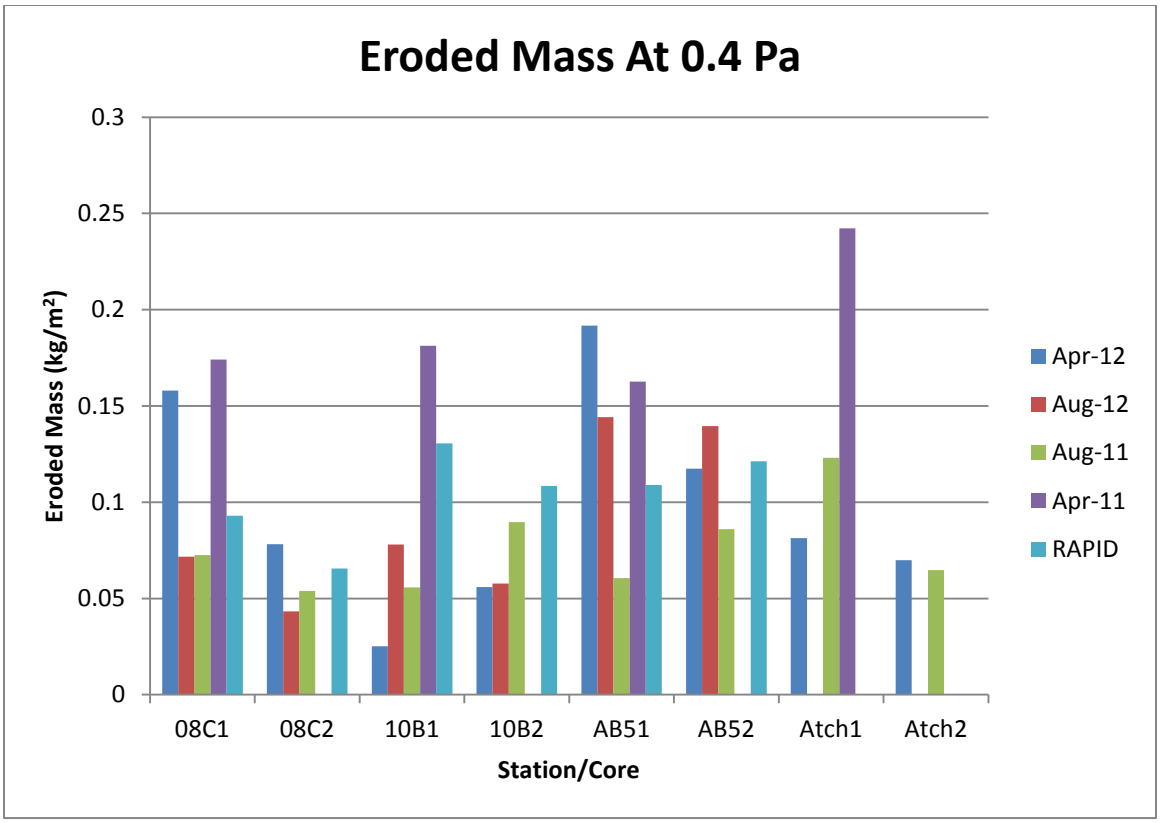

Figure 3-29. Bar graph representing the values of eroded mass calculated for the 0.4 Pa shear stress (data extracted from erodibility profiles). Station/Core designates the station sampled and from which of the dual cores the values were measured and calculated.

Table 4-1. Properties of sediment tracers in the model for river derived sediment. τ_{cr} is critical shear stress in Pascals. W_s is settling velocity in mm/s. Erosional rate in kg/m^2/s. Percent fraction of large and small floc types from Mississippi and Atchafalaya Rivers.

Sediment	Type	τ_{cr} (Pa)	W_s (mm/s)	Erosional Rate (kg/m^2/s)	Fraction
Mississippi	Large flocs	0.11	1	$5x10^{-5}$	50%
	Small flocs	0.11	0.1	$5x10^{-5}$	50%
Atchafalaya	Large flocs	0.03	1	$5x10^{-5}$	10%
	Small flocs	0.03	0.1	$5x10^{-5}$	90%

Table 4-2. Seabed sediment tracer properties used for all four sensitivity test for sediment transport in 2005. Seabed sediment fractions from usSEABED data (see Fig. 2-22).

Simulation	Seabed Sediment	Type	τ_{cr} (Pa)	W_s (mm/s)	Erosional Rate (kg/m^2/s)	Fraction
1	High Ws; Low E rate	Sand	0.13	10	$5x10^{-5}$	Spatially variable, see Fig. 2-20
		Mud	0.11	1	$5x10^{-5}$	
2	High Ws; High E rate	Sand	0.13	10	$5x10^{-4}$	
		Mud	0.11	1	$5x10^{-4}$	
3	Low Ws; Low E rate	Sand	0.13	1	$5x10^{-5}$	
		Mud	0.11	0.1	$5x10^{-5}$	
4	Low Ws; High E rate	Sand	0.13	1	$5x10^{-4}$	
		Mud	0.11	0.1	$5x10^{-4}$	

Table 4-3. Erosional and Depositional Depths (cm) calculated from shaded areas in Fig. 4-29 for all 5 sites studied for Hurricanes Katrina and Rita.

	Erosional Depth (cm)		Depositional Depth (cm)	
Site	**Katrina**	**Rita**	**Katrina**	**Rita**
AB5	31.53	37.67	12.7	36.84
River	75.9	52.73	14.53	2.12
10B	16.33	22.52	17.04	14.08
08C	0.72	36.29	0.77	27.29
Atch	1.29	4.54	1.2	5.64

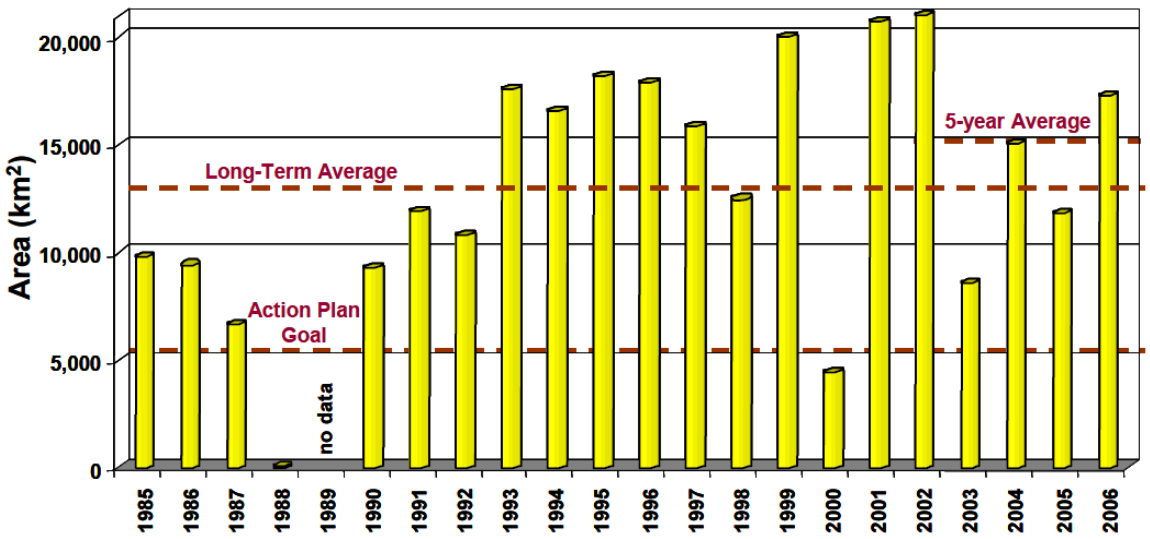

Figure 4-1. Estimated area of bottom-water hypoxia (dissolved oxygen < 2 mg/L) for mid-summer cruises, superimposed with long-term average, five-year average and 2015 goal of 5,000 km^2(Rabalais et al., 2006).

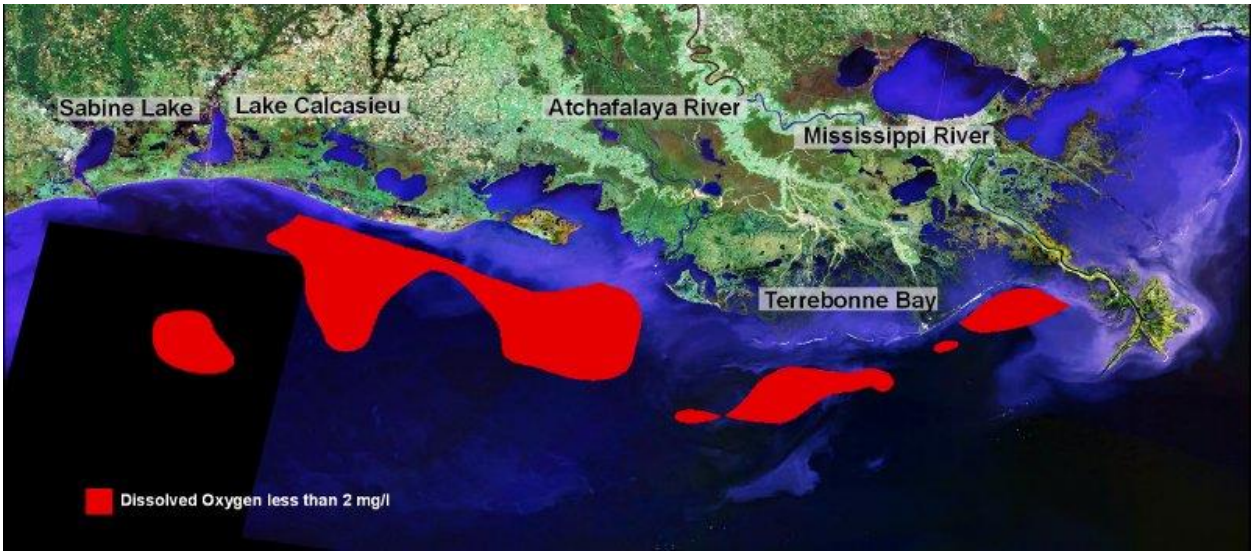

Figure 4-2. Areal extent of hypoxia for 2005 over the northern Gulf of Mexico; areas colored red indicated bottom water DO levels at or below 2 mg/L. Maps provided by Louisiana University Marine Consortium (LUMCON) <http://www.gulfhypoxia.net/Research/Shelfwide%20Cruises/all_cruises.asp>.

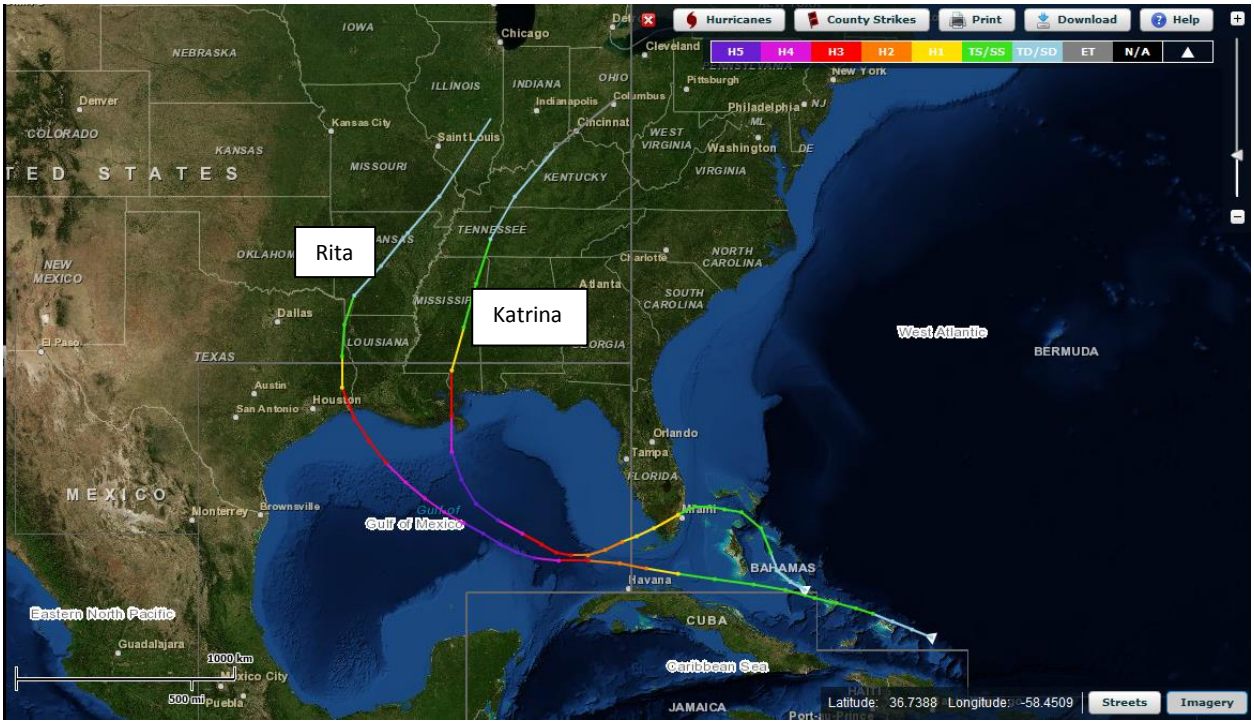

Figure 4-3. Paths and intensities (indicated by color) of Hurricanes Katrina and Rita. Category 5; Category 4; Category 3; Category 2; Category 1; Tropical Storm; Tropical Depression (csc.noaa.gov).

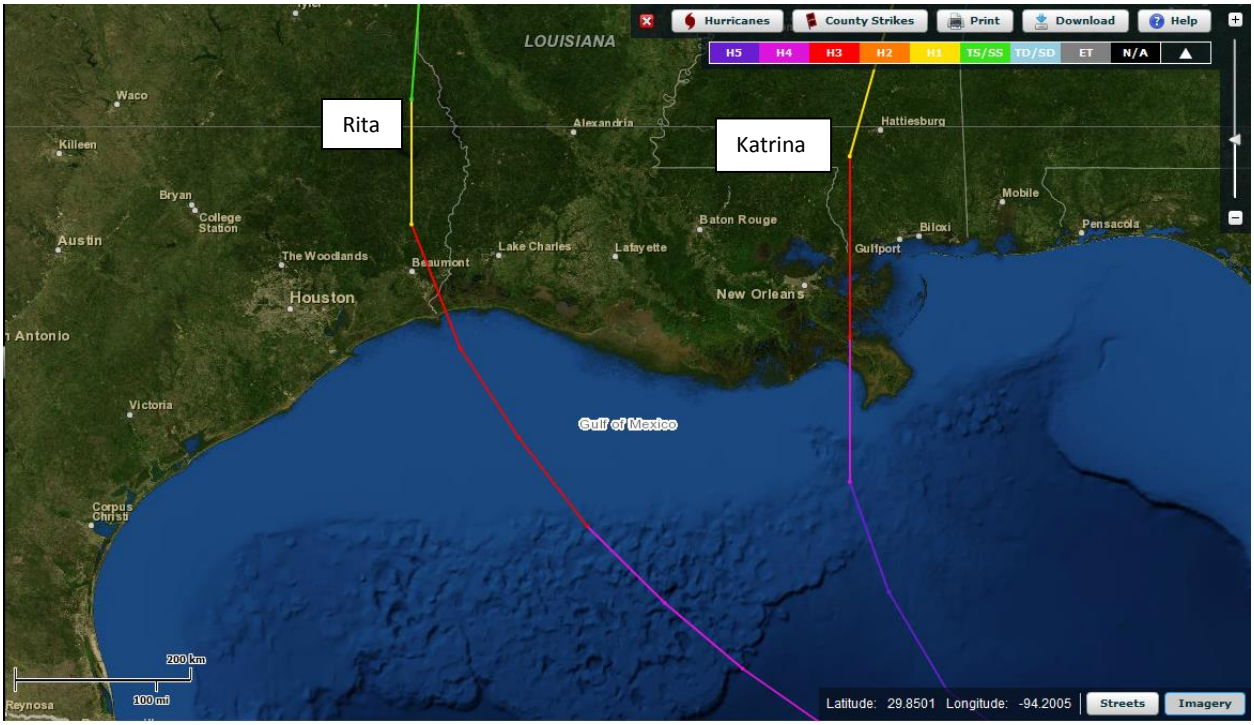

Figure 4-4. Landfall paths and intensities (indicated by color) of Hurricanes Katrina and Rita. Category 5; Category 4; Category 3; Category 2; Category 1; Tropical Storm; Tropical Depression (csc.noaa.gov).

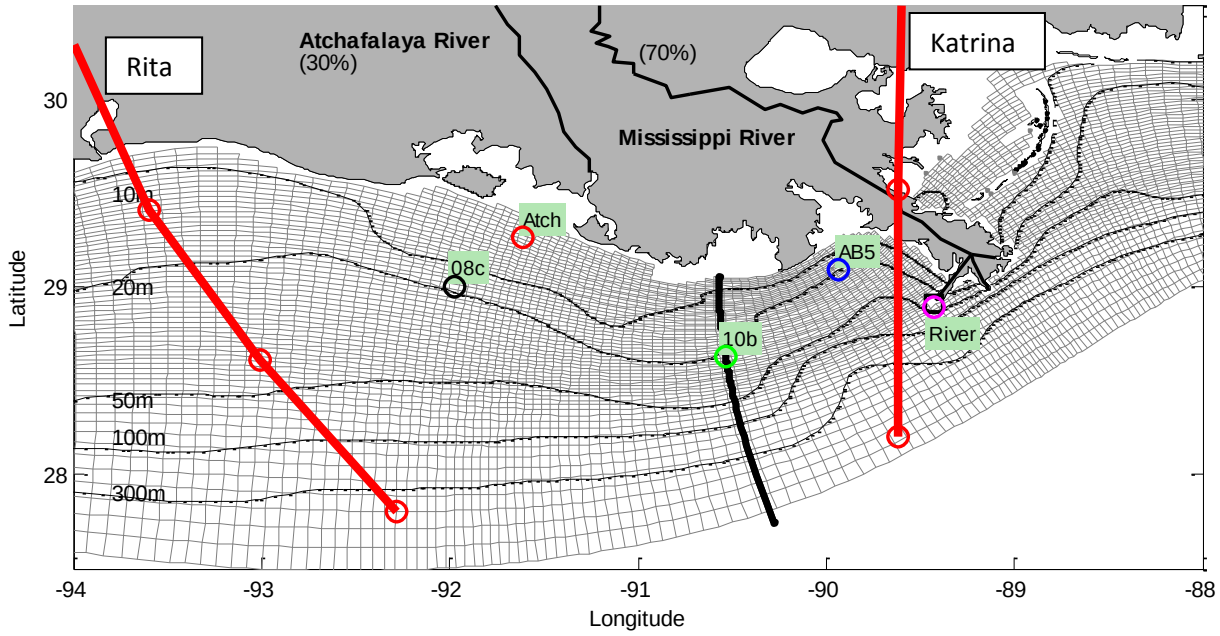

Figure 4-5. Curvilinear model grid for the Louisiana-Texas shelf. Isobaths contoured at water depths of 10, 20, 50, 100, and 300 m. The unfilled square indicates the location of the BURL 1 C-MAN weather station maintained by NOAA National Data Buoy Center (NDBC). Solid black line indicates hypoxic zone transect for profile analyses. Circles represent locations of stations River (BURL 1 C-MAN), AB5, 10B (mid hypoxic zone station), Atch, and O8C used throughout this study. Red lines indicate Hurricane paths through model domain.

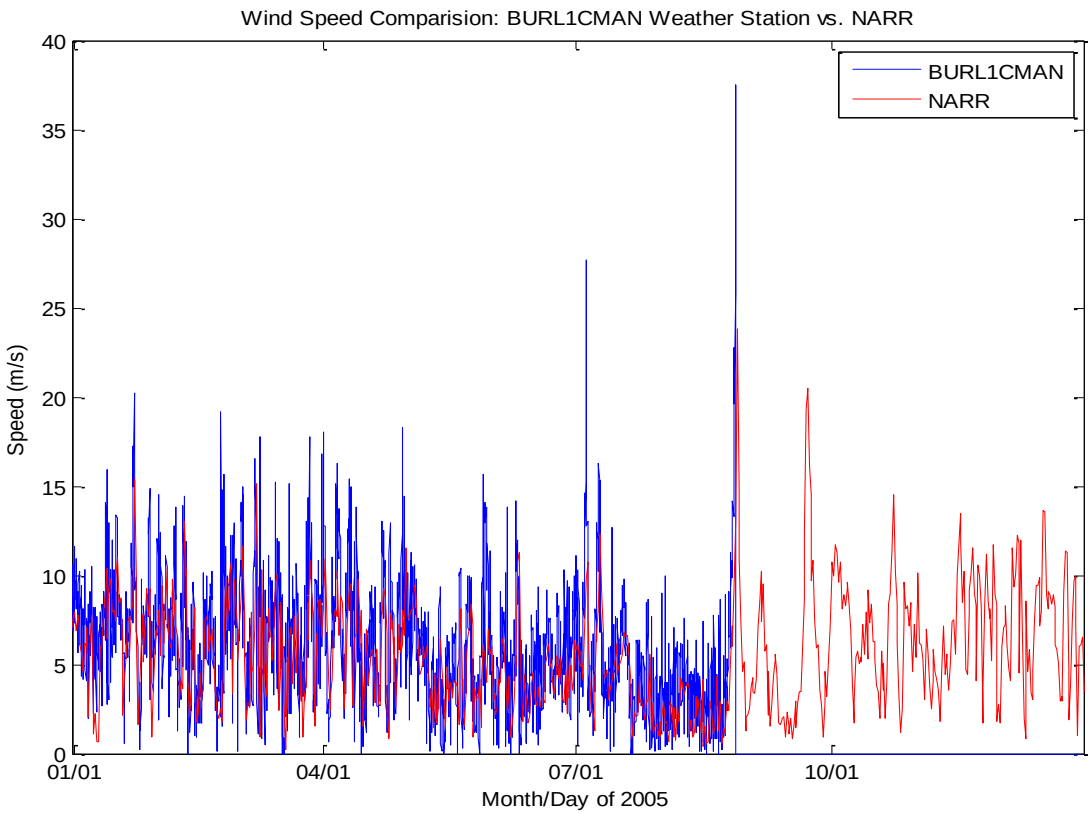

Figure 4-6. Time series comparison of wind speeds (m/s) at the BURL 1 C-MAN weather station (Blue) and wind speeds from NARR model (Red) for 2005. Blue line shows weather station data and missing data due to buoy malfunction during Hurricane Katrina.

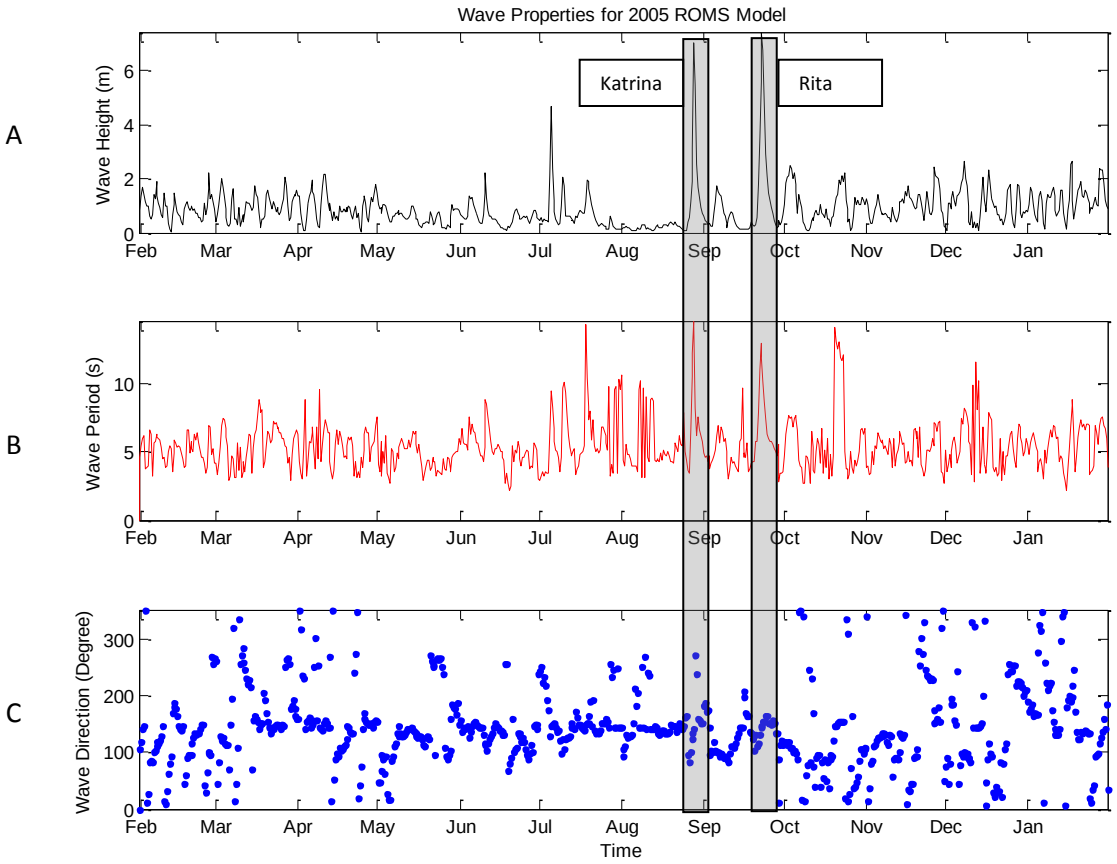

Figure 4-7. Time-series of wave input properties at station 10B (mid hypoxic zone) from WaveWatch III for 2/1/2005 to 2/1/2006. (A) Wave height (m). (B) Wave period (s). (C) Wave direction (degree).

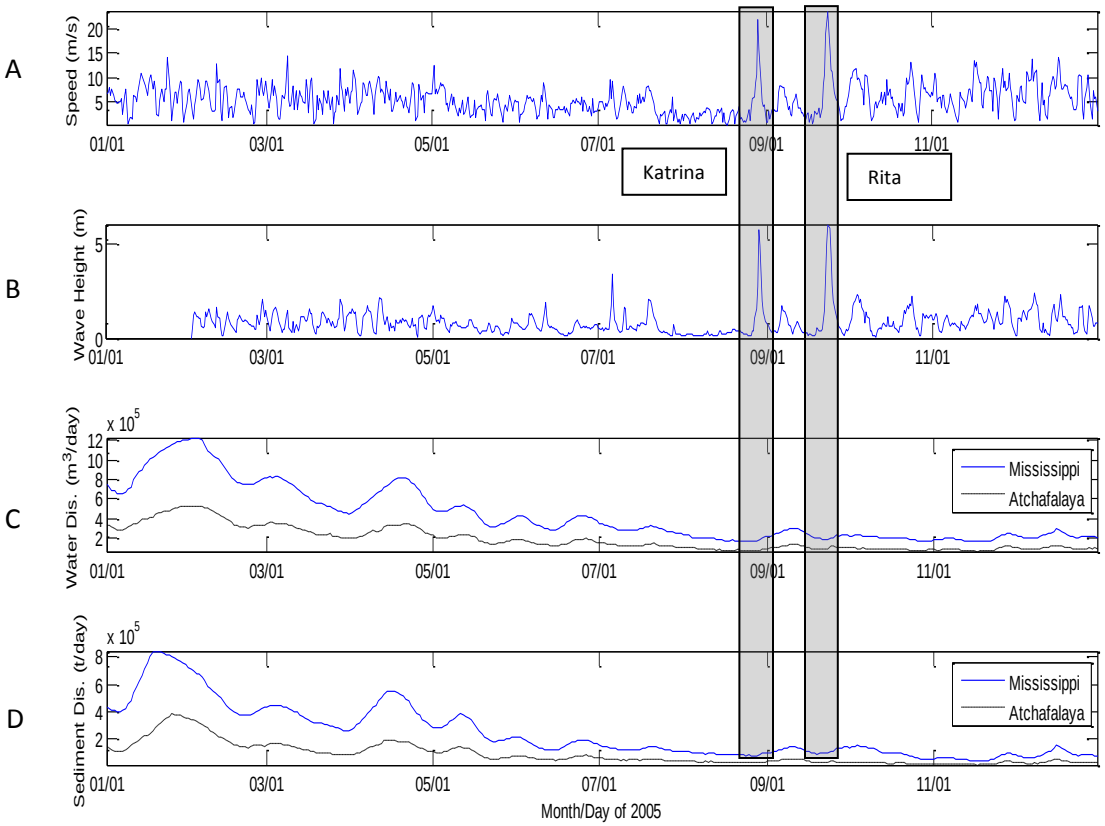

Figure 4-8. (A) Modeled wind speed from NARR at BURL 1 C-MAN weather station. (B) WW3 modeled wave height at BURL 1 C-MAN weather station. (C and D) Water and sediment discharge from the Mississippi and Atchafalaya Rivers. This paper focused on the following two periods in 2005 (shaded): Hurricane Katrina and Hurricane Rita.

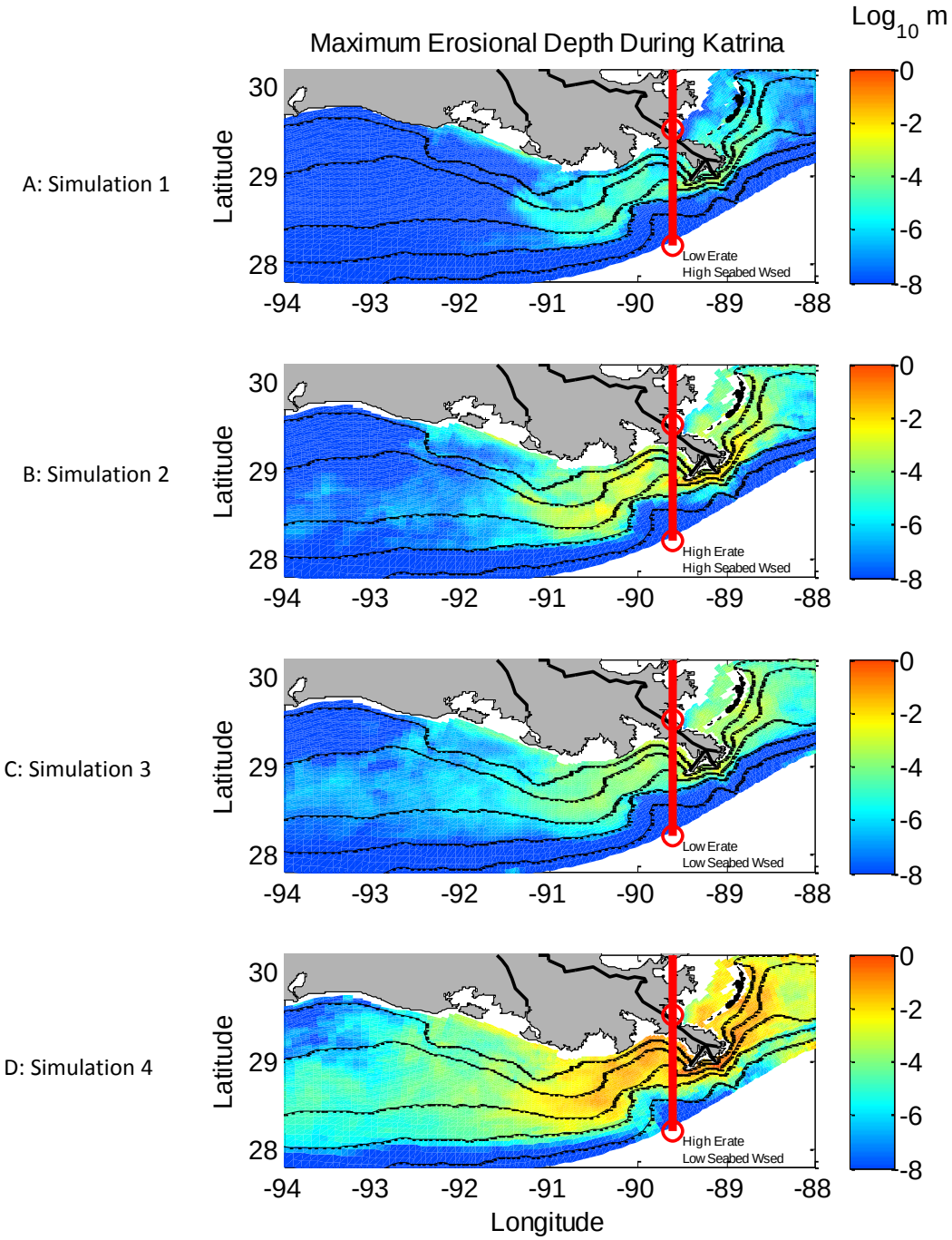

Figure 4-9. Maximum erosional depth (log10 m) during Hurricane Katrina.(A) Simulation 1: Low erosional rate (Erate) and High settling velocity (W_s) for seabed. (B) Simulation 2: High Erate and High W_s for seabed. (C) Simulation 3: Low Erate and Low W_s for seabed. (D) Simulation 4: High Erate and Low W_s for seabed. Red line and circles indicate Hurricane Katrina's path.

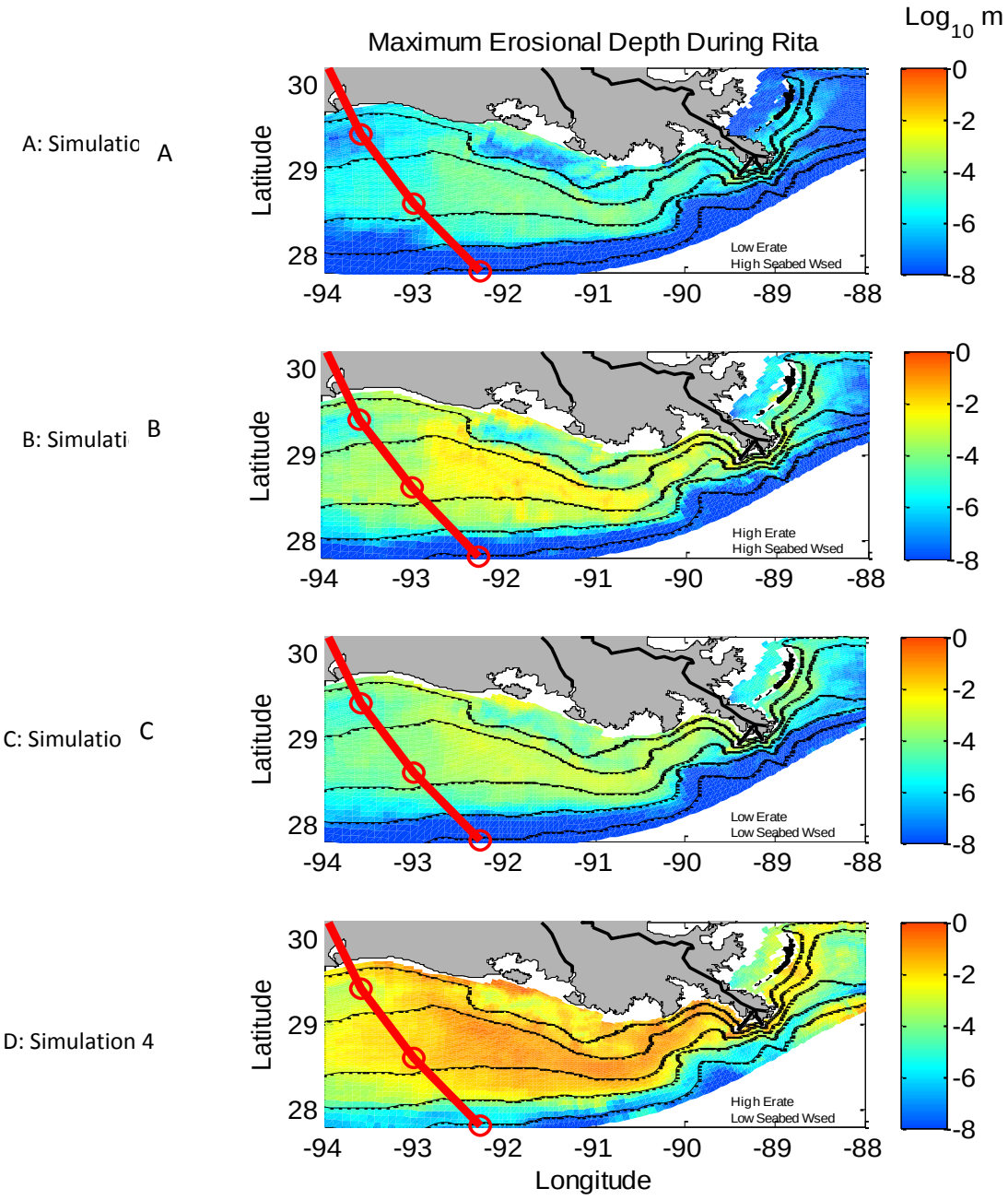

Figure 4-10. Maximum erosional depth (log10 m) during Hurricane Rita. (A) Simulation 1: Low erosional (Erate) and High settling velocity (W_s) for seabed. (B) Simulation 2: High Erate and High W_s for seabed. (C) Simulation 3: Low Erate and Low W_s for seabed. (D) Simulation 4: High Erate and Low W_s for seabed. Red line and circles indicate Hurricane Rita's path.

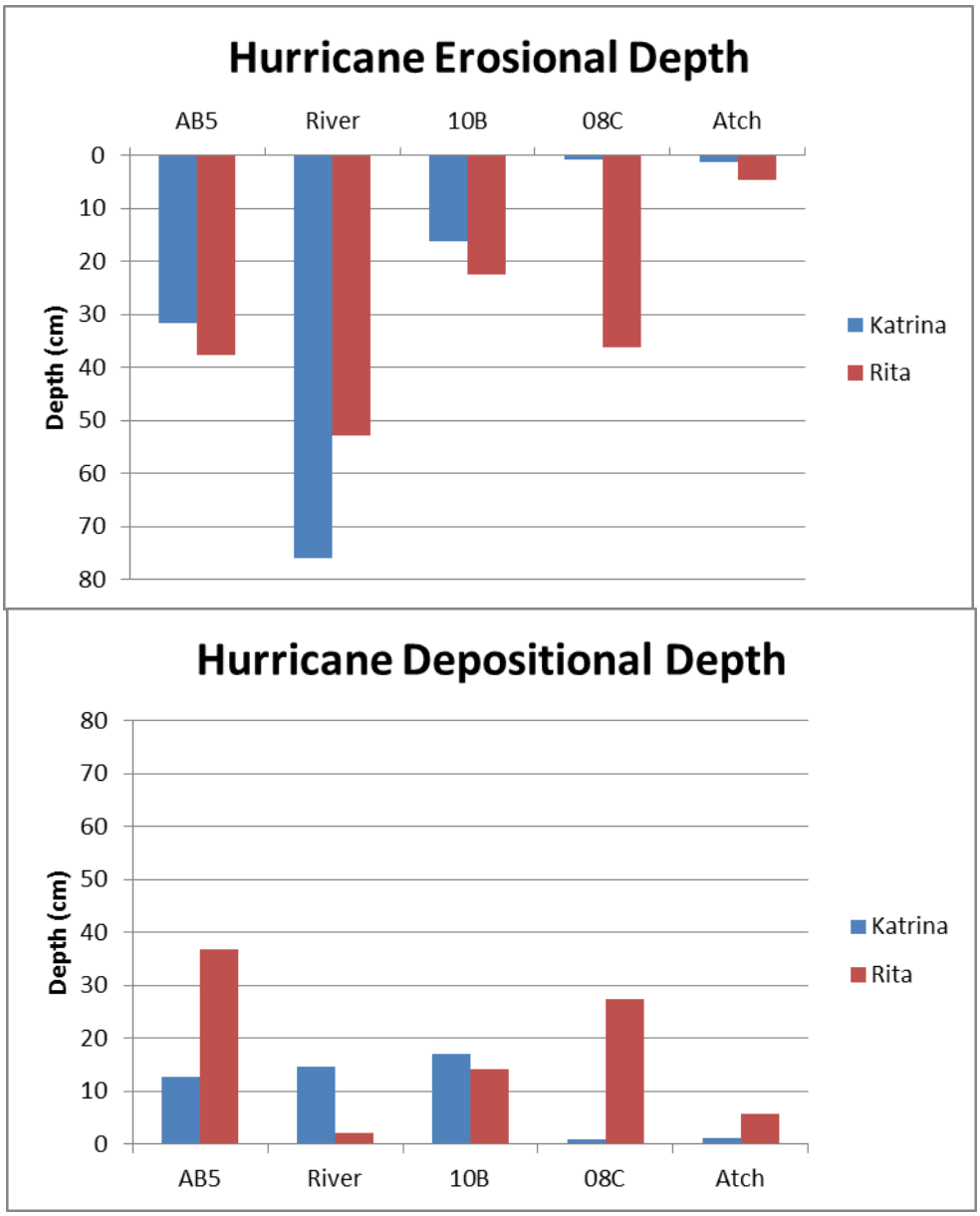

Figure 4-11. Erosional and depositional depths (cm) calculated from the shaded areas in figure 4-29 for Hurricanes Katrina and Rita.

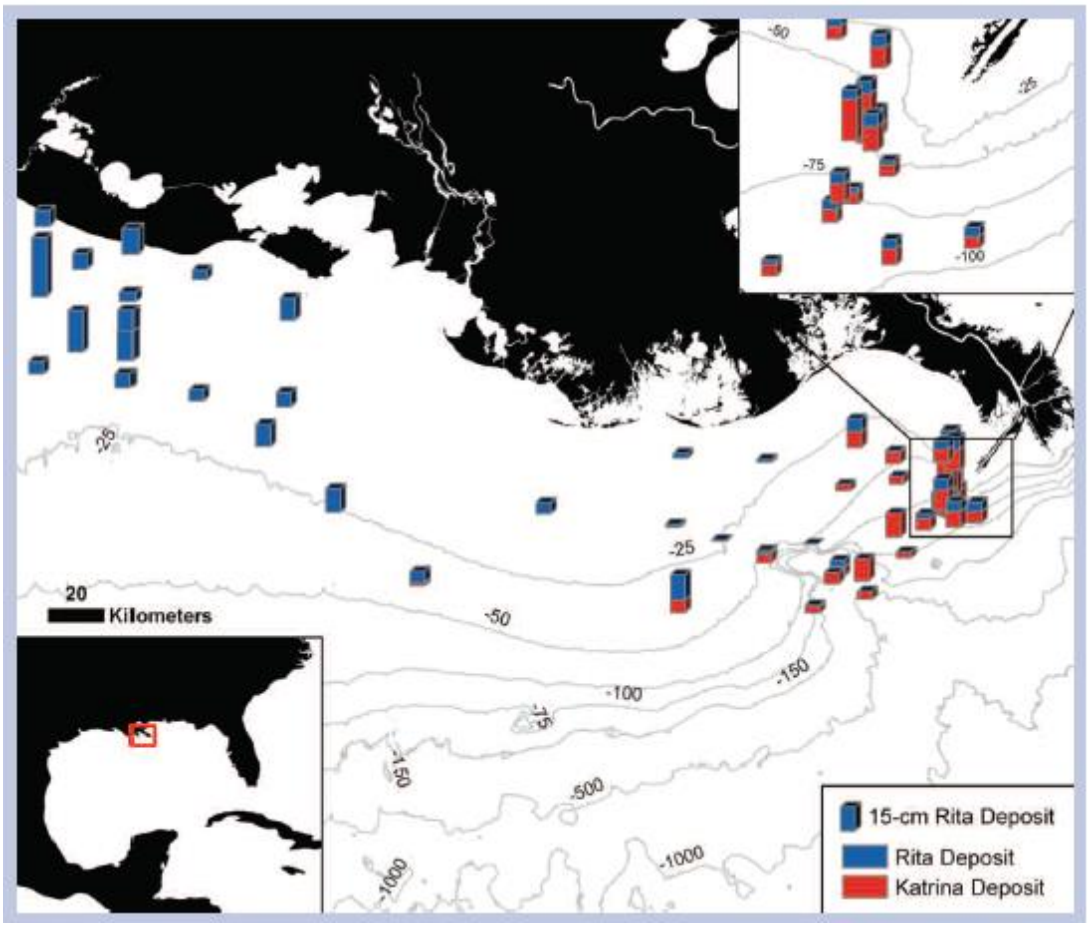

Figure 4-12. Map from Goni et al. (2007) illustrating the thickness (cm) of sediment deposits associated with Hurricanes Katrina and Rita.

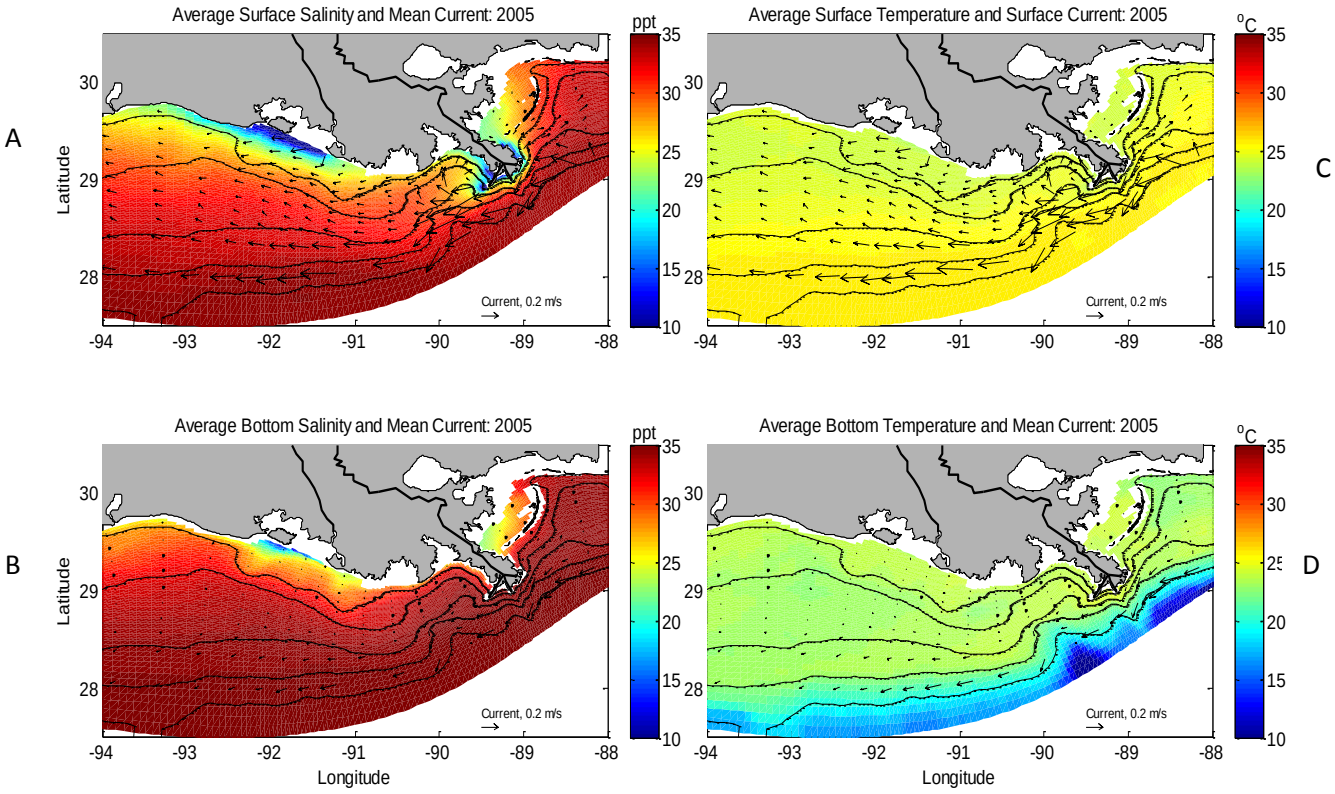

Figure 4-13. (A) Mean surface salinity (ppt) and mean surface current (m/s) arrows for 2005. (B) Mean bottom salinity and mean bottom current arrows for 2005. (C) Mean surface temperature (degree C) and mean surface current arrows for 2005. (D) Mean bottom temperature and mean bottom current arrows for 2005.

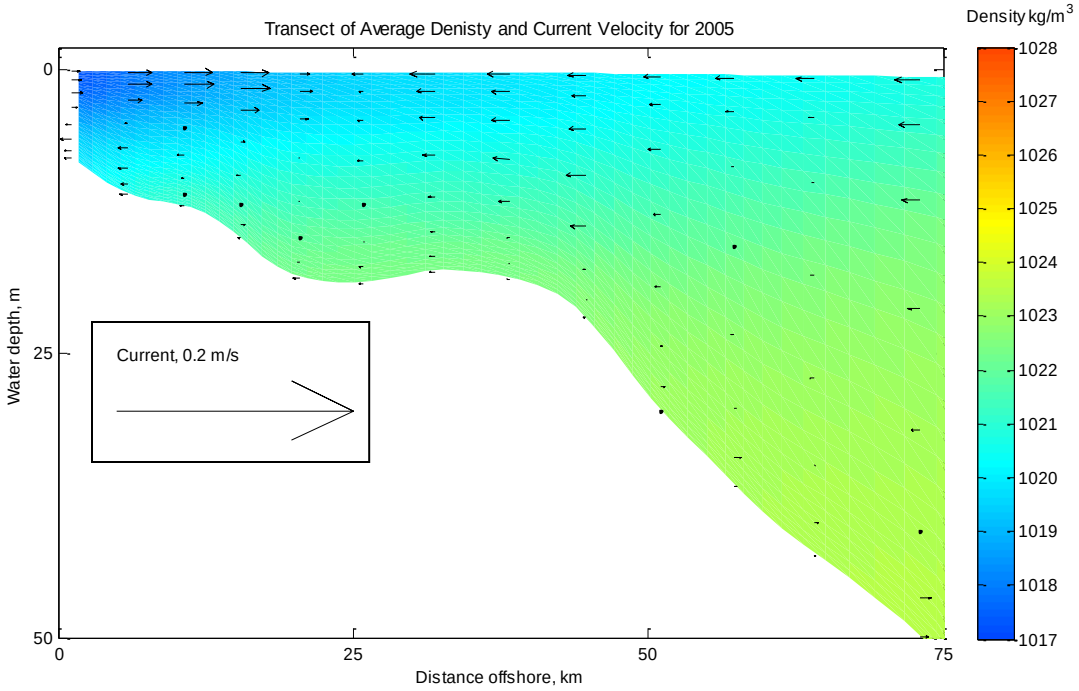

Figure 4-14. Mean density (kg/m^3) and current velocity (m/s) arrows for mid hypoxic region transect based on the means of the year 2005.

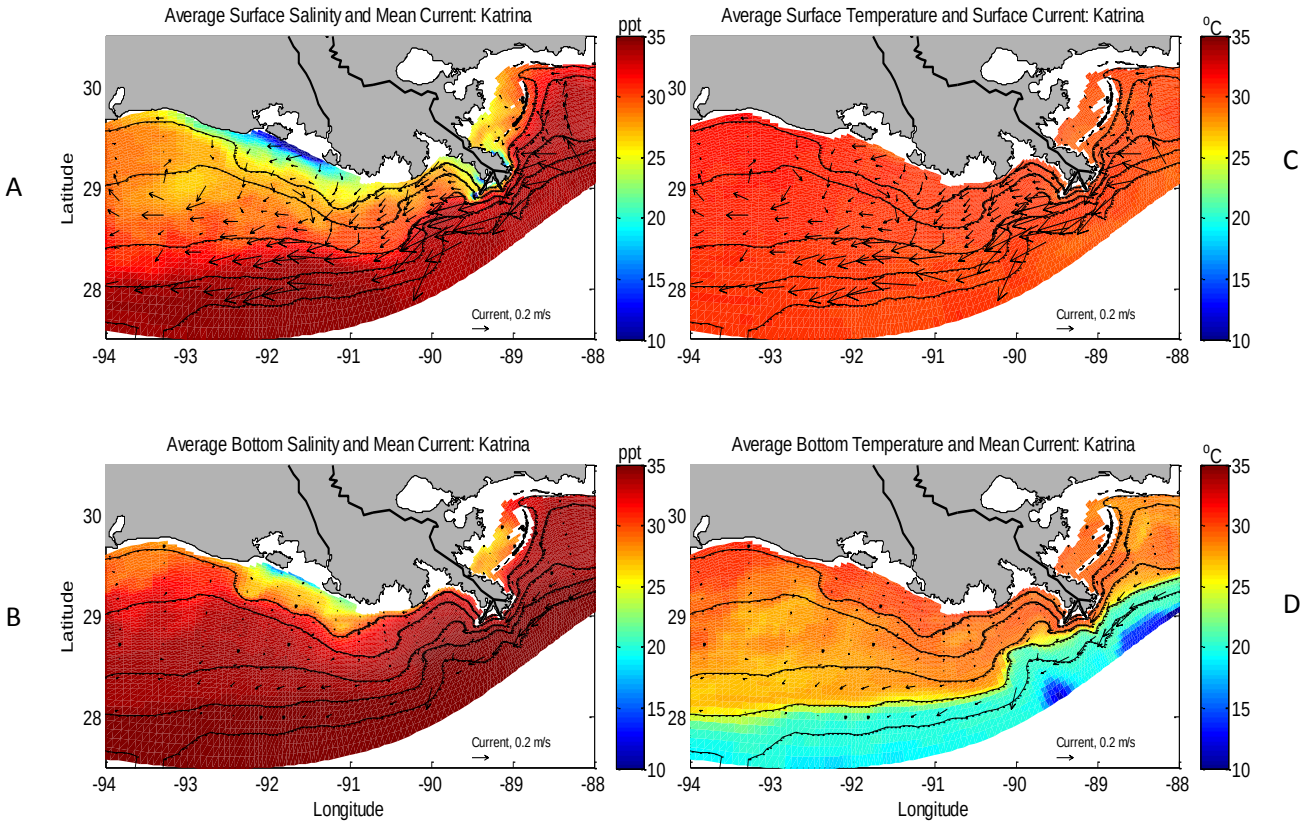

Figure 4-15. (A) Mean surface salinity (ppt) and mean surface current (m/s) arrows for Katrina 7-day period. (B) Mean bottom salinity and mean bottom current arrows for Katrina 7-day period. (C) Mean surface temperature (degree C) and mean surface current arrows for Katrina 7-day period. (D) Mean bottom temperature and mean bottom current arrows for Katrina 7-day period.

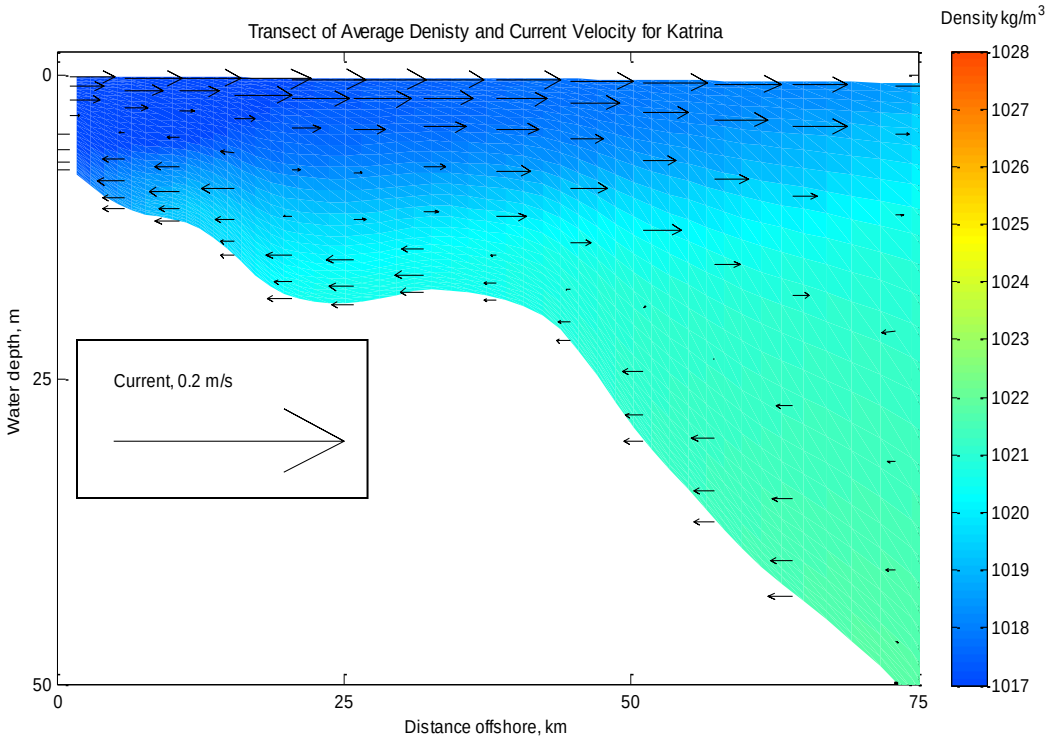

Figure 4-16. Mean density (kg/m^3) and current velocity (m/s) arrows for mid hypoxic region transect based on the means for Hurricane Katrina 7-day period.

A

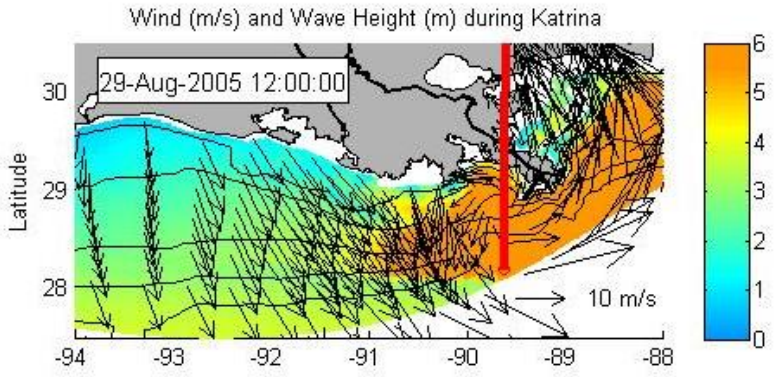

B

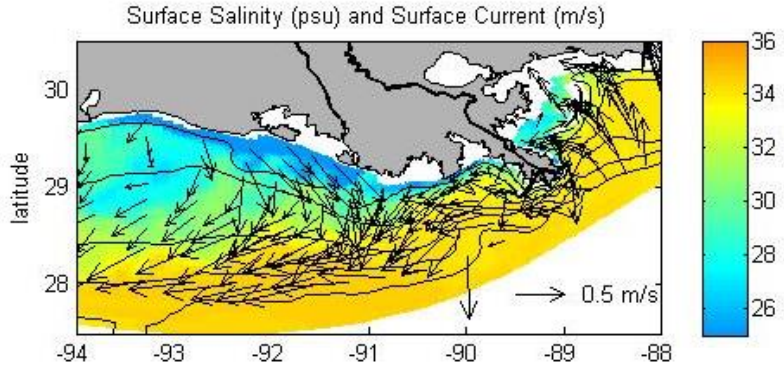

C

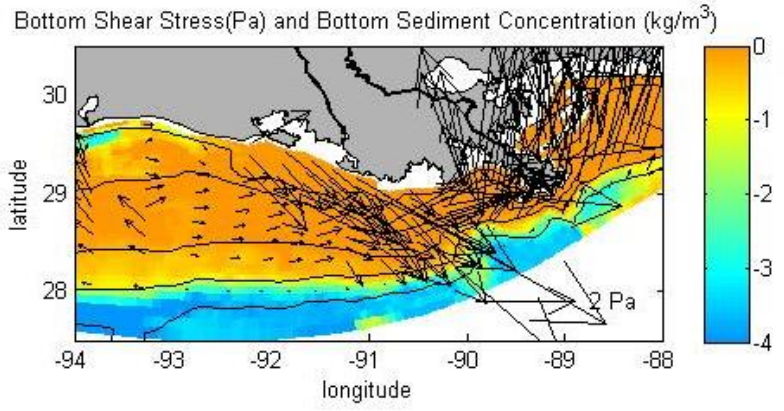

Figure 4-17. Peak characteristics of Hurricane Katrina over the model domain. A) Wind speed and direction (m/s) and wave height (m). B) Surface salinity (PSU) and surface current (m/s). C) Bottom shear stress (Pa) and bottom sediment concentration (kg/m^3).

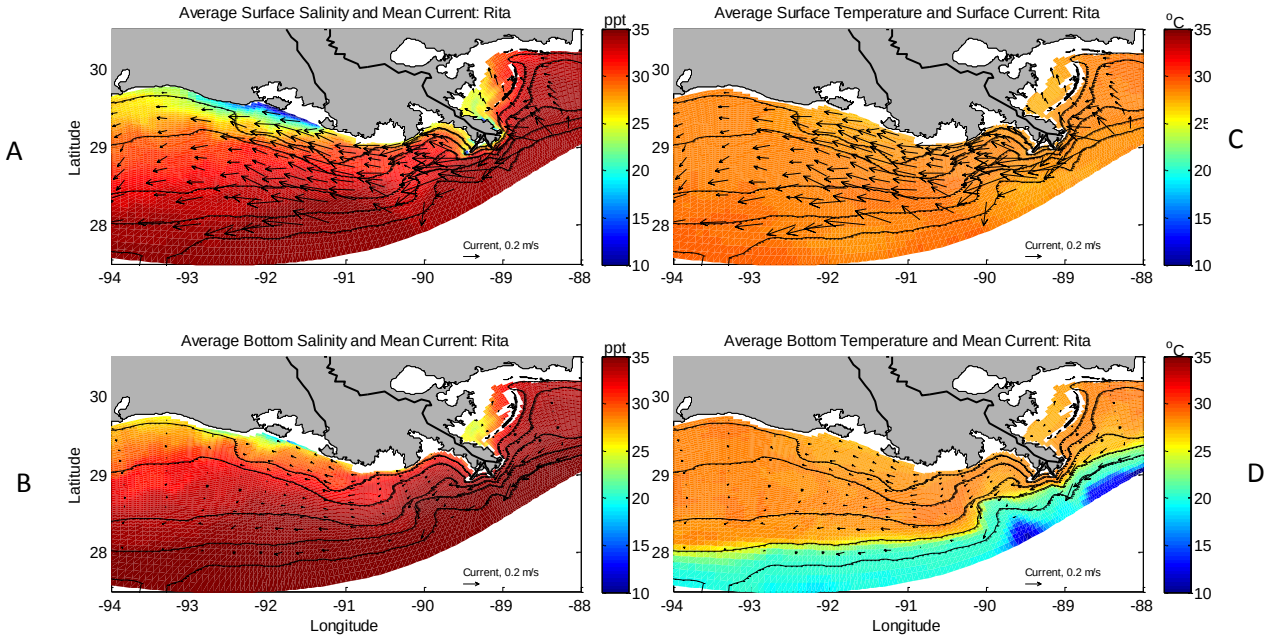

Figure 4-18. (A) Mean surface salinity (ppt) and mean surface current (m/s) arrows for Rita 7-day period. (B) Mean bottom salinity and mean bottom current arrows for Rita 7-day period. (C) Mean surface temperature (degree C) and mean surface current arrows for Rita 7-day period. (D) Mean bottom temperature and mean bottom current arrows for Rita 7-day period.

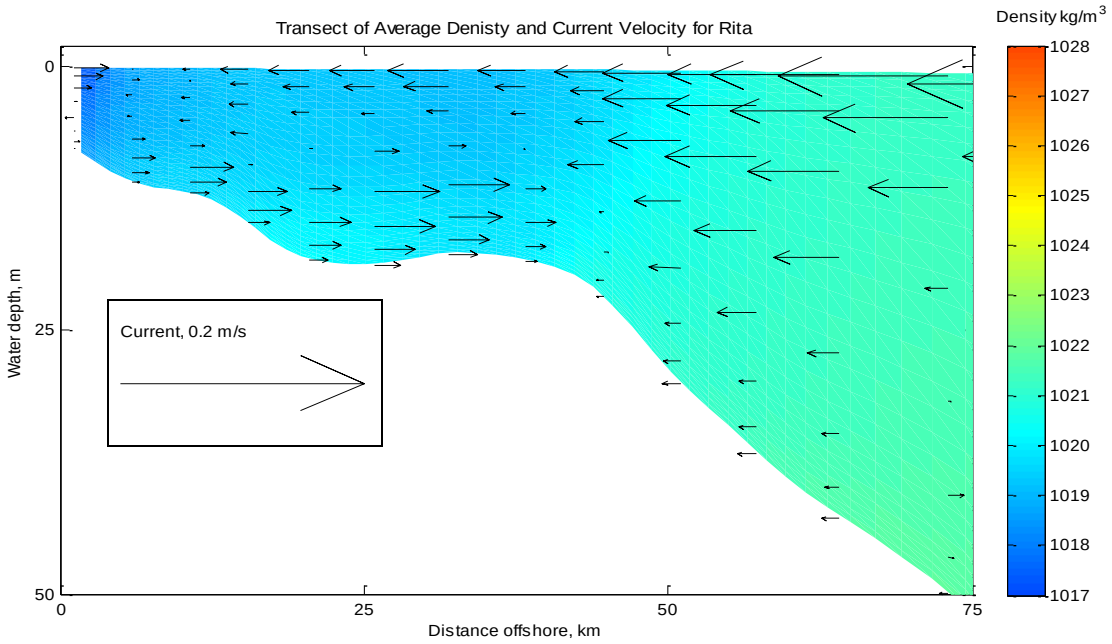

Figure 4-19. Mean density (kg/m^3) and current velocity (m/s) arrows for mid hypoxic region transect for Hurricane Rita 7-day period.

A

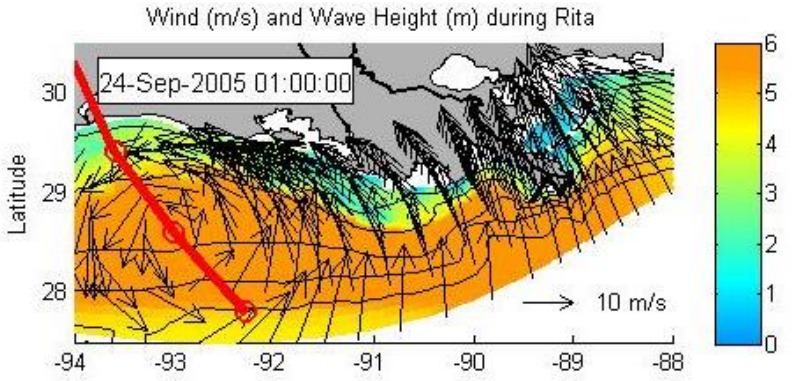

B

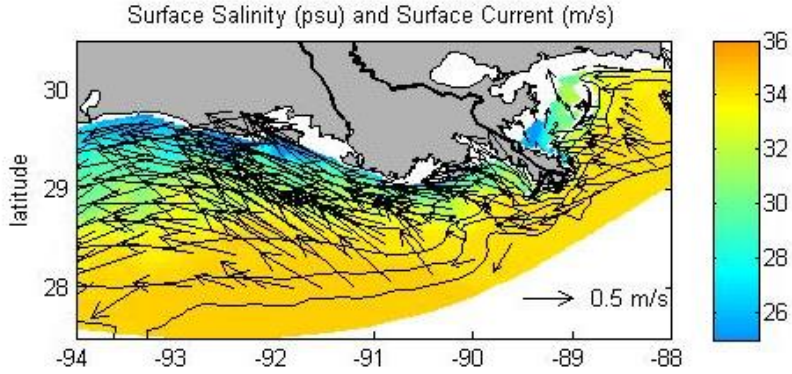

C

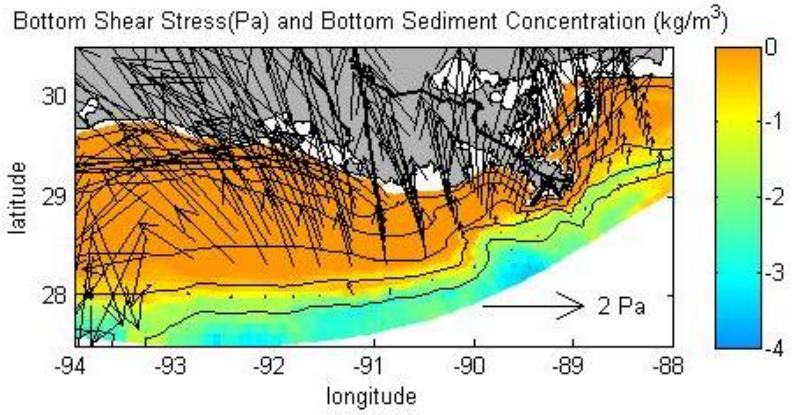

Figure 4-20. Peak characteristics of Hurricane Rita over the model domain. A) Wind speed and direction (m/s) and wave height (m). B) Surface salinity (PSU) and surface current (m/s). C) Bottom shear stress (Pa) and bottom sediment concentration (kg/m^3).

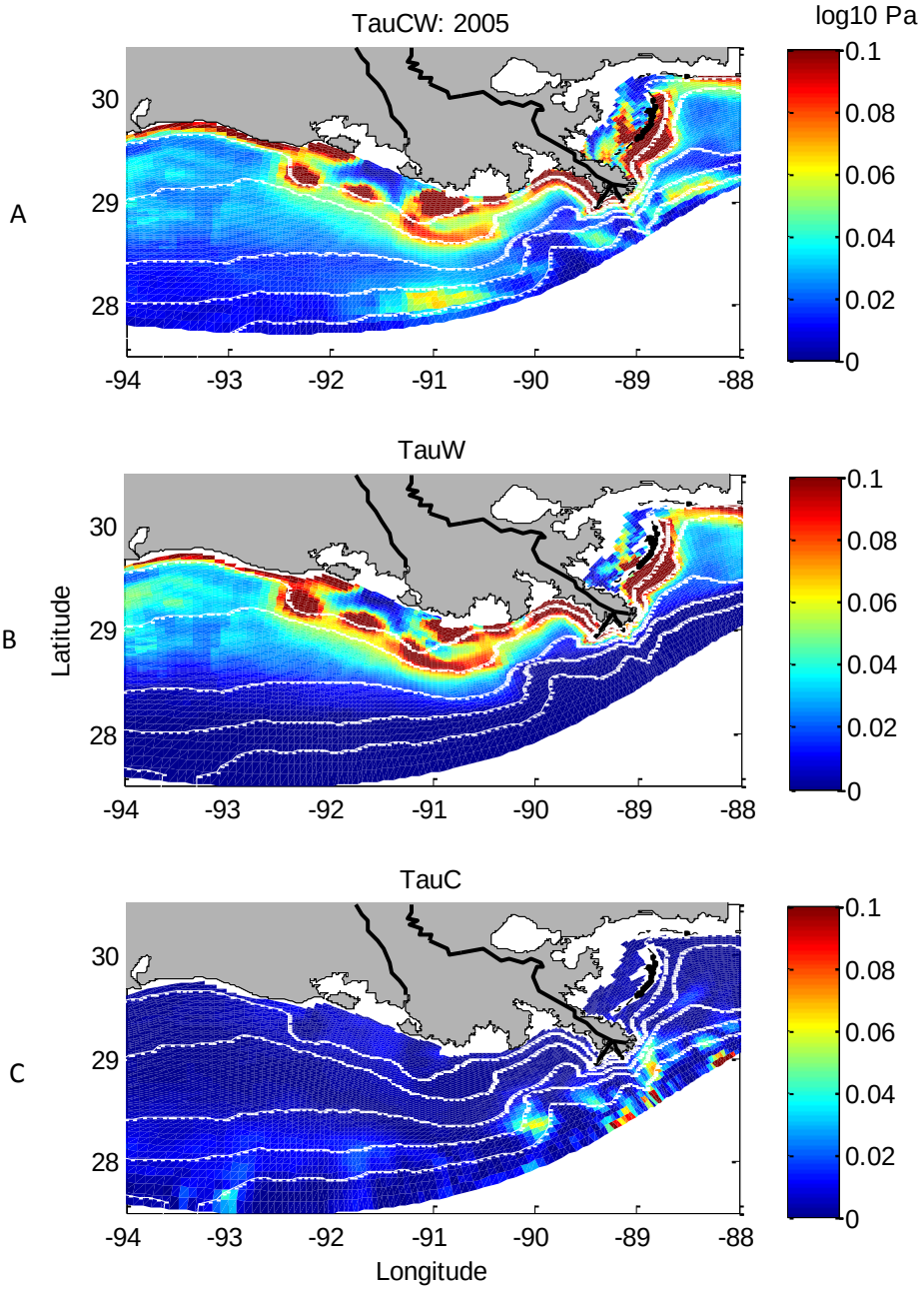

Figure 4-21. 2005 Annual mean shear stress (log10 Pa). (A) Combined wave and current shear stress. (B) Wave shear stress. (C) Current shear stress. White lines indicate depth contours (10m, 20m, 50m, 100m, and 300m).

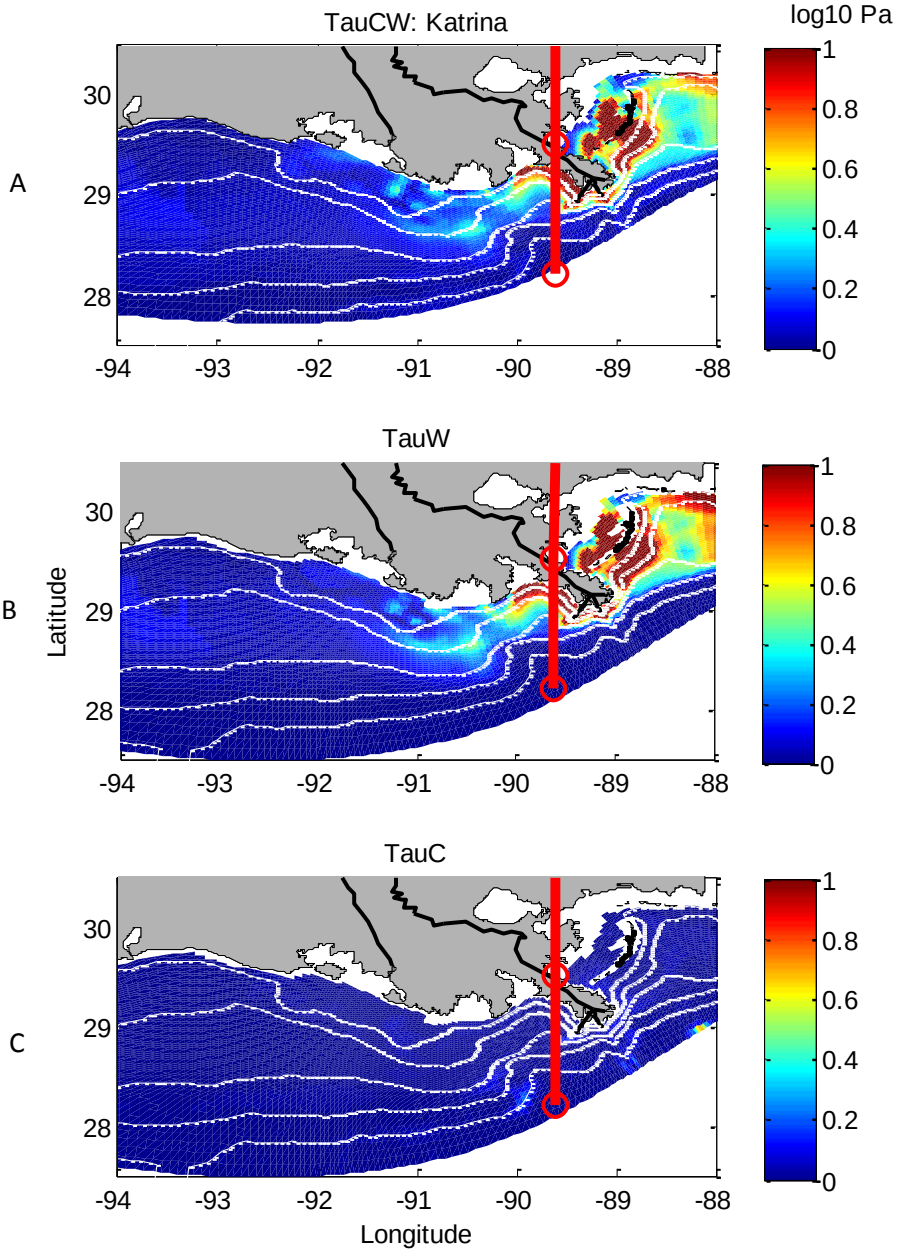

Figure 4-22. Mean shear stress (log10 Pa) during Hurricane Katrina 7-day period. (A) Combined wave and current shear stress. (B) Wave shear stress. (C) Current shear stress. Red line indicates hurricane path. White lines indicate depth contours (10m, 20m, 50m, 100m, and 300m).

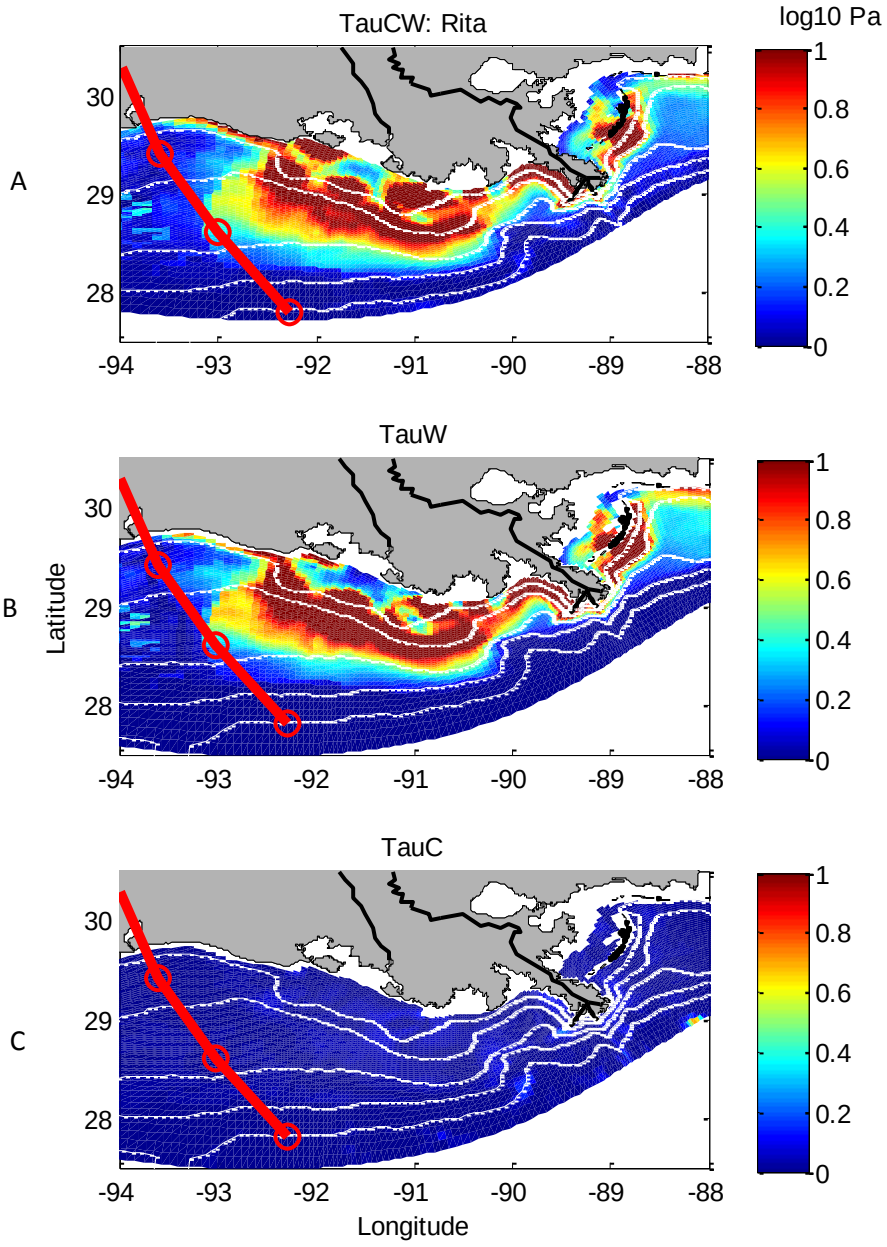

Figure 4-23. Mean shear stress (log10 Pa) during Hurricane Rita 7-day period. (A) Combined wave and current shear stress. (B) Wave shear stress. (C) Current shear stress. Red line indicates hurricane path. White lines indicate depth contours (10m, 20m, 50m, 100m, and 300m).

A

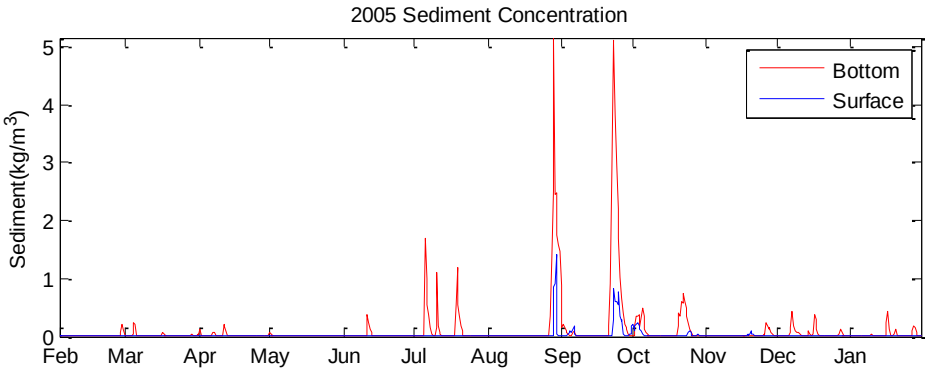

B

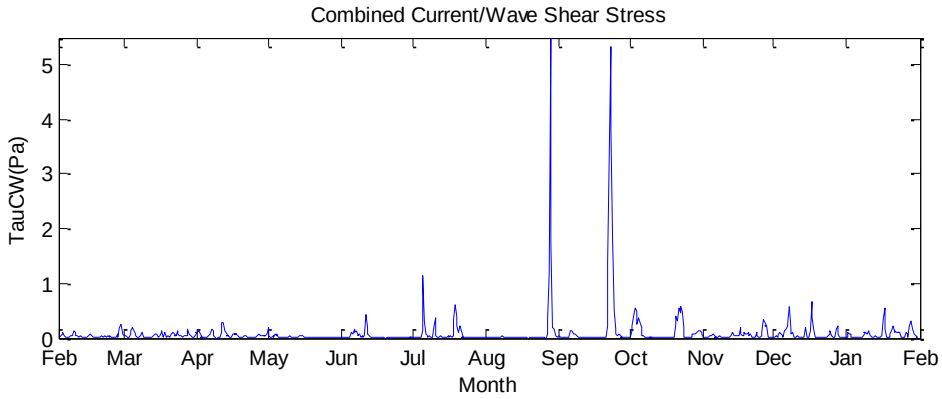

Figure 4-24. (A) Surface and bottom sediment concentration (kg/m^2) for the entire year of 2005 at station 10B. (B) Combined current and wave shear stress (Tau_{CW}) for the entire year of 2005 at station 10B.

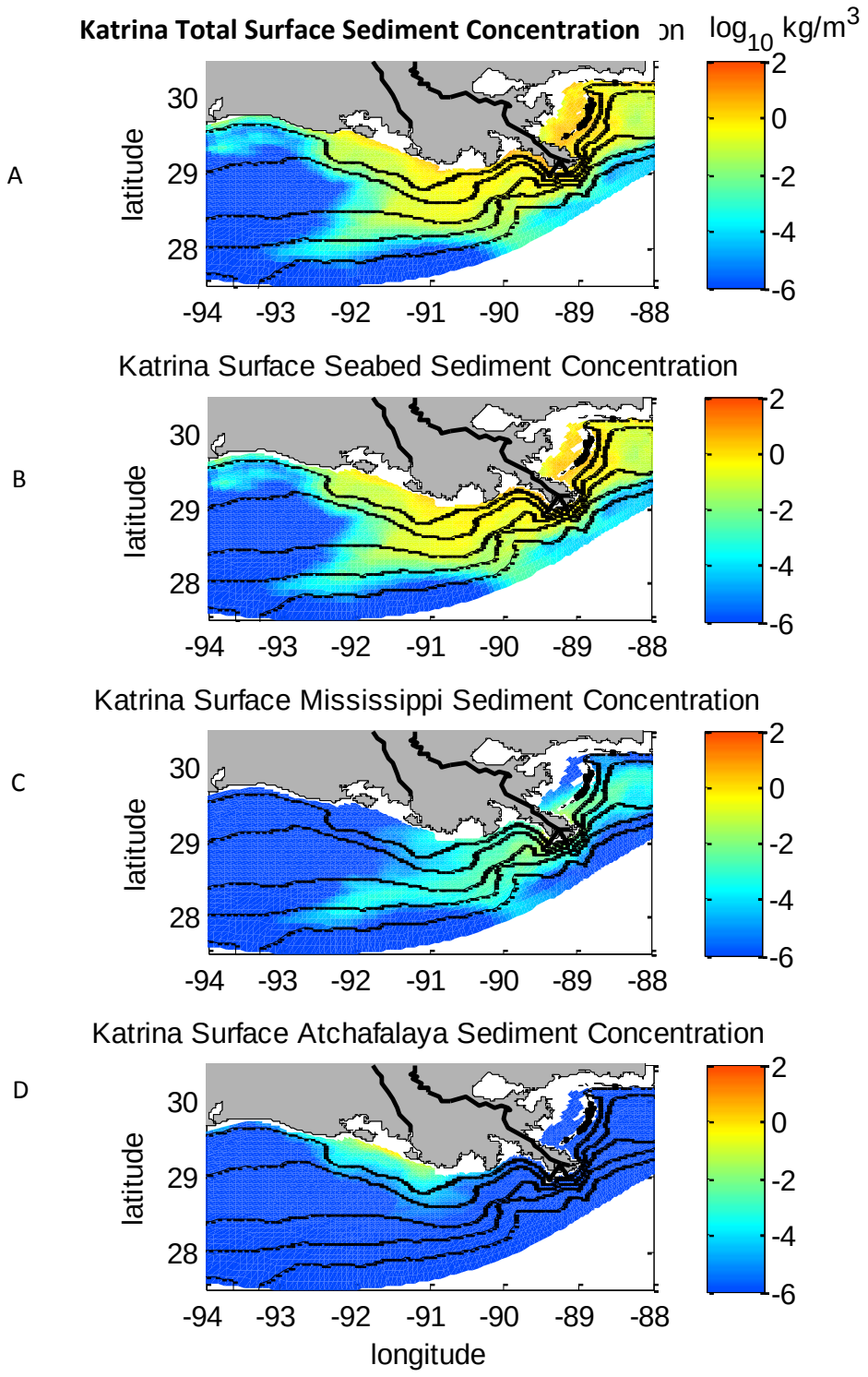

Figure 4-25. (A) Surface sediment concentration (log_{10} kg/m^3) including all sediment classes during Hurricane Katrina. (B) Surface sediment concentration of seabed sediment tracers during Katrina. (C) Surface sediment concentration of Mississippi sediment tracers during Katrina. (D) Surface sediment concentration of Atchafalaya sediment tracers during Katrina.

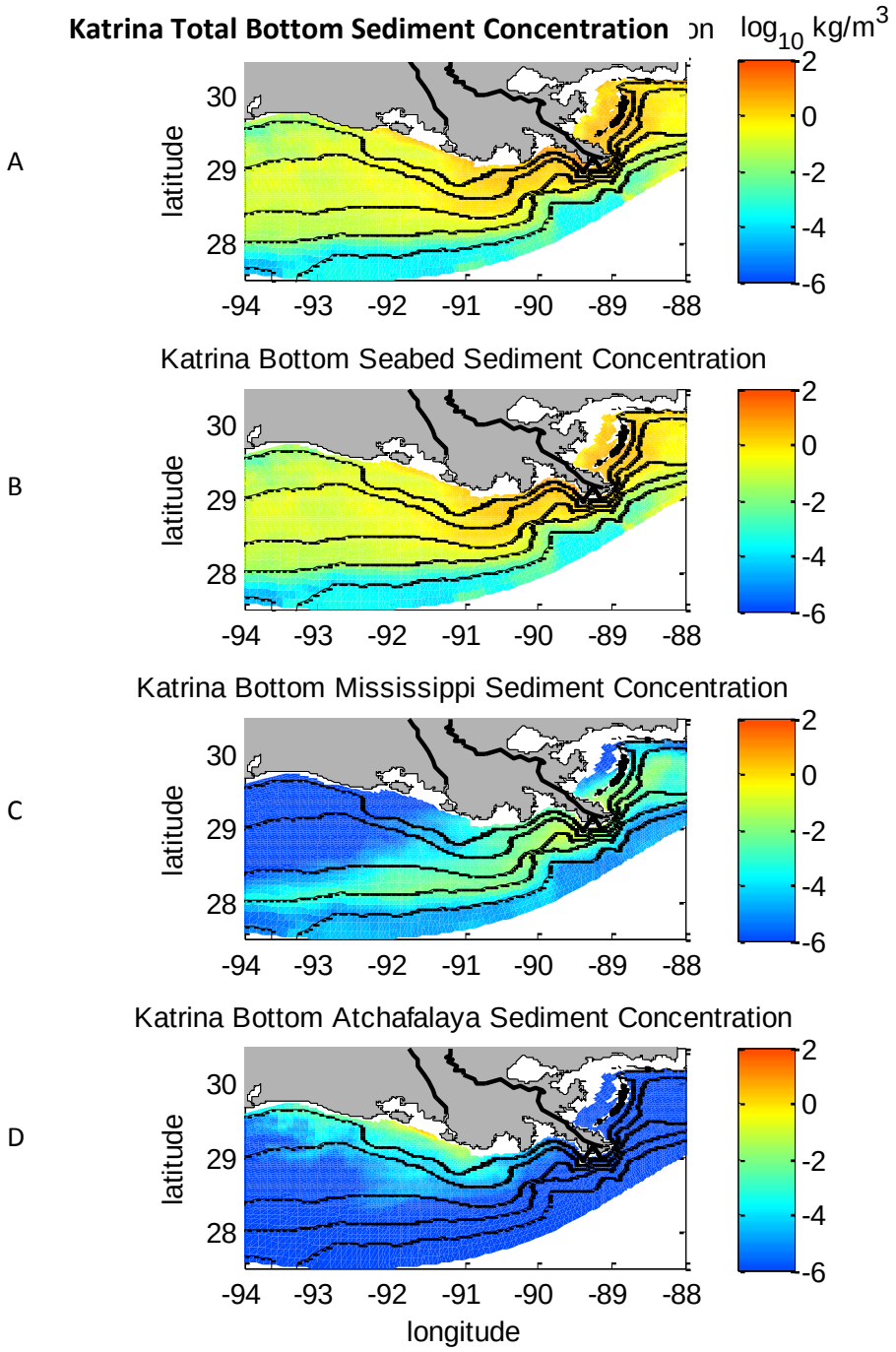

Figure 4-26. (A) Bottom sediment concentration (log_{10} kg/m^3) including all sediment classes during Hurricane Katrina. (B) Bottom sediment concentration of seabed sediment tracers during Katrina. (C) Bottom sediment concentration of Mississippi sediment tracers during Katrina. (D) Bottom sediment concentration of Atchafalaya sediment tracers during Katrina.

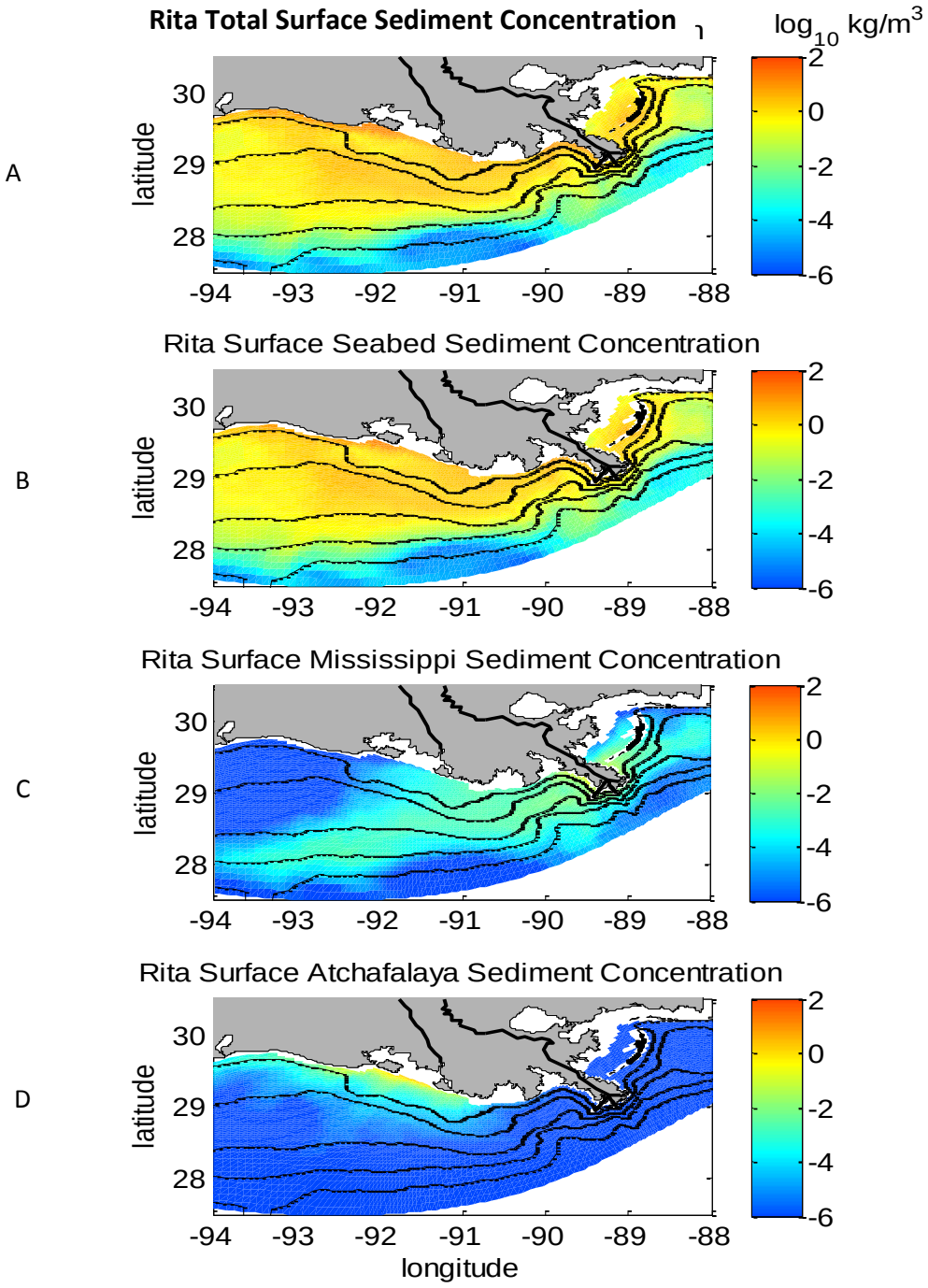

Figure 4-27. (A) Surface sediment concentration (log_{10} kg/m^3) including all sediment classes during Hurricane Rita. (B) Surface sediment concentration of seabed sediment tracers during Rita. (C) Surface sediment concentration of Mississippi sediment tracers during Rita. (D) Surface sediment concentration of Atchafalaya sediment tracers during Rita.

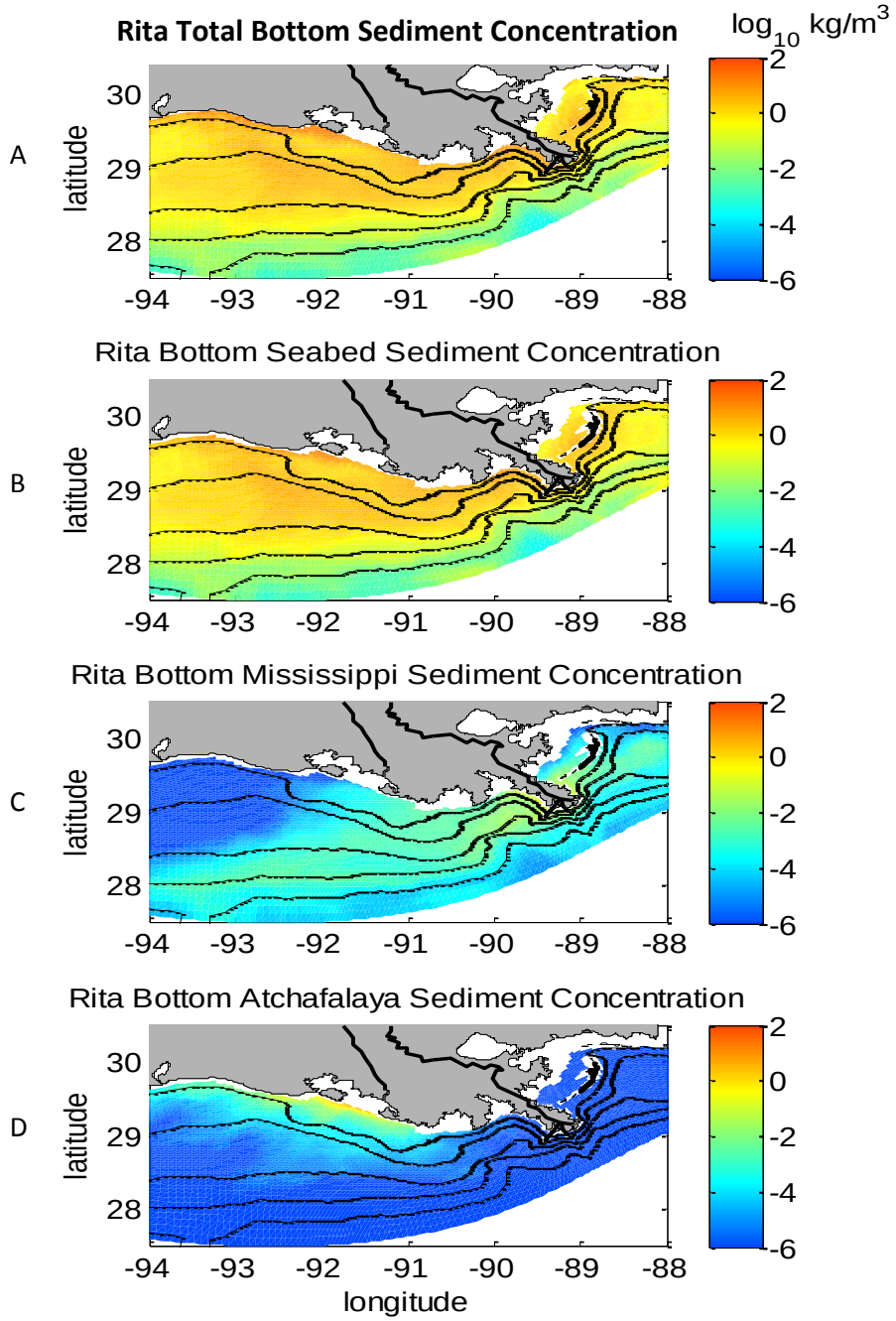

Figure 4-28. (A) Bottom sediment concentration (log_{10} kg/m^3) including all sediment classes during Hurricane Rita. (B) Bottom sediment concentration of seabed sediment tracers during Rita. (C) Bottom sediment concentration of Mississippi sediment tracers during Rita. (D) Bottom sediment concentration of Atchafalaya sediment tracers during Rita.

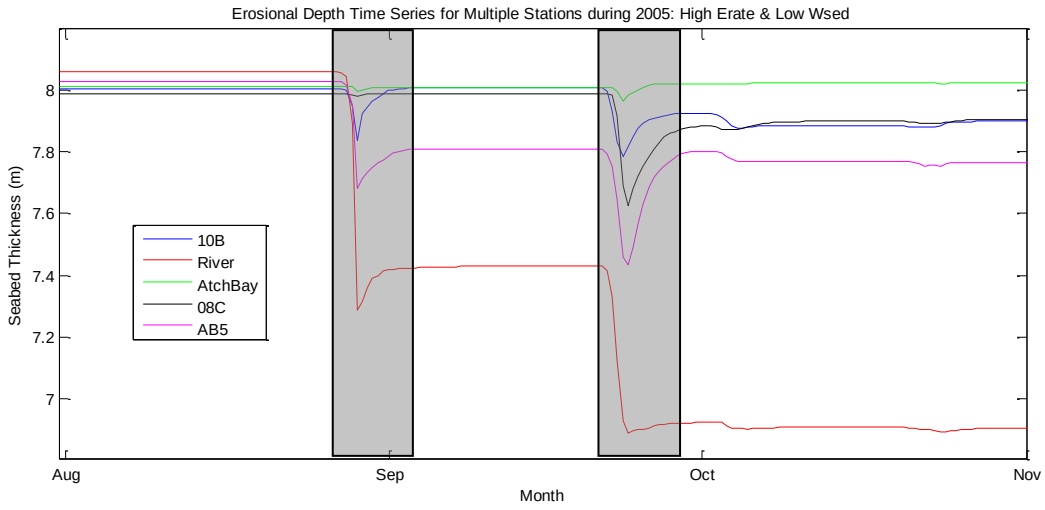

Figure 4-29. Seabed elevation changes (m) during and after Hurricanes Katrina and Rita at the 5 different stations (Fig. 5) for simulation 4; 8m was designated initial seabed thickness. Shaded areas used to determine erosional and depositional depth during and post hurricane.

A

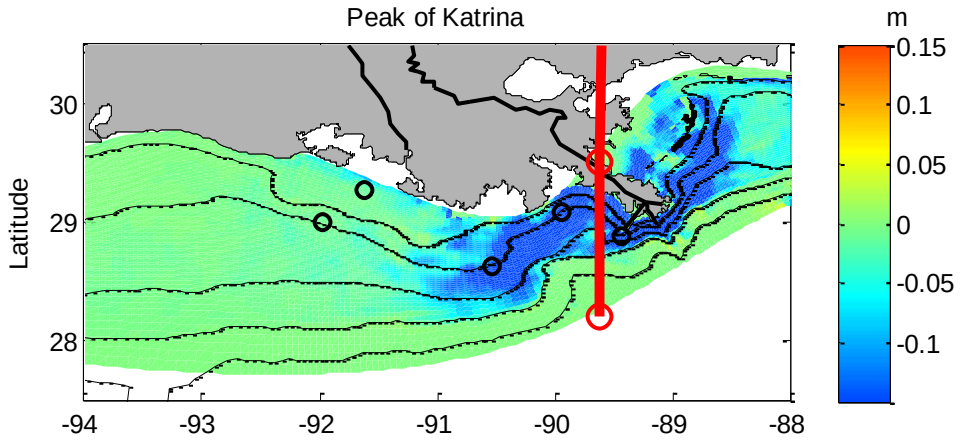

B

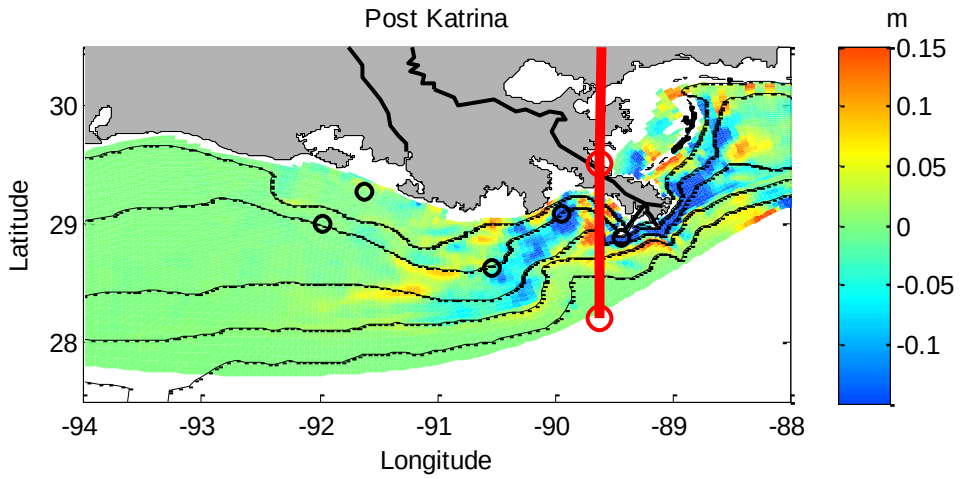

Figure 4-30. Seabed elevation changes (m) at peak of Hurricane Katrina (A) and post Katrina (B). Black circles represent 5 stations used in this study (refer to Fig. 4-5).

A

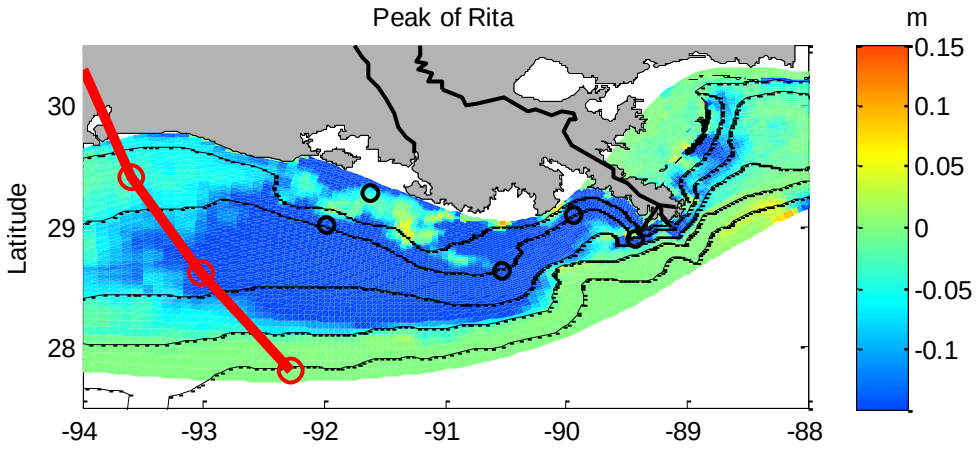

B

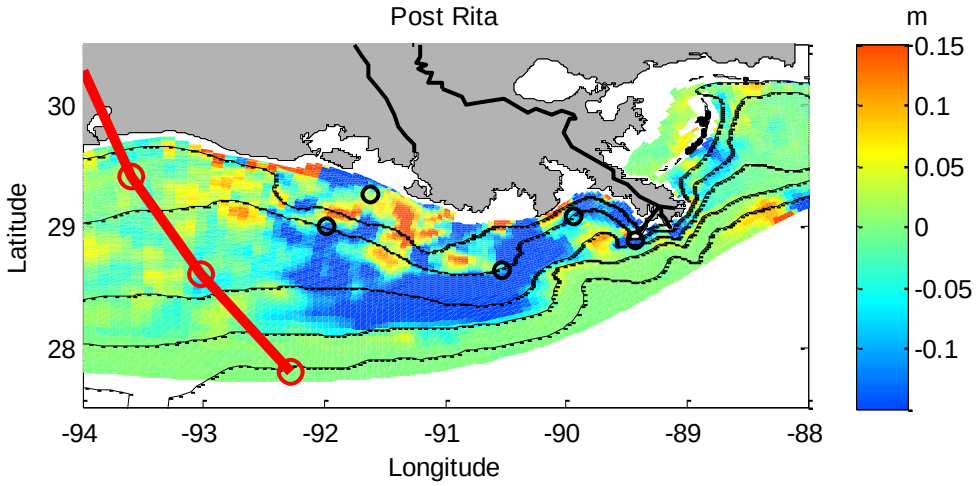

Figure 4-31. Seabed elevation changes (m) at peak of Hurricane Rita (A) and post Rita (B). Black circles represent 5 stations used in this study (refer to Fig. 4-5).

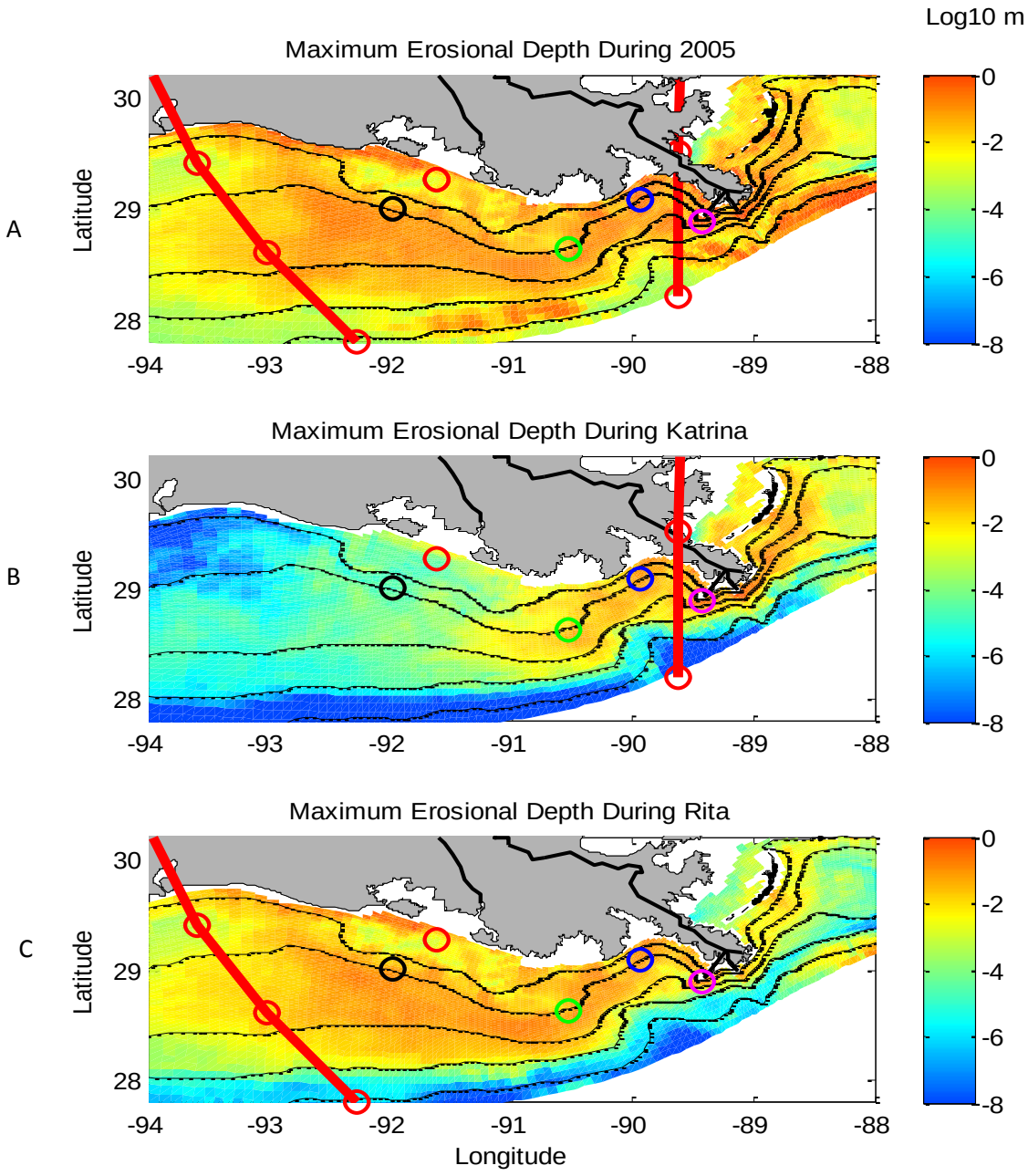

Figure 4-32. (A) Maximum erosional depth (log_{10} m) during 2005. (B) Maximum erosional depth during Katrina (7-day period). (C) Maximum erosional depth during Rita (7-day period). Red lines indicate hurricane path. Open circles represents 5 stations analyzed throughout this study.

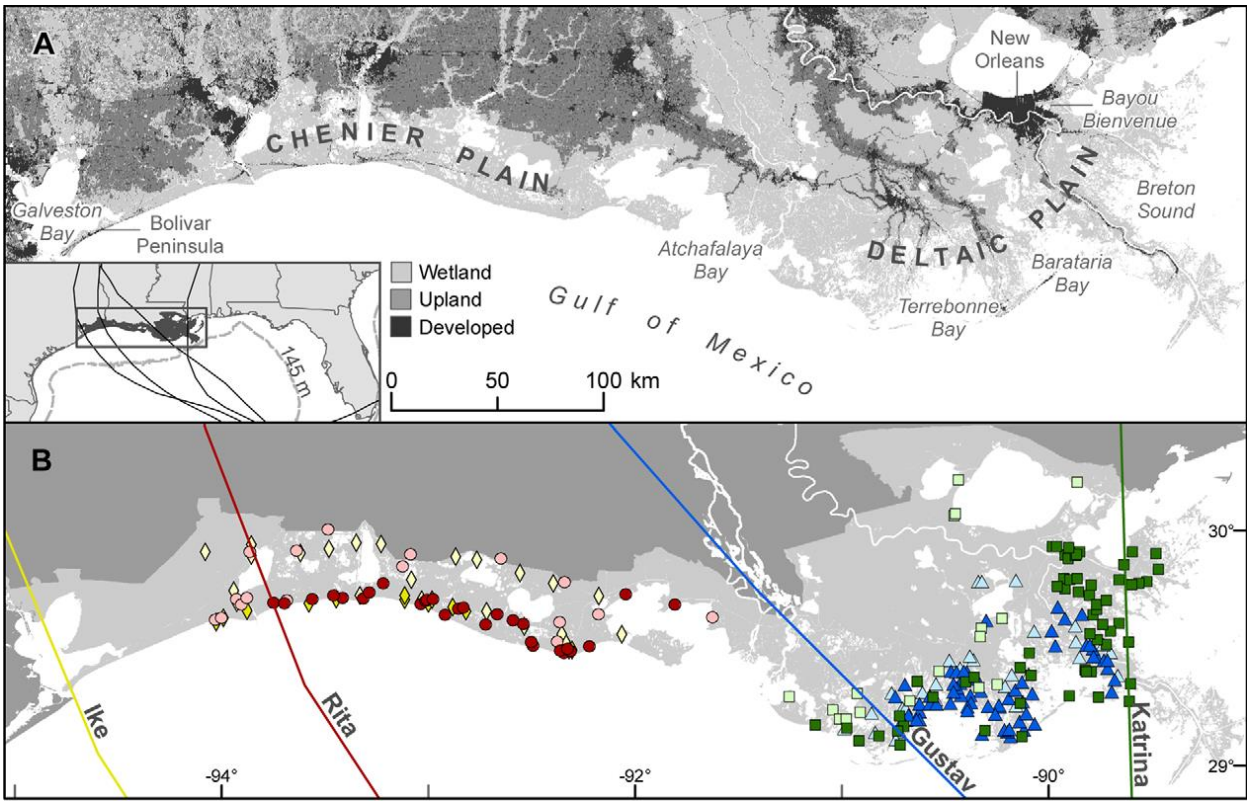

Figure 4-33. (A) Map showing locations of geographic names used in text. Inset shows general location of study area, hurricane paths (black lines), and 145 m isobath (dotted line). (B) Sampling locations and storm paths for Hurricanes Katrina (green square), Rita (red circle), Gustav (blue triangle), and Ike (yellow diamond). The dark colored symbols mark observed deposition and light colored symbols mark observation of no sediment. Taken from Tweel and Turner (2012).

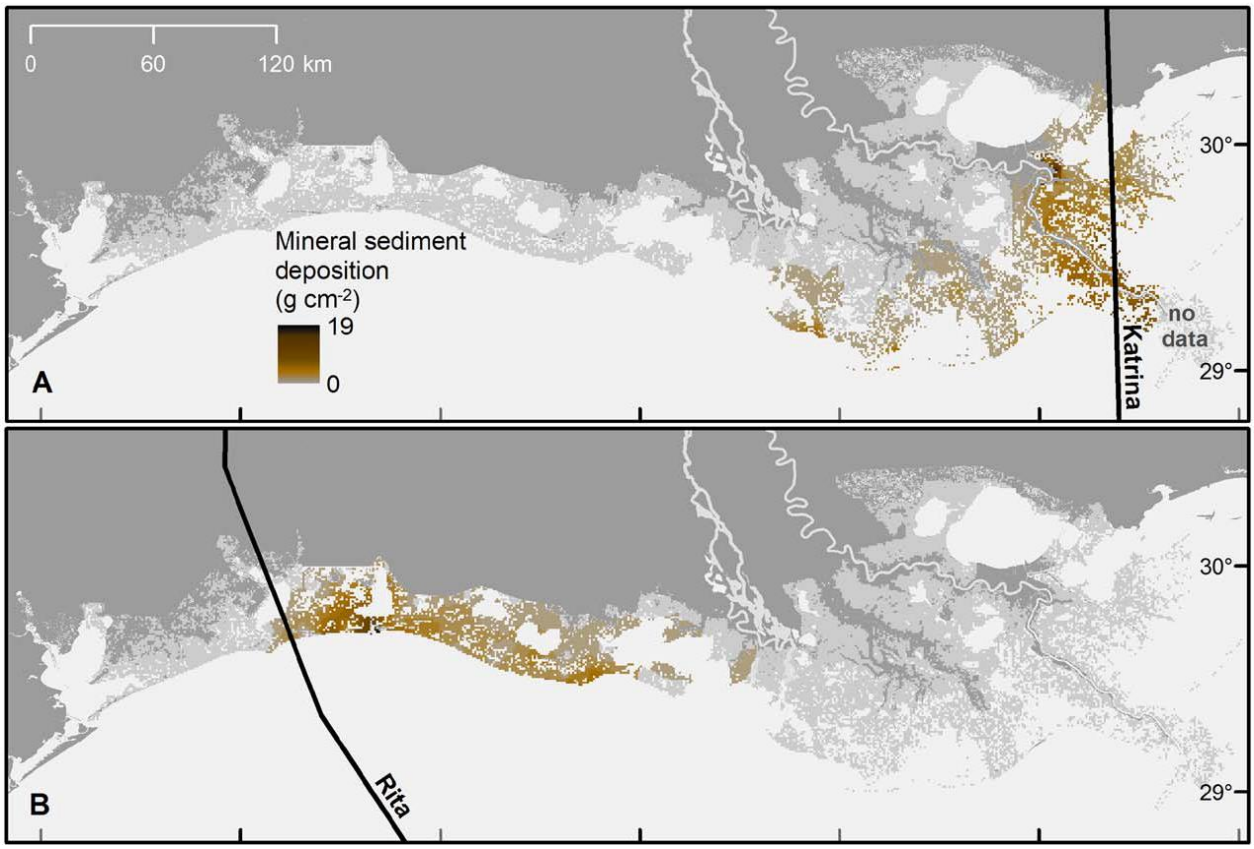

Figure 4-34. Wetland sediment deposition following two recent hurricanes. Mineral sediment deposition (g/cm^2) from Hurricanes Katrina (A), Rita (B). Black lines indicate hurricane path. Taken from Tweel and Turner (2012).

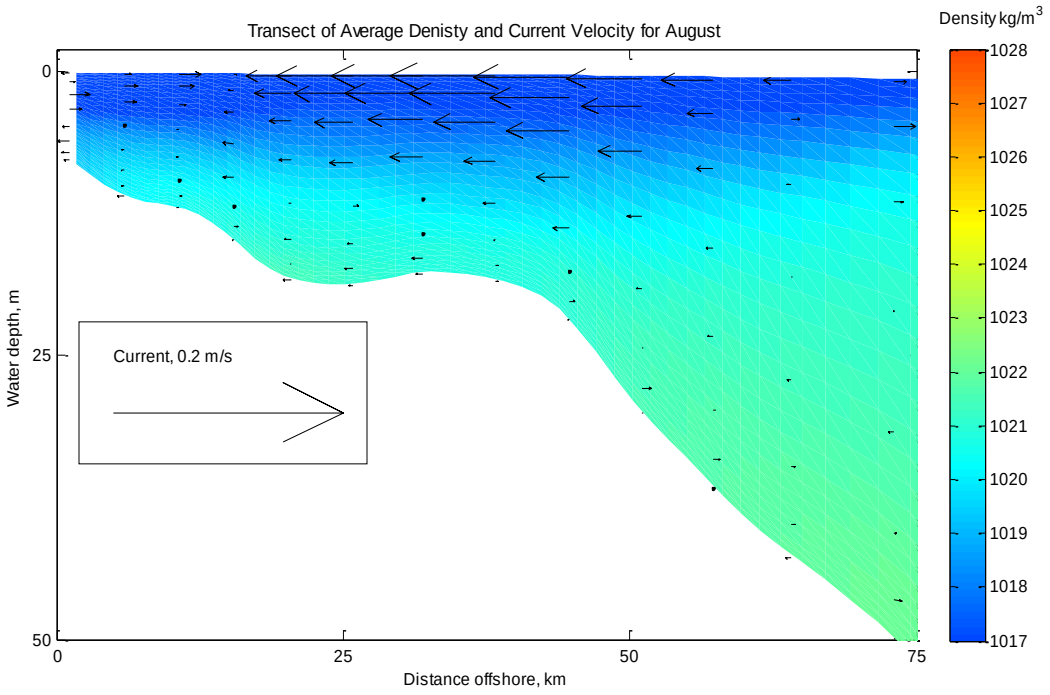

Figure 4-35. Mid-hypoxic zone transect of mean water column density (kg/m^3) and mean current velocity (m/s) arrows during August 2005.

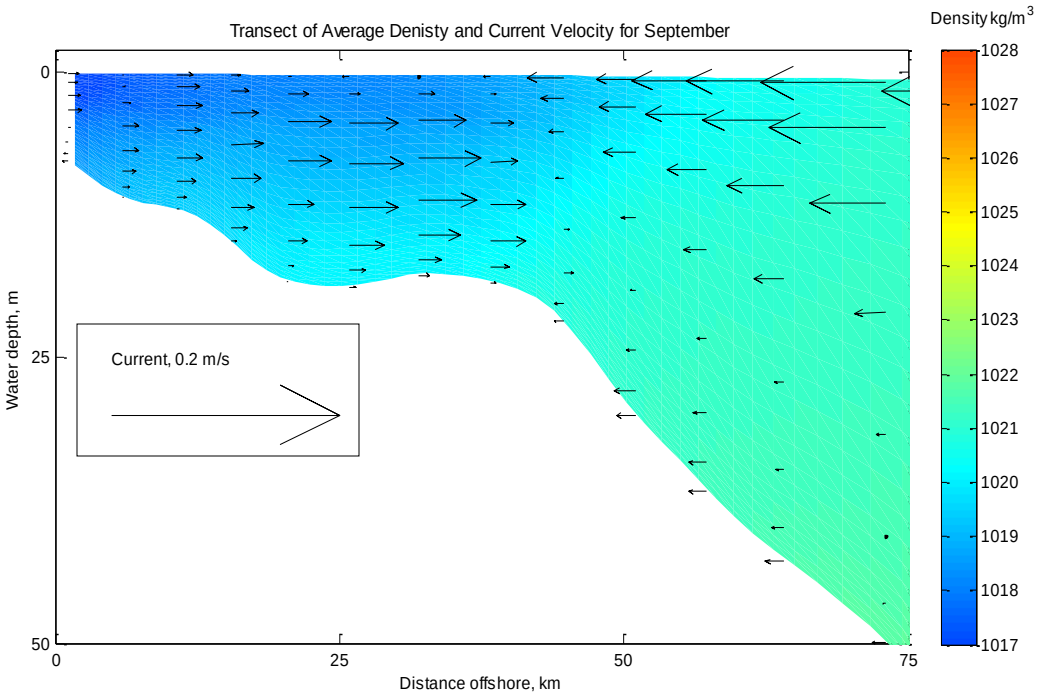

Figure 4-36. Mid-hypoxic zone transect of mean water column density (kg/m^3) and mean current velocity (m/s) arrows during September 2005.

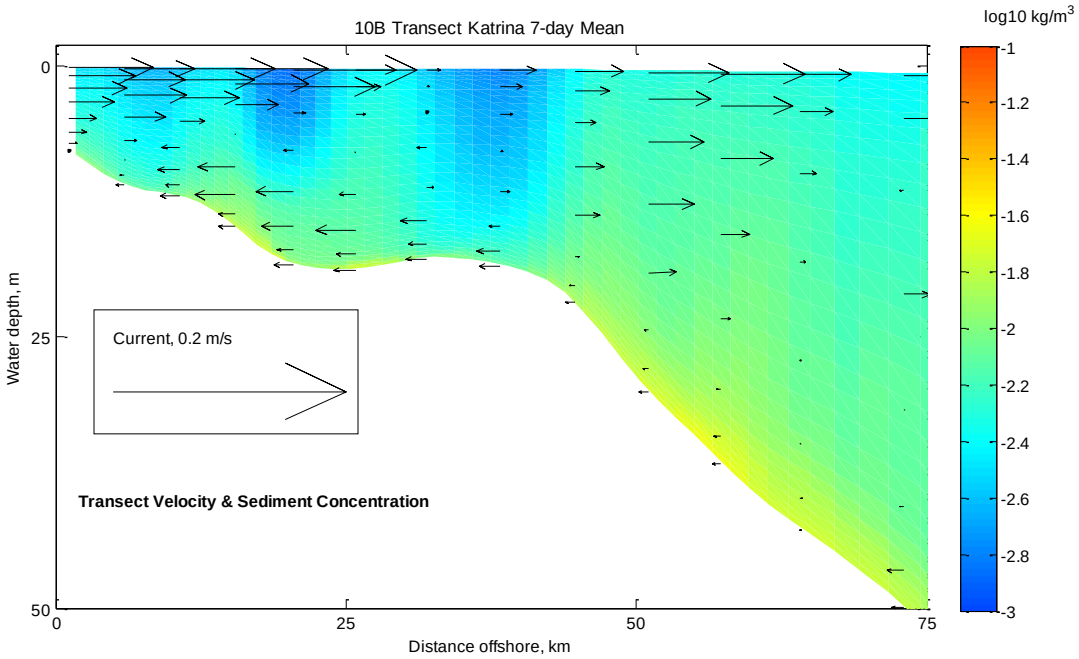

Figure 4-37. Mid-hypoxic zone transect of mean water column sediment concentration (log10 kg/m^3) and mean current velocity (m/s) arrows for Hurricane Katrina 7-day period.

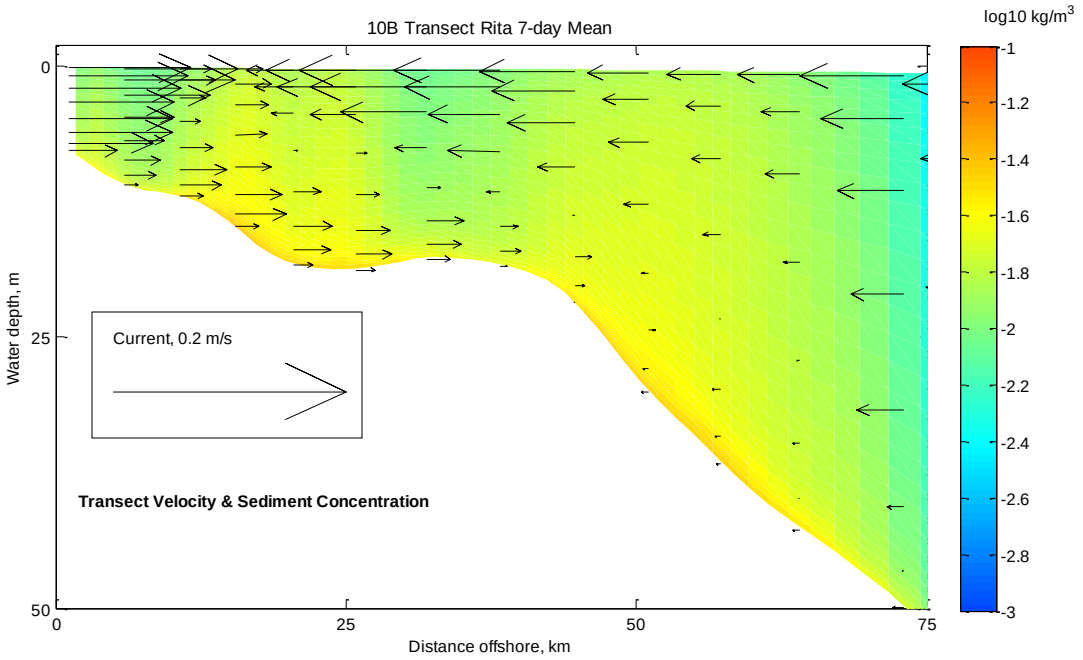

Figure 4-38. Mid-hypoxic zone transect of mean water column sediment concentration (log10 kg/m^3) and mean current velocity (m/s) arrows for Hurricane Rita 7-day period.